AKARI FIS Data User Manual

Version 1.3

Eva Verdugo[1], Issei Yamamura[2] and Chris Pearson[1,2]

with contributions from:

Mai Shirahata[2], Shuji Matsuura[2], Yoko Okada[2], Sin'itirou Makiuti[2],
Noriko Murakami[3] and Mitsunobu Kawada[3]

[1]European Space Astronomy Centre (ESAC), ESA
[2]Institute of Space and Astronautical Science (ISAS), JAXA
[3]Nagoya University, Japan

September 14, 2007

Revision Record

Date	Revision	Comments
Mar 2007	Version 1.0	Release of version 1.0
Mar 2007	Version 1.1	Updated toolkit setup instructions in Appendix A
Jun 2007	Version 1.2	Updated processing options explanation
Sep 2007	Version 1.3	FTS sections updated.
		FIS 01/02 sensitivity numbers updated
		Additional information about ghost added
		Appendix A updated according to the new pipeline version

Contents

Chapter 1

Introduction

1.1   Purpose of this document

This manual is intended to give the FIS observer all necessary information to produce their data products.

The FIS IDUM should make the observer familiar with the FIS instrument, its operations, the output data, the calibration and the processing. To achieve this the following subjects are addressed:

- The FIS instrument and its operations

- Some characteristics of the instrument that have implications for the data

- An overview of the data processing

- The calibration of the data and the accuracy

- A guide to the data products

- How to start with the data

- A cookbook for the usage of the processing tools

Since this manual is intended to give the observer up to date information on the processing and the calibration of the FIS instrument, it will be updated regularly. Every change in the FIS data reduction software, the calibration procedures or the file descriptions will be reflected in this manual.

1.2   Relevant information

AKARI Observer's Web

  The ISAS Web page contains the most up to date information:
  URL:*http://www.ir.isas.jaxa.jp/AKARI/Observation/*
  The ESAC page also includes up to date information:
  URL:*http://akari.esac.esa.int/observers/*

Helpdesk

  Any questions and comments on AKARI observations and user support are addressed to
  the AKARI Helpdesks:
  iris_help@ir.isas.jaxa.jp
  http://akari.esac.esa.int/esupport/

Chapter 2

Instrument and AOT Overview

The Far-Infrared Surveyor (FIS) Instrument is designed primarily to perform the All-Sky Survey in four wavelength bands. The instruments are operated such that data acquisition is continuously made as the telescope scans the sky, resulting in sets of strip data of sky brightness. This operation can also be used for pointed observations in a Slow-Scan mode. The FIS is also equipped with a Fourier Transform Spectrometer (FTS) that enables imaging spectroscopy over the full FIS wavelength range. FTS observations are only made as pointed observations.

2.1 Hardware Specification

2.1.1 Overview

The specifications of the FIS instrument are summarized in Table 2.1.1. It provides four photometric bands between 50 and 180 μm, two broad bands and two narrow bands. Individual detector systems are implemented for the two short and two long wavelength bands, respectively. The FTS covers the entire FIS wavelength range with a resolution of ~ 0.36 cm^{-1} ($R = 450$–150) or ~ 2.4 cm^{-1} ($R = 75$–23).

Table 2.1.1: Hardware Specifications of the Far-Infrared Surveyor (FIS)

Photometric mode				
Band	N60	WIDE-S	WIDE-L	N160
Wavelength Range (μm)[1]	50–80	60–110	110–180	140–180
Central Wavelength (μm)	65	90	140	160
Band Width (μm)[2]	21.7	37.9	52.4	34.1
Detector	Monolithic Ge:Ga[3]		Stressed Ge:Ga	
Array size	20×2	20×3	15×3	15×2
Operational Temperature	~ 2.0 K		~ 2.0 K	
Pixel size (arcsec)[4]	26.8		44.2	
Pixel pitch (arcsec)[4]	29.5		49.1	
Readout	Capacitive Trans-Impedance Amplifier (CTIA)			
Spectroscopic mode				
Spectrometer	Martin-Puplett type Fourier transform spectrometer			
Wavelength (μm)	N/A	60–110	110–180	N/A
Resolution (cm^{-1})	N/A	0.36 / 2.4		N/A

[1] The detector responsivity is higher than 20% of the peak.
[2] As defined by the bandwidth equation below
[3] The SW detector was manufactured by NICT.
[4] The values may change as more accurate telescope parameters become available.

The Central Wavelength is given to be a representative number of the band near the weight center of the band profile. The band width is then defined by the following equation for a flat spectrum, $\nu F_\nu =$const.

$$\Delta\nu \equiv \frac{\int r(\nu)T(\nu)F_\nu(\nu)d\nu}{r(\nu_c)T(\nu_c)F_\nu(\nu_c)} = \frac{\int r(\nu)T(\nu)d\nu/\nu}{r(\nu_c)T(\nu_c)/\nu_c}. \tag{2.1.1}$$

Together, the responsivity (r) and optical transmittance (T) define the system responsivity (R, the relative spectral response function : RSRF).

2.1.2   Optics and Filters

The FIS Optics

Figure 2.1.1 shows the bottom view looking out of the telescope (telescope and the sky are into the page) from the FIS instrument. The light path is indicated by the dash-dotted arrows. Optical elements are labeled. There are three moving parts, a shutter at the light entrance, a filter wheel, and the moving mirror of the FTS. The filter wheel can be rotated to switch between photometric and spectroscopic (FTS) modes. The shutter will be closed occasionally to obtain instrumental dark levels.
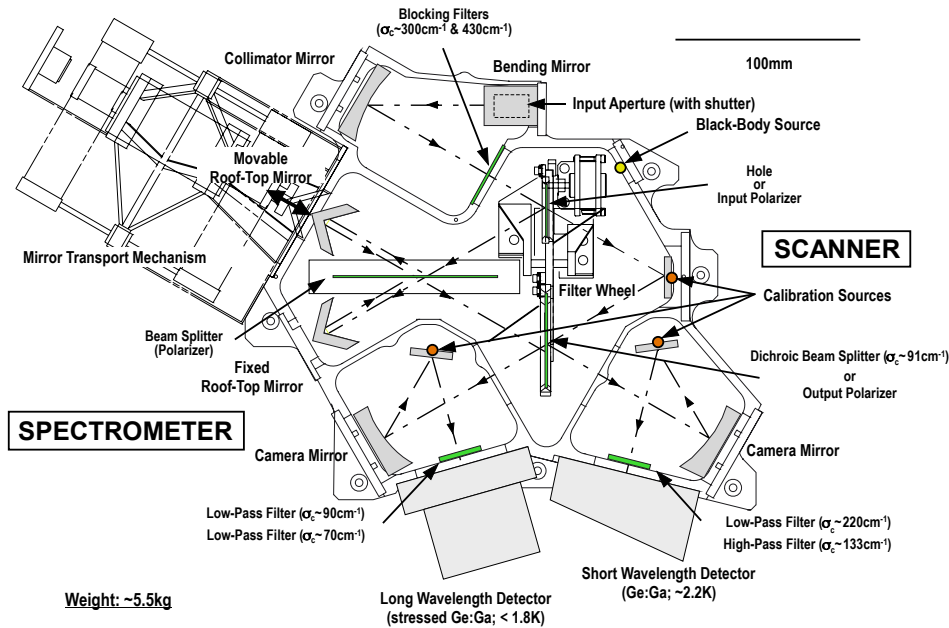
Figure 2.1.1: The optical paths within the FIS. Locations of the calibration lamps are indicated.

Filters and Photometric bands

Figure 2.1.2 describes the filter configuration of the FIS photometric bands. The LW narrow band filter was replaced in 2004 with a new filter with a cut-off at 70 cm^{-1} (143 μm). This extended the band profile shortward and results in a better effective responsivity. Following this change, we now denote the longest FIS band as "N160" instead of the previous name N170.

Calibration Lamps

Two sets of calibration lamps are installed in the FIS. The Cal-A system consists of two lamps placed in front of the SW and LW detector arrays. They can be operated individually so that the optimal calibration procedure for each detector array can be realized. An important role of the Cal-A lamp is to produce a pulse flash to simulate the passage of a real point source. The pulse flashes were planned periodically (e.g., every minute) to monitor and correct the time variation of the detector responsivity[1]. However, analysis of the PV-phase observations showed strong after effects due to slow transient response (see Section 3.2.6) thus the periodically pulse flashes (every minute) are now omitted for the pointed observations.

---

[1]In the current calibration sequence the duration of pulse is 0.47 sec for the LW array and 0.24 sec for the SW array

Incident photons

Blocking Filter (σ_c=430cm^{-1} & 300cm^{-1})

Dichroic Beam Splitter (σ_c=91cm^{-1})

LPF (σ_c=90cm^{-1})　　　LPF (σ_c=220cm^{-1})

LPF (σ_c=70cm^{-1})　　　HPF (σ_c=133cm^{-1})

| N160 ($\sim$180-140μm) | WIDE-L ($\sim$180-110μm) | WIDE-S (110-60μm) | N60 (80-50μm) |

stressed Ge:Ga array　　　Ge:Ga array

for FTS mode
dichroic BS is replaced by output polarizer
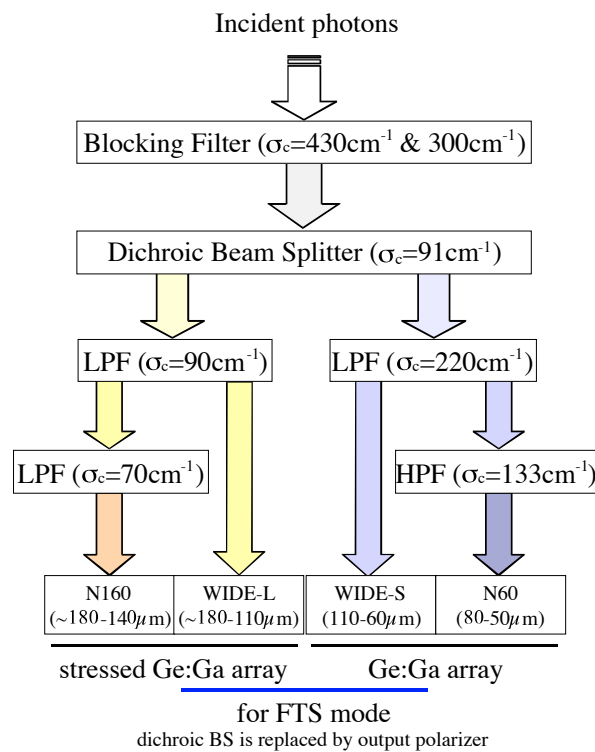
Figure 2.1.2: The filter configuration of the FIS photometric bands. LPF is the Low Pass Filter.

Occasionally the lamps are continuously turned on to provide a stable irradiation. In addition, the Cal-B system is a lamp located in the middle of the FIS optical path. Its' light passes through the beam splitter reaching both detector arrays. This Cal-B system will be used as a backup for the Cal-A system. Both of these two sets of lamps are used solely for monitoring the relative responsivity variation of the detectors. The absolute flux calibration will be made with celestial objects.

In addition to the calibration lamp sets, there is a black body source on the inner wall. It is used for calibration of the FTS.

Shutter

There is a shutter at the entrance aperture of the FIS. The instrumental dark level can be measured by closing the shutter. During the All-Sky Survey, the shutter is closed periodically to monitor the dark level. Leakage at the 1/200 (at every passage of the polar regions) level has been observed in the pre-flight measurement. No significant leakage has been observed although a detailed quantitative evaluation is yet to be made. The internal calibration sequence, calibration lamps and shutter operation for pointed observations are described in the AOTs (Astronomical Observation Templates).

2.1.3   Detector System

Arrays

The FIS has two kinds of detector arrays, a set of two monolithic Ge:Ga arrays[2] for the SW-channel (50–110 μm) and a stressed Ge:Ga array for the LW-channel (110–180 μm). They are operated at $\sim$ 2.0 K. Both the SW and LW channels consist of two photometric bands; i.e, the FIS will have four bands in total, which are operated simultaneously in scan mode. In the spectroscopy mode, only WIDE-S and WIDE-L are operated.

Figure 2.1.3 shows the FIS detector arrays in detail on the Focal-Plane. The upper detectors with three rows are the WIDE-S and WIDE-L bands, and the lower ones with two rows are the N60 and N160 bands. The FIS detector arrays are tilted with respect to the scan direction by 26.5 deg such that the interval between the neighbouring scan paths of the detector pixels is one half of the physical pitch of the pixels. As noted above, the SW and the LW detector arrays observe almost the same area on the sky. The slight difference in the sky coverage is due to the difference of the projected array size.
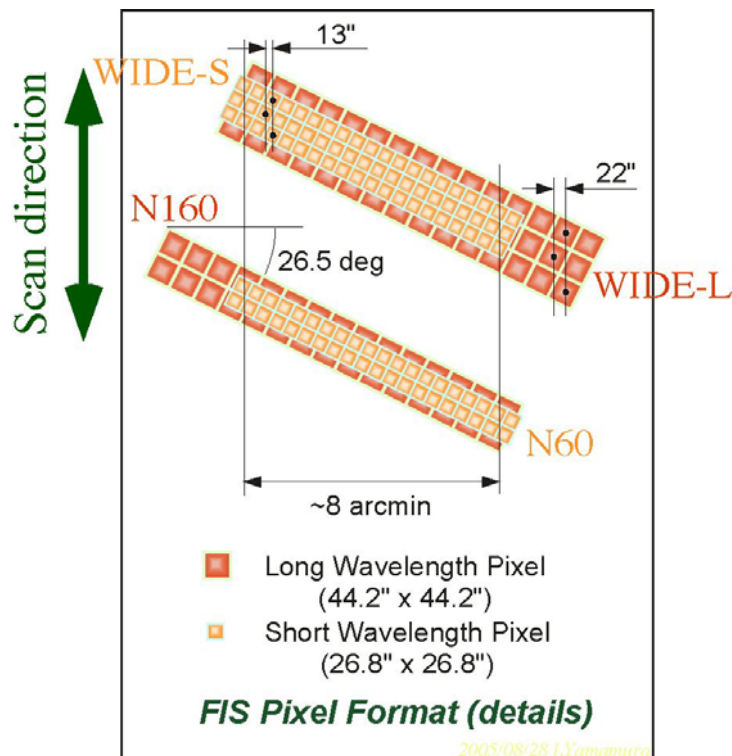
Figure 2.1.3: Focal-Plane layout of the FIS detectors.

Detector Readout Modes

The readout circuit of the FIS is a Capacitive Trans-Impedance Amplifier (CTIA). The signal from each pixel is accumulated in the capacitor as the detector observes far-infrared photons. The voltage at the capacitor is then read out at appropriate intervals. The charge level in the capacitor is periodically reset in order to avoid saturation. The accumulated signal between two resets is called a *Ramp*. Differentiation of the Ramps provides the data that should be proportional to the flux of the incoming radiation. The reset operation of the FIS detectors

---

[2]The SW detector was manufactured by NICT.

is synchronous, i.e., resets are inserted with a set time interval, regardless of the signal level of each pixel. Although the reset interval is carefully optimized to maximize the instrument performance, bright objects passing through the FIS FoV will possibly cause saturation of the detector signal.

Three different detector readout modes are considered.

Simple sampling mode is the basic operation sequence. Each sampled signal is downlinked to the ground after A/D conversion. This mode is used for the FTS observations.

Co-add (Nominal) mode samples the ramps at a higher rate, then the sums of every n samplings are transfered to the ground. This can reduce the noise by a factor of $\sim \sqrt{n}$ while preserving the data size, (n is fixed as 6 in the current design). The Co-add mode is referred to as the **nominal mode** and is generally used for both the All-Sky Survey and the Slow-Scan modes (FIS01, FIS02) of the FIS.

CDS (Correlated Double Sampling) mode is designed to avoid saturation in very bright regions, such as the inner galactic plane. The detectors are reset at every two samplings, and on board differentiation of these two samplings is retrieved as the signal. Therefore, the downlinked data is already differentiated. This mode is occasionally used in the All-Sky Survey and Slow-Scan mode (FIS01, FIS02).

Bias Light for the LW detectors

The Ge:Ga detectors generally have a strong transient response, i.e. the detector does not respond instantaneously to the incoming flux but rather has a delay of a few – hundreds seconds time scale (see Section 3.2.6). In the All-Sky Survey, a point source passes across a detector pixel in 1/4–1/7 seconds. This is too short for the detectors to reach a steady level corresponding to the source flux. Accordingly the point source sensitivity decreases. This effect is particularly serious for the LW detectors (stressed Ge:Ga detectors), and in the low flux condition (dark sky + weak sources).

In order to reduce the impact of this effect, we decided to add a 'bias light'. This takes the form of a set of thin stainless wires put in front of the LW aperture. During the survey a constant current will be used to give a steady photon flux into the detector array. The point source sensitivity for the All-Sky Survey is expected to recover by a factor of a few with this 'bias light'.

The SW detectors do not require such a mechanism.

2.1.4 The Fourier Transform Spectrometer (FTS)

The FIS provides the opportunity for imaging spectroscopy over its full wavelength range (60–180 μm) using the two wide-band arrays (WIDE-S and WIDE-L). The Fourier transform spectrometer of the FIS is of the Martin-Puplett type (Figure 2.1.4). This polarizing type Michelson interferometer uses input and output polarizers to create a linearly polarized beam, and another polarizer to split the beams to a fixed and moving mirror to make the interferogram. The input and output polarizers are mounted on the filter wheel. These polarizers reduce the optical efficiency of the instruments by 1/4 (ideal case) compared to the photometric mode. The total optical efficiency is thus 10–20%. The moving mirror, driven by an electromagnet, can shift ± 9.2 mm from its physical center. The optical center (zero path position) is displaced by 4.6 mm from the physical center and the optical path length is asymmetric to the center.

Two preset operation modes are provided for observers; *Full-resolution mode* and *SED mode* (Figure 2.1.5). They are in principle different only in the mirror scan path length, and accordingly in the resultant spectral resolution. The Full-resolution mode uses the full physical path
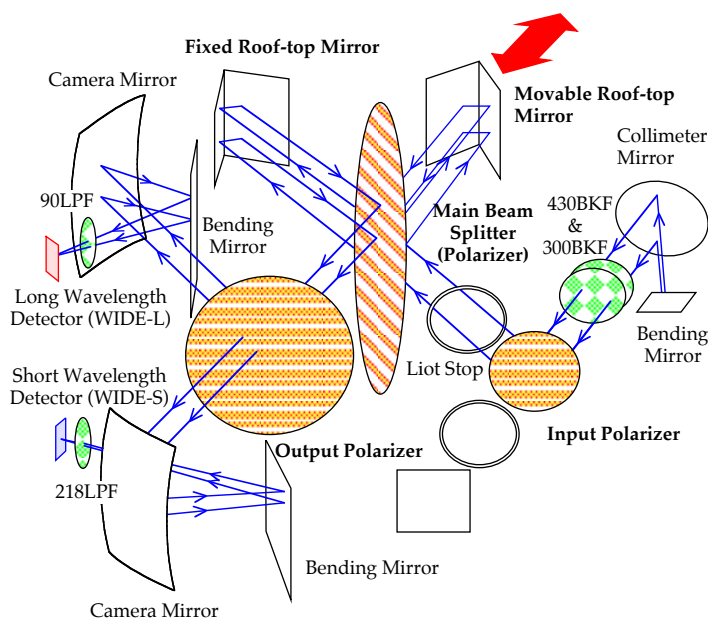
Figure 2.1.4: The optical diagram of the FIS Fourier Transform Spectrometer (FTS).

length, while the SED mode scans ±4.6 mm with respect to the optical center. The mirror moving speed is always a constant 0.367 mm/sec for SED mode and 0.382 mm/sec for Full-Resolution mode. Taking an interferogram (scanning one-way) takes 48 sec in Full-Resolution mode and 12 sec in SED mode.
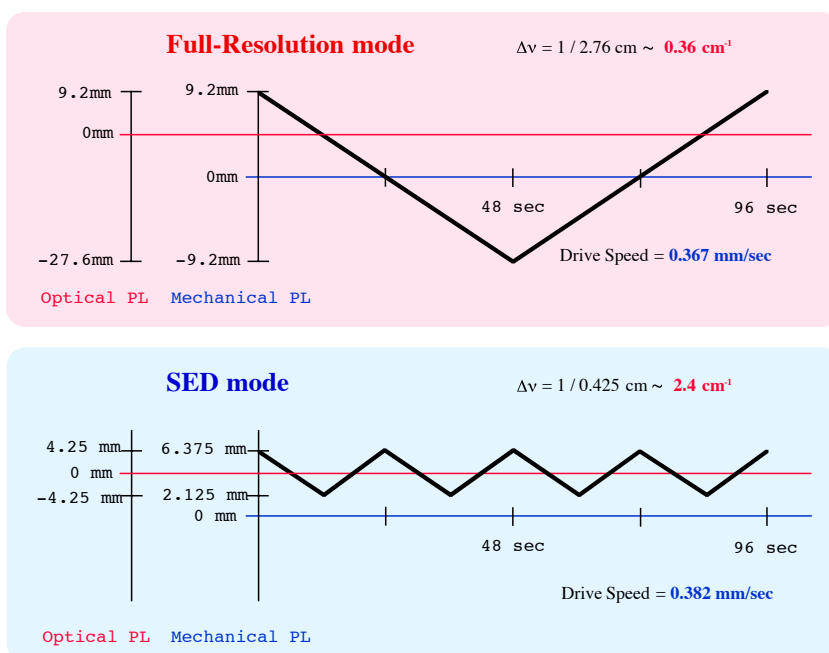
Figure 2.1.5: The mirror driving patterns of the FIS/FTS. There are two modes, *Full-Resolution mode* and *SED mode*.

The spectral resolution, defined as $1/L$ (L is the optical path length) is about 0.36 cm^{-1} for the Full-Resolution mode and 2.4 cm^{-1} for the SED mode, respectively. Note that these values

assume apodization at the spectrum reconstruction. Better spectral resolution may be obtained by optimizing the data reduction procedure. The specification of the FTS mode is summarized in Table 2.1.2.

In FTS mode, the WIDE-S and WIDE-L are operated simultaneously, with a higher sampling rate than in the photometric mode in order to properly sample the interferogram. The narrow band detectors, N60 and N160, are not used.

Table 2.1.2: Specifications of the FIS Fourier Transform Spectrometer (FTS) mode.

Wavelength (μm)	60–110 (WIDE-S), 110–180 (WIDE-L)	
Operation mode	Full-Resolution	SED
Mechanical Path Length (mm)	-9.2–$+9.2$	$+2.1$–$+6.3$
Optical Path Length (mm)	27.6	4.25
One scan time (sec)	48	12
Resolution (cm^{-1})	0.36	2.4
Resolution $\lambda/\Delta\lambda$	450–150	75–23

The actual position of the fields of view (FOV) of the detectors for the FTS mode are offset from one another compared to the originally designed position and is shown in Figure 2.1.6.
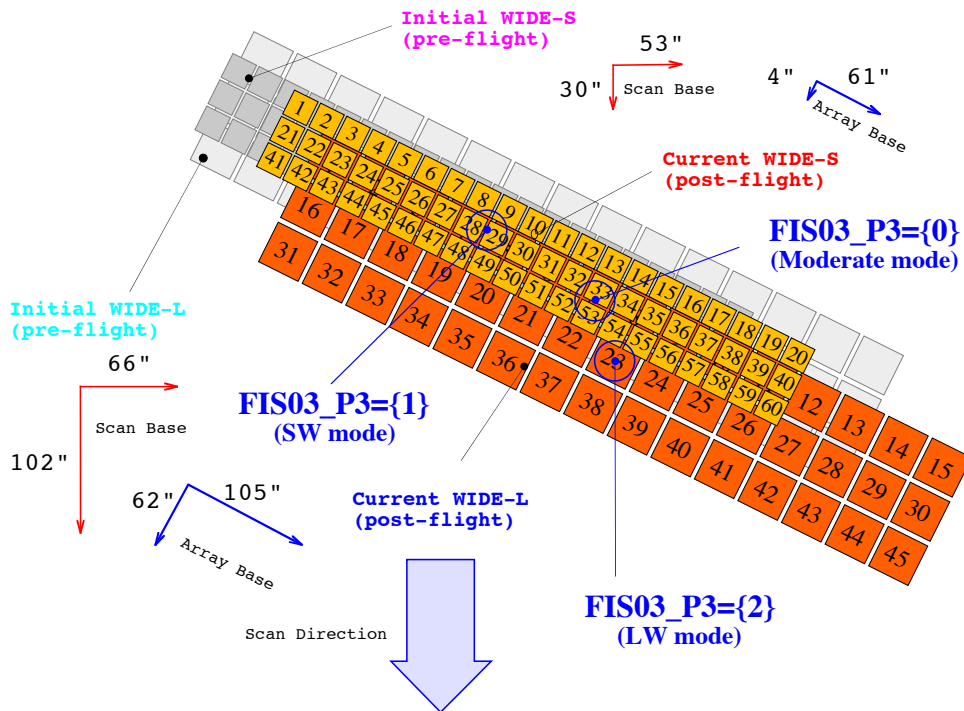
Figure 2.1.6: Actual schematic view of the FOV of the FIS detectors in FTS mode.

2.1.5   Instrument Operation

The data acquisition process of the FIS is programmed into the hardware sequencer. When the instrument begins an observation, a preset specified sequence pattern is repeatedly carried out and the data are edited into telemetry packets and sent to the satellite's main computer (Data Handling Unit: DHU). The data sampling timing is as accurate as the FIS internal clock and is quite stable. The FIS data acquisition is continuous and reset of detector charge and calibration lamps and the shutter are controlled by the FIS on-board software with an accuracy as good as the readouts. They can alternatively be operated by commands if necessary. The status of the shutter and calibration lamps are all recorded for the data processing.

The survey observation sequence and the AOTs (Astronomical Observation Templates) are designed by combining these elemental operation units.

2.2 The FIS Pointed Observations: AOTs

2.2.1 FIS01: Slow-Scan Observations for Photometry / Mapping of Small Area

The **FIS01** AOT is designed for photometry of point sources and/or mapping of small areas up to $\sim 25 \times 10$ arcmin^2.

Table 2.2.3: FIS01 summary.

Fixed parameters	
Observing Mode	Photometry
Band	N60, WIDE-S, WIDE-L, N160
Scan pattern	Two round-trip scans with a cross-scan shift
User specified parameters	
Sampling mode	Nominal* or CDS
Reset interval	0.5 or 1 or 2 sec (for Nominal sampling mode)
Slow-Scan speed	8 or 15 arcsec/sec
Shift length	70 or 240 arcsec

* = Co-add mode

[Instrument Operation]
The instrument is operated in the photometry/imaging mode; all four FIS photometric bands (N60, WIDE-S, WIDE-L, N160) retrieve data. The detector operation parameters are fixed at the recommended values provided by the instrument team. Two readout modes are possible: Nominal and CDS.

[Scan Operation]
An observation consists of two sets of round-trip scans in the in-scan direction with a shift in the cross-scan direction. The round trip scan is mandatory to ensure data redundancy. The cross-scan shift is used to increase the redundancy or to observe a wider area of the sky. The scan speed is either 8 or 15 arcsec/sec. These speeds are selected to maximize the performance (sensitivity) while enabling observations of a certain size area of sky.

[User specified parameters]
The following inputs are given by the observer.

Detector readout mode (Nominal / CDS) CDS mode should only be used for the brightest targets that would normally saturate the detector in Nominal mode. See Section 2.1.3 for the details of the readout methods.

Reset interval This parameter is only relevant for the Nominal readout mode and is chosen based on the brightness of the targets. Generally, a longer reset interval improves sensitivity in the amplifier but at the same time increases the risk of saturation. On the other hand, a shorter reset looses more data points at the resets.
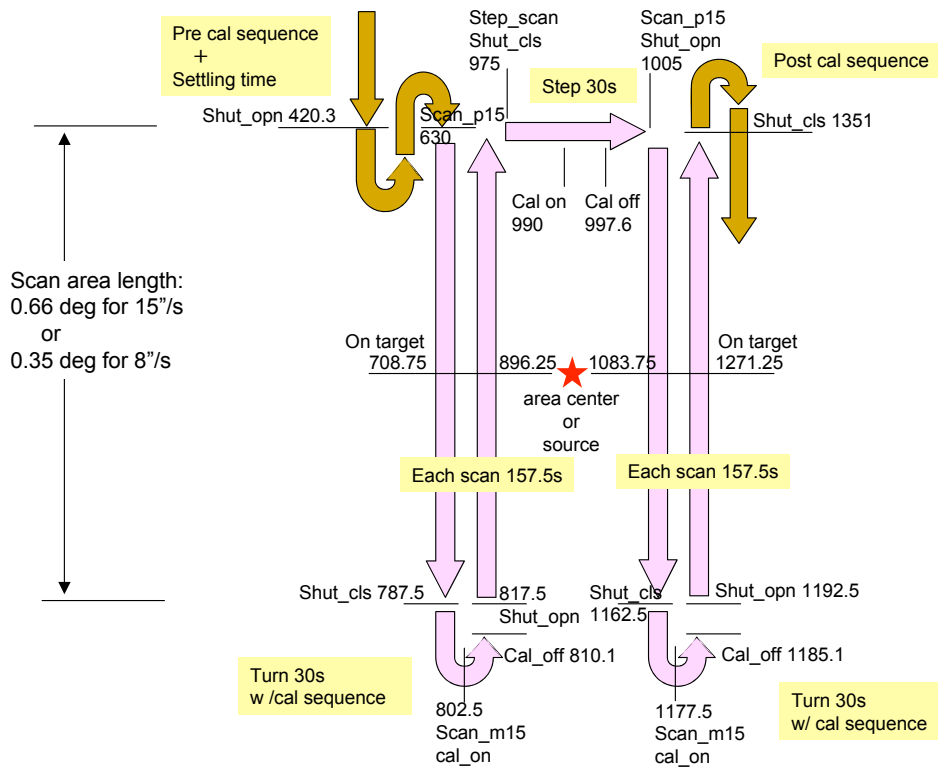
Figure 2.2.7: The scan sequence of the AOT FIS01 (numbers are in seconds).

Scan parameters Two numbers are given to define the scan pattern; A scan-speed and a cross-scan shift length. A scan-speed of 8 arcsec/sec balances depth and sensitivity with scan area for data redundancy and is used for photometry of small numbers of sources. A higher scan speed of 15 arcsec/sec is used to observe larger areas to a slightly shallower sensitivity.

A cross-scan shift length of 70 arcsec is used for point source photometry, and 240 arcsec for small area mapping.

Target position The satellite is operated such that the target position is located at the center of the scanned area.
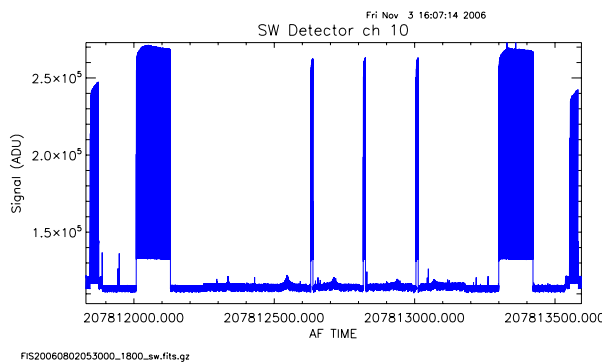
Figure 2.2.8: Example of FIS01 in-flight data from the PV phase. Time series raw signal with pre and post calibration sequences and the three w/cal sequences can be seen.

2.2.2 FIS02: Slow-Scan Observations for Mapping of Large Areas

The **FIS02** AOT is designed for the mapping of relatively large areas. An observation covers a long strip of ~ 1 degree.

Table 2.2.4: FIS02 summary.

Fixed parameters	
Observing Mode	Photometry
Band	N60, WIDE-S, WIDE-L, N160
Slow-Scan speed	15 or 30 arcsec / sec
Scan pattern	One round trip scan
User specified parameters	
Sampling mode	Nominal* or CDS
Reset interval	0.5 or 1.0 or 2.0 sec
Slow-Scan speed	15 or 30 arcsec/sec

* = Co-add mode

[Instrument operation]
The operation of the instrument with this AOT is the same as FIS01, except that FIS02 carries out a single round-trip only, and that the choice of scan speed is 15 or 30 arcsec/sec.

[Scan operation]
The difference of this AOT from FIS01 is that an observation consists of only a single round-trip scan. The scan speed is chosen from 15 or 30 arcsec/sec. The scan length is approximately 1 and 2 deg. depending on the scan speed.

[User specified parameters]
The following inputs are given by the observer.

Detector readout mode (Nominal / CDS) Same as FIS01.

Reset interval Same as FIS01

Target position The satellite is operated such that the target position is located at the center of the scanned area.

Pre cal sequence
+
Settling time

630 Scan_p15

Post cal sequence

Shut_opn 420.3

Shut_cls 1351

Scan area length:
1.44 deg for 15"/s
or
0.77 deg for 8"/s

On target
802.5

On target
1177.5

area center
or
source

Each scan 345s

Shut_cls 975

1005 Shut_opn

Turn 30s
w /cal
sequence

997.6 Cal_off

990 Scan_m15, Cal_on

Figure 2.2.9: The scan sequence of the AOT FIS02.

2.2.3   Performance of FIS01 & FIS02

Photometry (imaging) observations by the FIS in pointed observation mode is always carried out with the Slow-Scan operation. At the moment the performance of Slow-Scan mode has not been systematically evaluated, because of various technical problem on the calibration and data reduction. Therefore, the performance given in this section are estimated by scaling the All-Sky Survey detection limits by factors which are functions of the scan speed and the reset interval. However, because of the nonlinear responsivity, transient effects, and other complicated characteristics of the instruments, the scaling law is not always straightforward. Table 2.2.5 lists the sensitivities for the three scan speeds incorporated into these 2 FIS AOTs, Note that confusion is not included in these estimates.

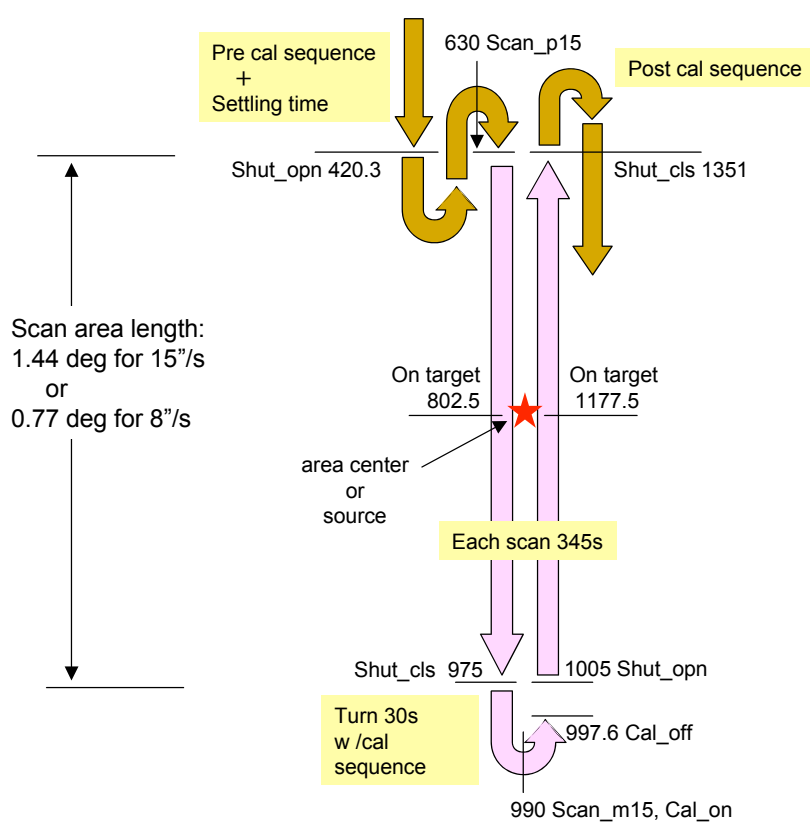The numbers in the table are 5σ noise levels for a single scan. In principle, the sensitivity should increase as the inverse square root of the number of scans such that four scans in FIS01 should improve the detection limit by factor of 2. On the other hand, this redundancy can alternatively be used to increase the reliability of the results. In such a case, the detection limit remain unchanged. We leave this at the discretion of the user. As the "standard" rule of thumb, we propose to apply the numbers per one round-trip scan. So for FIS01, which carries out two round trips, a sensitivity of $1/\sqrt{2}$ of the value in the table can be assumed.

Following the resent results of careful analysis of the FIS in-orbit performance the sensitivity of the FIS has been further updated from the previous IDUM. In summary, the SW bands (N60, WIDE-S) detection limits are worse than the pre-launch predicteions (i.e. as documented in the Observer's manual) by factor of 2–3. For the LW bands (N160, WIDE-L), various factors have brought the sensitivity to a level a factor of four (0.5 sec integration) to eight (2 sec integration) worse with respect to the pre-launch values published in the Observers Manual.

It should be mentioned that these numbers are not the results of source extraction and number counting. Further technical charanges are needed to draw the maximum performance of the FIS instrument.

Table 2.2.5: The 5σ detection limits for the FIS AOTs FIS01 & FIS02 (See Tables 2.2.3, 2.2.4 for relevant scan speeds for the two AOTs). Numbers are per scan, see text for details.

Point Source (mJy)											
Scan speed	8 arcsec/sec				15 arcsec/sec				30 arcsec/sec			
Reset	0.5 s	1.0 s	2.0 s	CDS	0.5 s	1.0 s	2.0 s	CDS	0.5 s	1.0 s	2.0 s	CDS
N60	260	180	130	3800	400	280	200	6100	630	420	420	9800
WIDE-S	52	39	26	890	84	60	42	1400	130	92	92	2200
WIDE-L	130	95	67	1600	200	140	100	2400	390	270	230	4400
N160	670	470	330	7560	1000	710	500	11000	1900	1400	1100	21000
Diffuse Source (MJy/sr)											
Scan speed	8 arcsec/sec				15 arcsec/sec				30 arcsec/sec			
Reset	0.5 s	1.0 s	2.0 s	CDS	0.5 s	1.0 s	2.0 s	CDS	0.5 s	1.0 s	2.0 s	CDS
N60	5.6	4.5	2.8	97	8.4	5.6	4.3	120	11	8.4	8.4	170
WIDE-S	1.2	1.0	0.6	22	1.8	1.2	0.9	28	3.0	1.8	1.8	42
WIDE-L	1.0	0.7	0.5	8.5	1.3	0.9	0.7	12	2.0	1.3	1.1	24
N160	5.0	3.5	2.3	41	6.7	4.8	3.3	57	9.7	6.8	5.5	110

The performance of the FIS detectors is influenced by cosmic ray hits. The induced glitches in the detector signal (at a frequency of about of approximately one per minute) contributes to the final noise figure. After such hits, the noise increases by a factor of a few for around ten seconds. This degrades the S/N ratio worse than the values listed in Table 2.2.5. Therefore,

we recommend for observers to repeat scans several times in order to obtain good sensitivity close to the limits in Table 2.2.5 . The performance of the LW bands (Stressed Ge:Ga detector array) is particularly worse than pre-launch prediction. This is attributed to two factors. Before launch, we expected that the responsivity should increase at least by a factor of two in space, (as observed in the case of IRAS, ISO, IRTS, and Spitzer). However, after launch, the bias voltage had to be reduced in order to avoid unstable behavior. As the result of this, the responsivity is, now, nearly equal to that on the ground and the detection limit has correspondingly been degraded compared to the pre-launch expectations. In addition to this, it was assumed, before launch, that the noise of the LW channels would depend on the integration time as the power of t^{-1}, that is, $S/N \sim t^{-1}$ based on the ground test results. However, after launch, the observed noise of LW arrays instead was found to follow a dependence of on the time as $t^{-1/2}$, that is, $S/N \sim t^{-1/2}$. As the result of these two factors, the LW sensitivities are degraded by a factor of 8 (= 2 x 4) in 2-second integration, and by a factor of 4 (= 2 x 2) in the 0.5-second integration case.

2.2.4   Saturation Limits for FIS01 & FIS02

The saturation limits are functions of the reset interval only. These limits are defined such that the integration ramps of the high sensitivity pixels reach a level where the reproductivity of the ramp shape becomes bad. Beyond this level we still obtain data from the lower-sensitivity pixels but photometric accuracy and quality of reconstructed image map may be significantly degraded. The in-flight measurements of the saturation limits are yet to be assessed although may be similar to those quoted in the Observer Manual. Table 2.2.6 gives the (Observers Manual) saturation levels for these FIS AOTs.

Table 2.2.6: The saturation limits for FIS01 and FIS02 AOTs. Note that at present these saturation numbers have not been confirmed in the flight configuration

Point Source (Jy)				
Reset (sec)	0.5	1.0	2.0	CDS
N60	280	140	70	3600
WIDE-S	60	30	15	700
WIDE-L	120	50	15	1500
N160	300	130	60	3500
Diffuse Source (GJy/sr)				
Reset (sec)	0.5	1.0	2.0	CDS
N60	4.0	2.0	1.0	50
WIDE-S	0.8	0.4	0.2	10
WIDE-L	1.0	0.42	0.12	13
N160	2.5	1.10	0.5	30

2.2.5 FIS03: FTS Spectroscopy

The **FIS03** AOT is designed for spectroscopic observations with the FTS.

Table 2.2.7: FIS03 summary.

Fixed parameters	
Observing Mode	Spectroscopy
Band	WIDE-S, WIDE-L
Scan pattern	Staring (no Step-Scan)
User specified parameters	
Sampling mode	Nominal (fixed)
Reset interval	0.1, 0.25, 0.5, or 1.0 sec (see text)
Resolution	Full-resolution / SED
Target position	0, 1, 2 (see text)

[**Instrument operation**]
The instruments are set up for the FTS mode. The filter wheel is rotated to switch from the empty hole to the polarizer. Detector readout mode is switched to high-frequency sampling mode. Only data from the WIDE detector arrays are acquired. During the observation, the moving mirror is driven. Two path lengths, i.e., spectral resolutions, are available (See Section 2.1.4). The spectral resolution is ~ 0.36 cm^{-1} for the *Full resolution* mode and ~ 2.4 cm^{-1} for the *SED* mode. The SED mode provides better quality spectra than the Full-resolution mode spectra after being smoothed to a corresponding resolution. There are four choices for the reset interval, similar to the other FIS AOT's. However, CDS readout mode is not available.

[**Scan operation**]
The FTS spectroscopic observation is operated in a staring pointing mode. To minimize the dead time, No Step-Scan, Micro-Scan, nor Slow-Scan is carried out during a pointed observation.

[**User specified parameters**]
The following inputs are given by the observer. Target position is a new parameter added after launch.

Resolution mode Full-resolution or SED. See the description above.

Reset interval Four choices from 0.1[3], 0.25, 0.5, and 1.0 sec are available. As the CDS mode for the brightest targets cannot be used for the FIS03 AOT, a shorter reset interval of 0.1 sec is alternatively provided. This shortest reset interval is available thanks to the 5–7 times faster detector sampling rate in this operation mode.

Target position (New) Due to the misalignment of the detectors (see Section 2.1.3 and Figure 2.1.6) three different positions are defined:

  Position 0: Target at the overlapping region of the two detectors (pixel 7 for WIDE-L and pixel 33 for WIDE-S)

---

[3]The actual reset interval is 0.14 sec.

Position 1: Target is located on the 2nd column of the WIDE-S detector array near pixel 28,29.

Position 2: Target is at the center of the WIDE-L array (pixel LW 23).

2.2.6   Performance of FIS03

The flight sensitivity of the FIS03 (FTS) mode is known to be worse than the pre-flight values given in the Observers' Manual. Although a quantitative evaluation of the flight-performance is given below, users of FIS03 are still urged to contact the FTS team in Japan via Helpdesk.

The flight sensitivity of the FIS03 (FTS) mode has been estimated from the signal-to-noise ratio of bright sources for a portion of the observation modes and specific pixels. Noise is defined as the dispersion between different scans in one pointed observation.

The sensitivity for the continuum emission is estimated from Neptune observed with the AOT position parameter 0, i.e. it is derived only for the SW33 and LW07 pixels. The 5σ detection limit is roughly 20Jy for 65–85 cm^{-1} (LW07), and 50Jy and 100Jy for 90–120 cm^{-1} and > 120 cm^{-1}, respectively (SW33).

The sensitivity for the line emission is estimated from diffuse bright regions towards the Galactic center. For [C II] 158 μm and [O III] 88 μm in LW30 and SW15, respectively, the 5σ detection limit is estimated to be 7.3×10^{-8} and 8.0×10^{-7} W m^2 sr^{-1}, respectively. Considering the relative sensitivity among different pixels (Fig. 3.5.20) and the estimate that the PSF in spectroscopic mode is larger by $\sim 20\%$ than that in photometry mode (section 3.1), these correspond to 5σ detection limits of 3×10^{-15} W m^{-2} and 5×10^{-14} W m^{-2} for [C II] 158 μm and [O III] 88 μm, respectively, with the AOT position parameter 0.

If the reset anomaly is not correctly interpolated, it produces artificial features at the corresponding wavenumber. Table 2.2.8 lists the possible wave numbers which are affected by these artificial features.

Table 2.2.8: The list of the possible wave numbers affected by artificial features caused by reset anomaly.

Reset interval [sec]	Wave number affected by the reset structure [cm^{-1}]
	SED mode
0.1	96.9, 193.8
0.25	(48.4), 96.9, 145.4, 193.8
0.5	(24.2, 48.4,) 72.7, 96.9, 121.1, 145.4, 169.6, 193.8
1.0	(12.1, 24.2, 36.3, 48.4,) 60.6, 72.7, 84.8, 96.9, 109.0, 121.1, 133.2, 145.4, 157.5, 169.9, 181.7, 193.8
	Full-Resolution mode
0.1	93.1, 186.2
0.25	46.5, 93.1, 139.6, 186.2
0.5	(23.3, 46.5,) 69.8, 93.1, 116.4, 139.6, 162.9, 186.2
1.0	(11.6, 23.3, 34.9, 46.5,) 58.2, 69.8, 81.5, 93.1, 104.7, 116.4, 128.0, 139.6, 151.3, 162.9, 174.6, 186.2

Chapter 3

Instrumental characteristics

In this chapter the different effects (due to the properties of the detector, instrumental effects caused by the electronics and optics and other external influences) to be corrected during the processing of the FIS observations are described.

3.1 Imaging Quality

3.1.1 Point Spread Function (PSF)

It was impossible for the AKARI team to carry out a ground based end-to-end performance test for the telescope and instruments in the cryogenic environment. After the launch, the telescope focus was adjusted using the IRC data. During the PV phase and the calibration time in Phase 1 & 2 various measurements of the PSF were carried out. As expected, the actual image from the FIS observations is influenced by many complicated instrumental characteristics. Investigation of the most reliable PSF information is still ongoing. Only preliminary data is shown at the moment.

Figure 3.1.1 and Figure 3.1.2 compare the measured PSF with a Gaussian and theoretical PSF model (Airy function of the telescope + FIS instrument optics). The central part (± 2 arcmin for SW, ± 3 arcmin for LW) of the observed PSFs can be well fitted by a Gaussian function of FWHM=37 ± 1, 39 ± 1, 58 ± 3, & 61 ± 4 arcsec for N60, WIDE-S, WIDE-L, and N160 respectively. The measured PSFs are based on the observations of asteroids. Theoretically, the PSF of broad band imaging observations depends on the colour of the target. However, we have not detected any significant difference between the PSF measured from the observations of asteroids and luminous infrared galaxies. The evaluation is continuing.
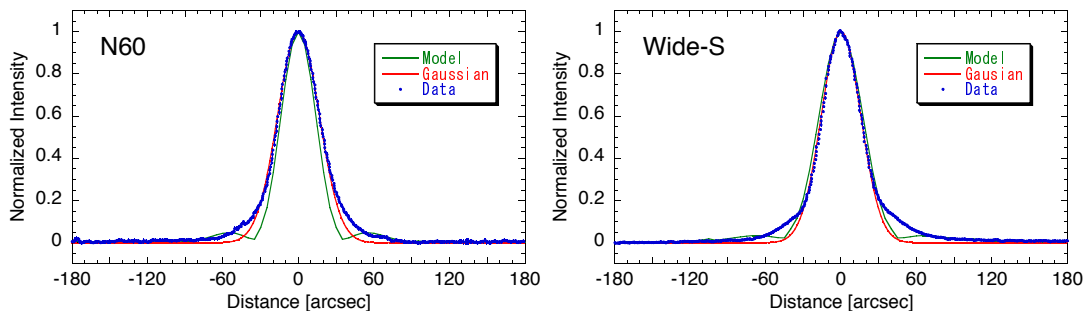

Figure 3.1.1: Comparison of the measured and modeled PSF for the SW detector.
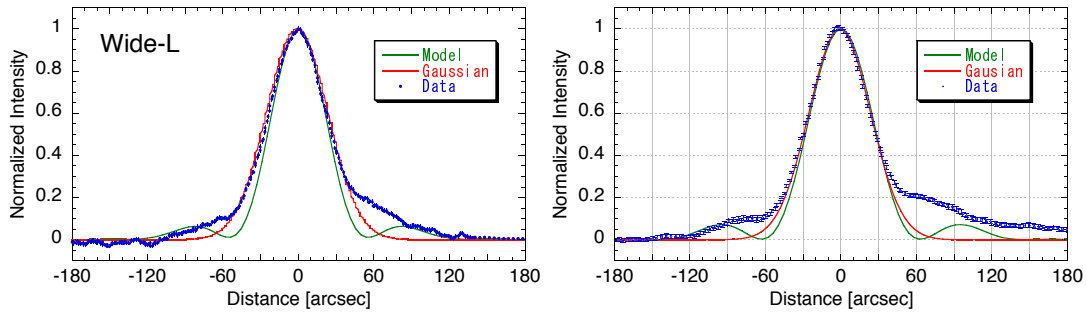
Figure 3.1.2: Comparison of the measured and modeled PSF for the LW detectors

There are large deviation in the 'skirt' part of the measured PSF from the model. The reason for this deviation has not yet been well understood.

3.1.2   Cross-talk and ghosts

Cross-talk between the detector pixels will broaden the effective FWHM of a point source image. Moreover, it will increase the effective number of glitches, and complicate the transient response. This effect is more serious in the SW detector, since it is a monolithic structure.
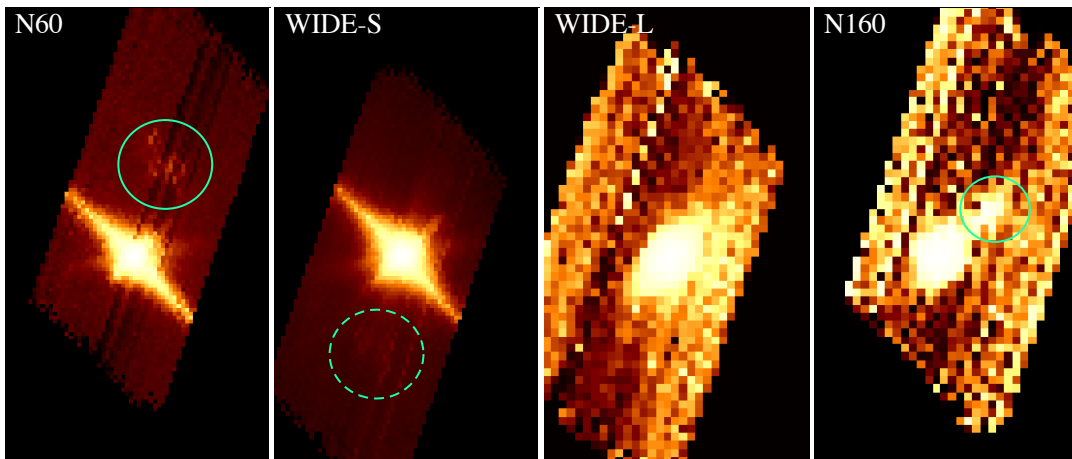
Figure 3.1.3: Cross-talk and ghost effects as seen in a FIS01 observation of a bright point source. See text for details.

A FIS01 observation of a bright point source is shown in Figure 3.1.3 (the colour scale is adjusted to emphasise the faint features). Points to note are:

- The target on the SW images does not look like a point source but shows long extensions along the detector array dimensions. It is more significant in the direction of 20 pixels (cross-scan). These extensions are considered to be due to cross-talk between the pixels. Both optical cross-talk and electrical cross-talk possibly contribute to this. The phenomenon has not yet been completely understood. therefore, at present, users should administer special care when they discuss the detailed morphology of targets.

- We also see spider-like features around the target that are probably due to the telescope optics.

- We observe ghost images in all detectors. The ghost image on the N60 detector appears when the target object is passing through the WIDE-S detector. The same relation holds for ghosts on WIDE-S, as well as the WIDE-L, N160 pair (though it is not clearly recognized in the WIDE-L band in Figure 3.1.3). The cause of these ghost images is not yet clear. The strength of the ghost image is less than 1% (probably $\sim 0.3\%$ of the target in the same image for the SW, and around 10% in the LW detectors). Users should take special care when looking at images of bright targets.

Figure 3.1.4 and 3.1.5 show time profiles of the detector signals from wide and narrow band detectors. These plots clearly demonstrate that the ghost signal appears in one detector when the other detector observes a bright object.
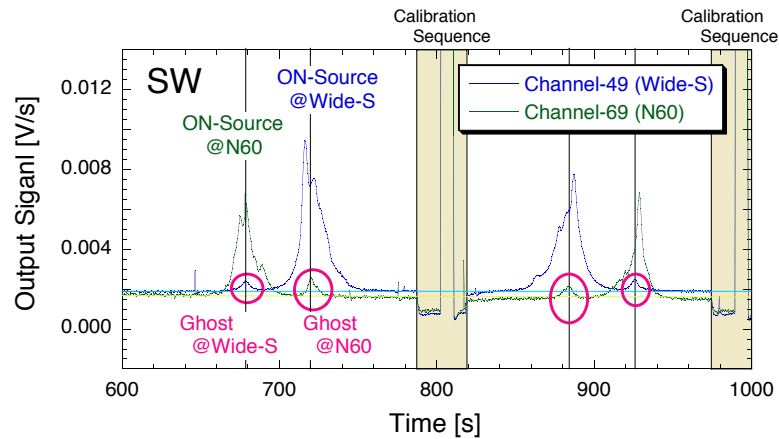
Figure 3.1.4: Time profile of signals from two SW detector pixels during one round trip scan of a Slow-Scan observation of a very bright source. The target passes from N60 to WIDE-S, then back again after the calibration sequence in the middle of the operation. A ghost signal is observed when the other detector was looking at the target.
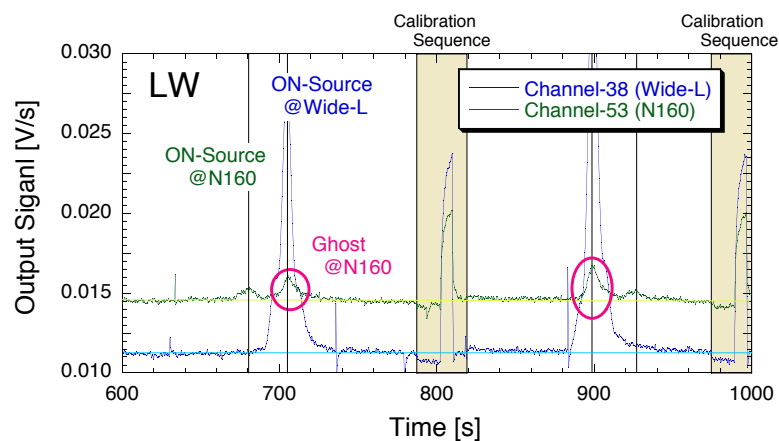
Figure 3.1.5: Same as Figure 3.1.4 but for the LW detectors. Only the ghost in the N160 is shown. Ghosts in the WIDE-L band appear in different detector pairs and are not shown in this plot.

The relative displacement of the ghost from the source object are approximately evaluated

and summarized in Table 3.1.1. The direction of the ghost is most easily understood when the NARROW and WIDE images are aligned in time domain such that the edges in the in-scan direction of the two images are overlaid to each other. The ghost appears where the source is observed in the other bands. See Figure 3.1.3.

Table 3.1.1: Relative displacement of the ghost from the source object. The uncertainty of the values is about 0.2 arcmin.

Detector	SW	LW
In-scan (arcmin)	5.4	3.6
Cross-scan (arcmin)	0.2	2.0
Distance (arcmin)	5.4	4.1

3.1.3   Leakage

A combination of two blocking filters at the entrance aperture are expected to reduce the short wavelength light leakage to factors of 10^{-5} at 10 μm and 10^{-9} at 0.5 μm optimally. However, no end-to-end measurement has been made and the leakage could be as worse as 10^{-5}–10^{-6} at 0.5 μm. Note that we have not detected any signature of blue light leakage from the blocking filter so far.

3.1.4   Distortion

Figure 3.1.6 shows the detector shape projected onto the sky. Due to the fact that the FIS aperture entrance is about 20 arcmin away from the center of the focal plane (boresight), and that the FIS optics are an off-axis design, significant distortion of the detector shape is observed (red lines). The shape without optical distortion is also plotted for comparison (blue). This distortion data is provided as part of the data reduction pipeline package. The distortion will be further evaluated with the in-flight data and the information will be correspondingly updated in the future.
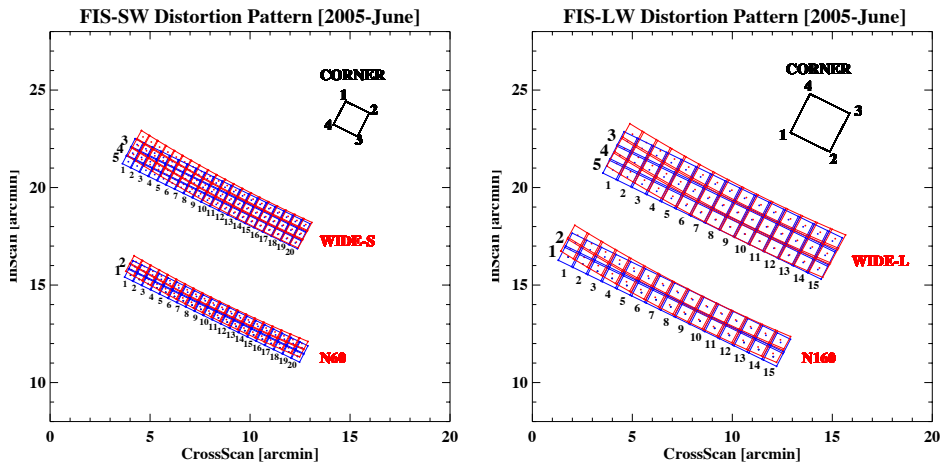

Figure 3.1.6: The FIS detectors projected onto the sky, with (red) and without (blue) optical distortion.

3.1.5 Polarization

The dichroic beam splitter used in the FIS is known to have polarization. In Figure 3.1.7 the transmittance and reflectivity of the filter is given. The reflection was measured at two different angles perpendicular to each other. A difference in performance at a few specific wavelengths at approximately 160 and 180 cm^{-1} (corresponding to 63 and 55 μm, respectively) was observed. Unfortunately the angle of the filter in the flight module instruments is not accurately known, and this difference will result in an uncertainty in the measurement of the polarized light.

Optical performance of Dichroic Filiter (non-FM)
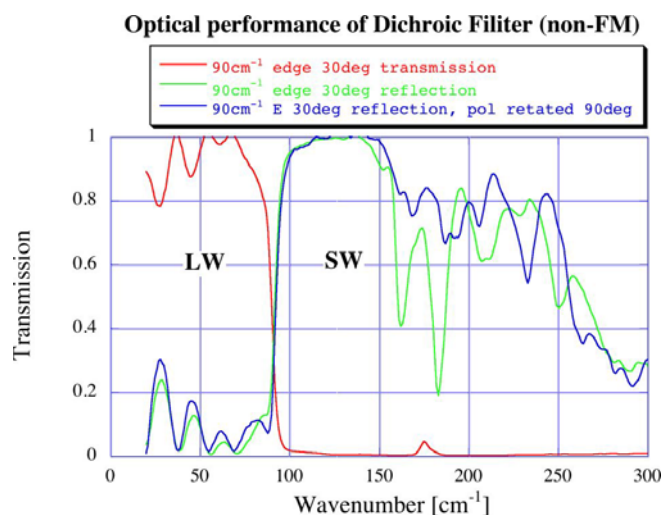
Figure 3.1.7: The reflectivity and transmittance of the dichroic beam splitter. The blue and green curves are the reflectivity in the SW channel side. The two curves deviate around 160 and 180 cm^{-1}.

3.1.6 Stray Light

It is found that the light from the Earth can enter the cryostat under certain configurations of the current orbit. Ideally, such light should be reflected back outside the telescope into space, however, a small amount of scattered light may in fact enter the telescope and be detected in the IRC and FIS instruments.

The stray light is most strongly observed over about 100 days with a maximum at the Summer solstice, when the telescope is observing the northern sky. The effect was most significant during observations of the NEP region in Phase 1. Most of the Mission programmes and Open Time proposals were carried out after September, when the stray light should be much smaller.

The intensity of the stray light seems to be 20–100% of the dark sky. Also, it is larger at the beginning and end of a pointed observation.

Two methods are suggested to remove stray light effects in the standard Slow-Scan data reduction tool (Section 4.2.5). For point source observations, median filtering methods can remove all large scale radiation components.
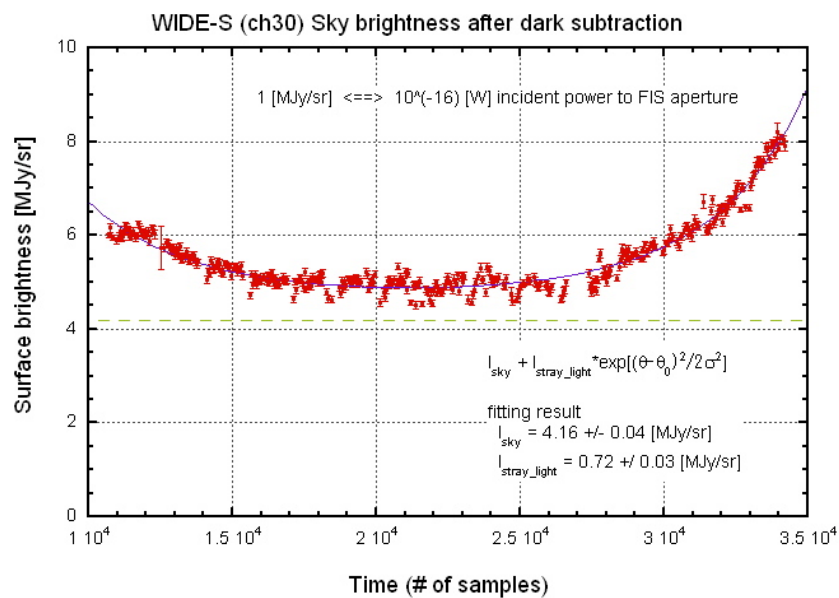
Figure 3.1.8: Time profile of a WIDE-S detector signal during a Slow-Scan observation over about 15 minutes. the stray light component is seen as a global variation of the background level. Brightness scale is based on an old calibration and may not be accurate.

3.2 Detector and instrument responsivity

3.2.1 Dead pixels

The SW- and LW-arrays are known to have 4 and 7 dead pixels, respectively. In addition one SW pixel has a large noise level and an unstable signal output. Figure 3.2.9 shows the positions of the dead and more badly performing pixels. In addition, one SW pixel (98) is very noisy and one LW pixel (42) shows strong non-linearity in the integration ramps. They are masked by the data reduction toolkit and not used in the data reduction.
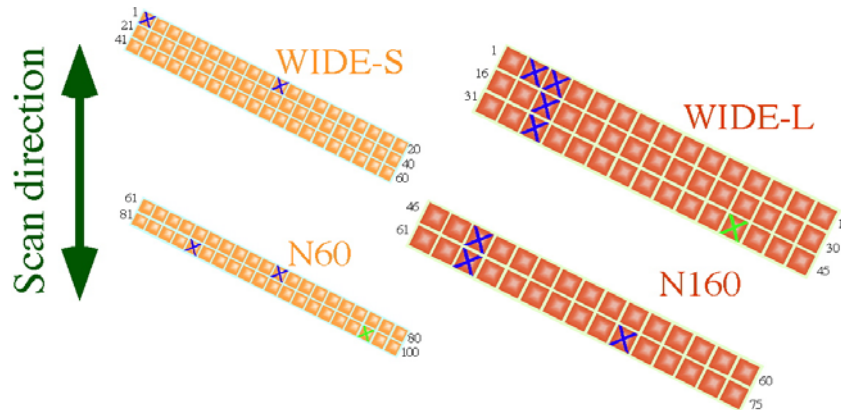
Figure 3.2.9: The positions of dead (blue cross) and badly performing (green cross) pixels in the FIS detector arrays. Definitions of the pixel numbering indices are also presented.

3.2.2 Responsivity and Uniformity

Figure 3.2.10 shows the in-flight and pre-flight responsivities of all the SW detector pixels. The values are calculated for a $\nu I\nu = $ constant spectrum at the central wavelength defined in Table 2.1.1. The same information is shown for the LW detectors in Figure 3.2.11.
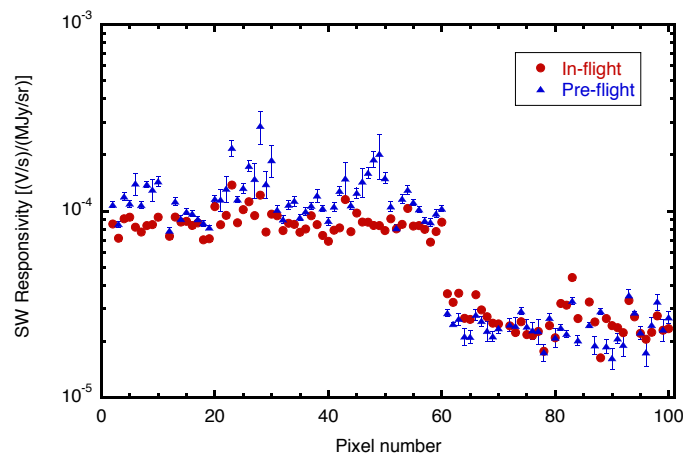
Figure 3.2.10: In-flight and pre-flight responsivities of all pixels in the SW detector arrays. See figure 3.2.9 for the definition of the pixel number.
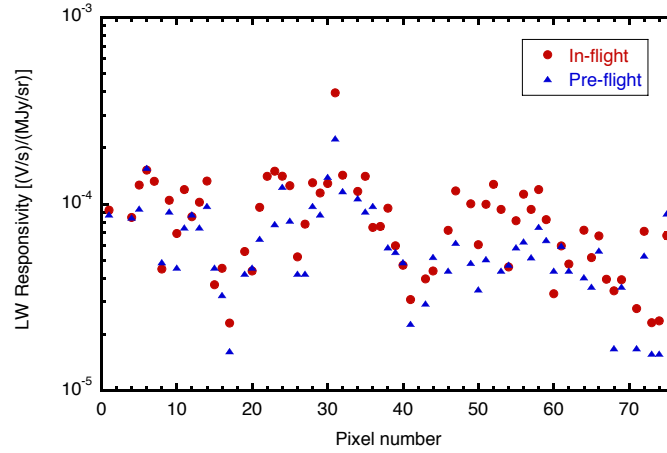
Figure 3.2.11: In-flight and pre-flight responsivities of all pixels in the LW detector arrays. See figure 3.2.9 for the definition of the pixel number.

3.2.3 Excess Noise

After the results of the early FM performance tests, the FIS introduced two noise filters, the first in the cryogenic part near the detector and the other outside the cryostat. These filters successfully reduced the noise significantly.

The typical frequency of the excess noise is close to the data sampling rate. Therefore, the noise component especially affects the All-Sky Survey observations which uses every data sampling. A software module to reduce this noise component has been implemented into the survey data reduction pipeline and is working successfully. On the other hand, the Slow-Scan data reduction toolkit calculates the slope of every integration ramp to derive the sky signal and is relatively robust to the high-frequency noise.
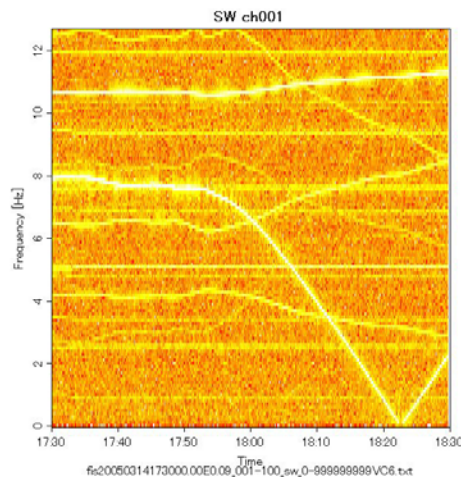
Figure 3.2.12: Noise spectral profile of a SW detector pixel. Time variation of the noise spectra taken during the laboratory test under dark conditions. White stripes are excess noise components. We observe a number of components at specific frequencies. Some of them move with time.

3.2.4   Ramp curve

Ideally the output signal of the FIS detector should be proportional to the number of incoming photons, but this is not the case in reality. The actual ramp curves show deviations from the optimal linear line even when the data is taken under constant incoming radiation. The SW detector shows this effect more prominently (Figure 3.2.13). As the slope of the ramp curve gives the instantaneous flux, any deviation from linearity means that the responsivity changes along a ramp. Currently, the SW ramp curve becomes flatter as an integration progresses. The non-linearity of the LW detector is 5–10%.

If the shape of the ramp curve is reproducible, and if the curve is monotonic with incoming flux, it will be possible to correct this effect.

Analysis of the flight data has shown that the ramp shape is relatively stable over a period of several months. The ramp curve correction module works effectively, except in the case of a few pixels that require further investigation. in addition, the ramp curve correction for observations in extremely dark or bright sky conditions can be further improved.
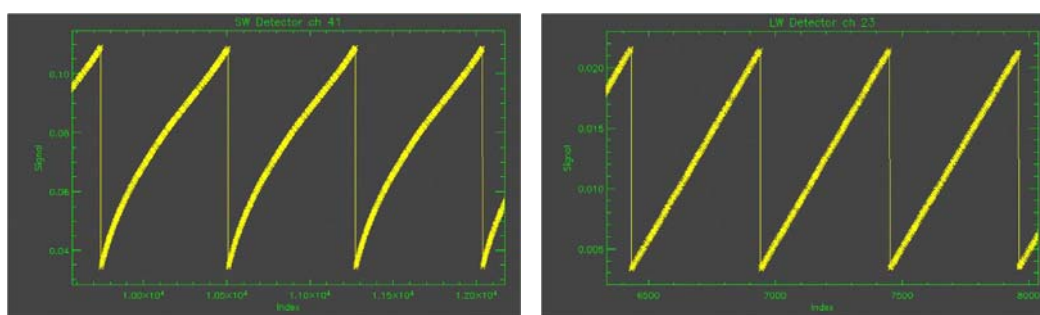
Figure 3.2.13: Comparison of integration ramps under constant irradiation levels. The LW detector (right) shows an almost linear response while the SW signal (left) deviates from linearity as the integration progresses.

### 3.2.5   Saturation After Effect

It is found that the saturation of the detector is followed by a decrease in the signal level (Figure 3.2.14). This effect is more obvious in the LW channel. The effect appears more significantly when the saturation is heavier. It seems that the effect is already present when the integrated signal has reached about half of the full saturation level. The recovery time scale is of the order of a minute. This effect is still under quantitative analysis and is not yet implemented in the data reduction software.

3.2.6   Transient response

It is known that the Ge:Ga type detectors show a strong transient response; the detector output signal does not respond instantaneously to a change of incoming flux but rather has a delay of a few – hundreds seconds time scale.

Figure 3.2.15 demonstrates how the transient response of the FIS detectors changes with a step change of incoming flux. In order to simulate the real flight conditions, a calibration lamp is turned on weakly to provide a background level for the SW detector, and a *Bias Light* (Section 2.1.3) is used for the LW array. In both these cases, the time constants are 10–30 sec.

Since AKARI/FIS almost always observes the sky in scanning mode, an understanding of the effect of the transient response to the observed data is essential. The most extreme case is
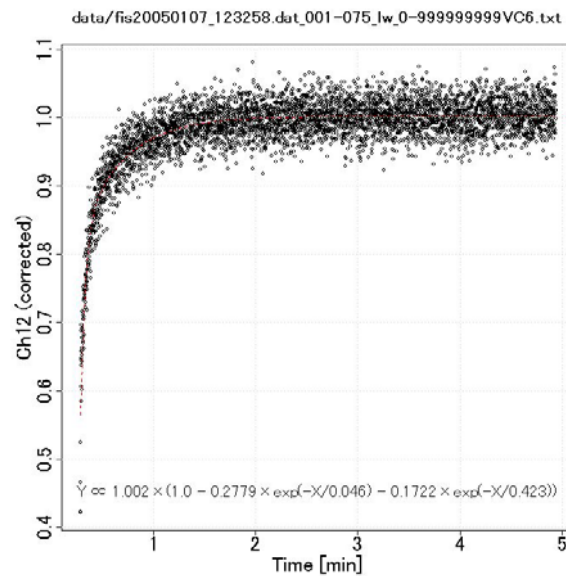
Figure 3.2.14: An example of Saturation after effect for a LW detector pixel. The differential signal for a constant irradiation is plotted against time after the saturation. In this figure an attempt is made to fit the data by a two component exponential function. More detailed analysis is ongoing.

the All-Sky Survey, in which a point source is scanned in only 0.2–0.4 sec, much smaller than the transient time constant, resulting in a lower output signal than expected by a factor of a few (Figure 3.2.16). This also affects the detection limits. The effect is less severe for the Slow-Scan mode for the pointed observations.

Ideally, the transient response should be understood and reproduced by modeling the charge transfer in the detector element. However, strong non-linear physics prevent us from making a perfect model. The analysis is continuing. For the All-Sky Survey data, the point source flux is planned to be corrected empirically by tables comparing the signals for the instantaneous and continuous flux levels.
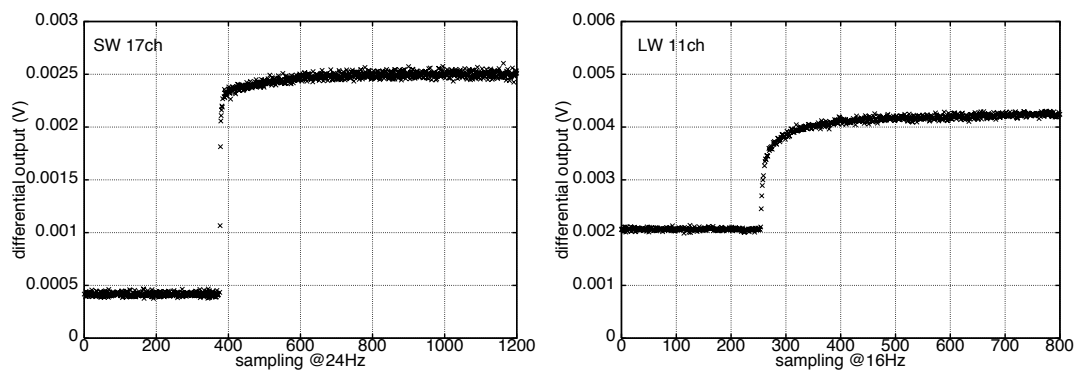
Figure 3.2.15: Examples of transient response for the FIS detectors for a step-wise change of the incident flux.
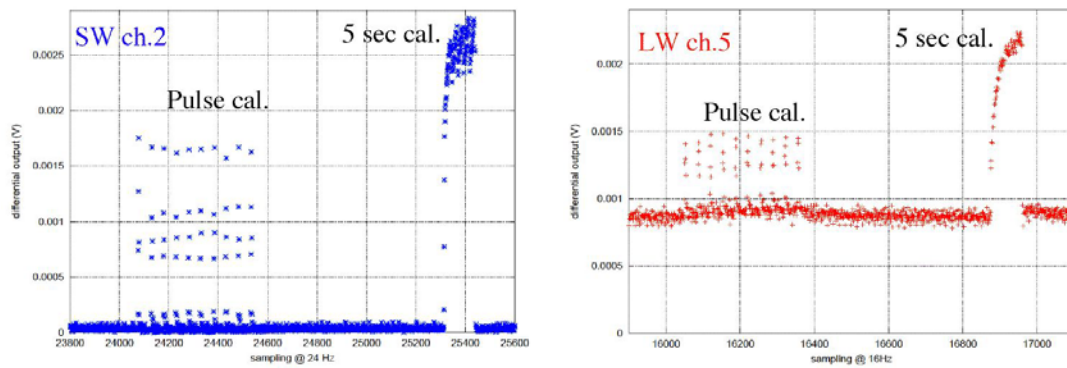
Figure 3.2.16: Transient response to pulse irradiation. On the left side of the each figure the calibration lamps are flashed at very short periods simulating the passage of a point source in the All-Sky Survey. While on the right, the lamps are turned on continuously for 5 sec. The intensity of the calibration lamps was the same for both cases. Although 5 sec is not enough time for the detectors to reach a constant output level, it is obvious that the output signal for flashes is smaller than that of the 5 sec case. This ratio will be used for the flux calibration of point sources.

3.2.7 Spectral Responsivity

The relative spectral responsivity of the FIS system is presented in Figure 3.2.17. The responses are normalized at their central wavelengths. The filter transmittance as well as the efficiency of the optical elements, and the detector spectral responsivity are taken into account. The filters and optics were measured in the end-to-end system configuration at room temperature. The narrow band filters for N60 and N160 were measured individually at the cryogenic temperature, since it was known that these filters showed a temperature dependent variation.
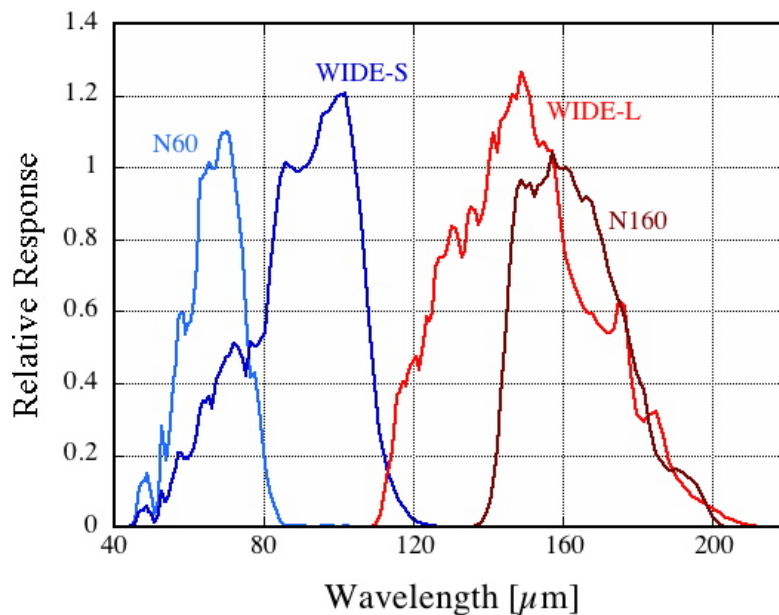
Figure 3.2.17: The spectral response curves of the four FIS photometric bands normalized at the central wavelength of each band. These profiles should be regarded as 'typical' for the bands.

The detector spectral responsivity was evaluated using the FTS of the FIS itself, with a blackbody source at different temperatures. Each pixel of the detector shows a different spectral response. This difference is larger in the LW detector, which is stressed Ge:Ga type. The difference arises from the non-uniform effective stress on the detector tips. The stronger the stress (pressure) on the detector element, the longer the wavelength limit can be extended. It is observed that the cut-off wavelength (the longest wavelength at which the detector is sensitive) varies from one pixel to another, probably because of inhomogeneous stress among the pixels. Figure 3.2.18 demonstrates the pixel by pixel variation of the spectral responsivity of the LW channel. It is seen that the cut-off wavelength ranges from 165–185 μm. The N160 band extends longer than the WIDE-L band as the detectors are under even higher pressure.

The plots in Figure 3.2.17 are regarded as the 'typical' profiles. Revision of the overall RSRF with the in-flight data has not yet been completed.
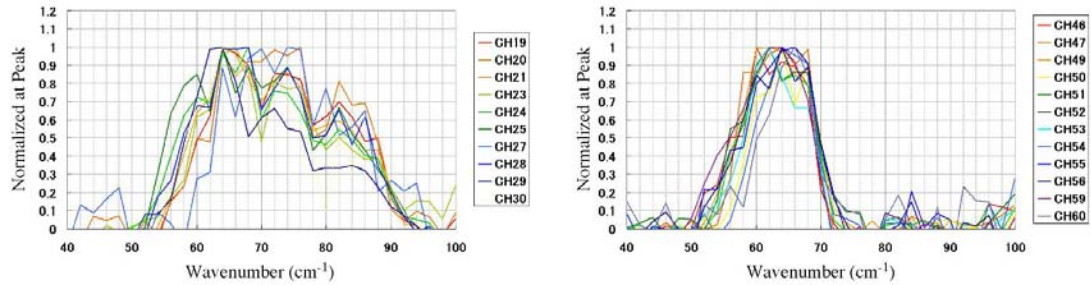
Figure 3.2.18: Pixel by pixel variation of the spectral response of the LW detector.

The difference in wavelength profile directly influences the photometric accuracy, especially for cool targets such as molecular clouds. The error in photometry is less than a few per cent for sources warmer than 100 K, but is more than 10% for a target of 30 K.

3.3   Charged Particle Hits (Glitches)

The preliminary in-orbit measured average glitch rate on the FIS detectors is ~ 1 / pixel / min for both the SW and LW arrays. There are also observed after effects of the glitches. The LW detectors show the strongest effects, with after effects of time scales of $\sim$1 sec. At present, such data are recommended to be discarded in the data reduction process.

   Observations carried out immediately after SAA passage have also been carefully checked but seem to show little difference in quality compared to the data taken in more quiet regions. Some observations that were carried out while the spacecraft passes through the polar-cap region, where many electrons hit the detectors show significant enhancement of glitches, although the effect differs from observation to observation and carefully inspection of the data may be required in these circumstances.

3.4   Diffuse and Point Source Confusion

For a realistic evaluation of the FIS sensitivity, external sources of noise in addition to the intrinsic Instrumental noise have to be considered. The sky confusion noise is observational dependent and can arise from both the superposition of sources in crowded fields and from extended structures which vary in surface brightness on scales of the telescope and instrument resolution. For the FIS instrument, the major components are the sky confusion due to the dust emission from irregular interstellar clouds at high galactic latitudes known as the "infrared galactic cirrus" and the confusion due to the fluctuation of the extragalactic background built up by the superposition of individual faint sources below the resolution of the telescope beam.

   Confusion can cause centroid position shifts and flux uncertainties leading to positional errors and spurious sources, therefore careful consideration must be given to the treatment of confusion noise and the confusion limit, as in reality, the confusion noise is a convolution of the observational phenomenon and the observing instrument.

   At present there are no in-flight measurements for the confusion noise for AKARI observations, therefore users are directed to the pre-launch estimates of confusion for the mission.

3.4.1   Confusion Due to Diffuse Background Emission

The galactic cirrus is a function of galactic latitude and is serious for wavelengths longer than 60 μm. The formalisation of Helou & Beichman (1990) can be used to provide an estimate of the confusion noise (σ/mJy) due to infrared Cirrus as a function of Cirrus brightness $< B_\lambda >$ for the AKARI telescope;

$$\frac{\sigma(\lambda)}{1\mathrm{mJy}} = 0.732(\frac{\lambda}{100\mu\mathrm{m}})^{2.5}(\frac{D}{0.7\mathrm{m}})^{-2.5}(\frac{< B_\lambda >}{1\mathrm{MJysr}^{-1}})^{1.5}, \qquad (3.4.1)$$

   Table 3.4.2 shows the estimated confusion limit over a range of average Cirrus brightnesses, $< B_\lambda >$.

3.4.2   Confusion Due to Point sources

The point source (galaxy) confusion limit is defined as the threshold of the fluctuations in the background sky brightness below which sources cannot be discretely detected in the telescope beam $\sim \lambda/D$. Point source confusion will affect AKARI observations in the faint flux regime and in crowded fields.

   As a benchmark for observations, a useful, practical benchmark for the confusion limit is adopted by assuming a limiting the number sources per beam before the beam becomes confused

Table 3.4.2: Estimated confusion limits due to galactic cirrus in AKARI FIS bands assuming the model of Helou & Beichman (1990). The tabulated FIS sensitivity is the 5σ limit for a single Slow-Scan with a 2 second integration and scan speed of 15 arcsec/s.

Band	Sensitivity	Confusion Limit (5σ, mJy) for $< B_\lambda >$		
	5σ (mJy)	0.5 MJy/sr	3 MJy/sr	10 MJy/sr
N60	78	0.37	5.49	33
WIDE-S	16	0.77	11	68
WIDE-L	85	3.6	54	330
N160	198	4.3	63	388

of 1/20 sources per beam (20 beams per source). Table 3.4.3 tabulates the source confusion limit assuming the above criteria for the FIS bands. From the table it can be seen that source confusion will only become problematical in the WIDE FIS bands.

Table 3.4.3: Estimated confusion limits (in mJy) due to point sources for AKARI FIS bands. The tabulated FIS sensitivity is the 5σ limit for a single Slow-Scan with a 2 second integration and scan speed of 15 arcsec/s.

Band	5σ Sensitivity (mJy) Slow-Scan Mode	Source Confusion Limit (mJy) 20 beam/source
N60	78	3
WIDE-S	16	7
WIDE-L	85	45
N160	198	50

3.5   FTS mode

3.5.1   Transient Effects on the FTS data

In the FTS mode, the detectors have to observe a rapidly changing signal from the interferogram. Naturally, strong transient effects appear in the output signal. Figure 3.5.19 plots the interferograms corresponding to the *forward* and *backward* motion of the mirror. Large deviations are seen.

Correction of transient effects in the FTS data is being investigated.
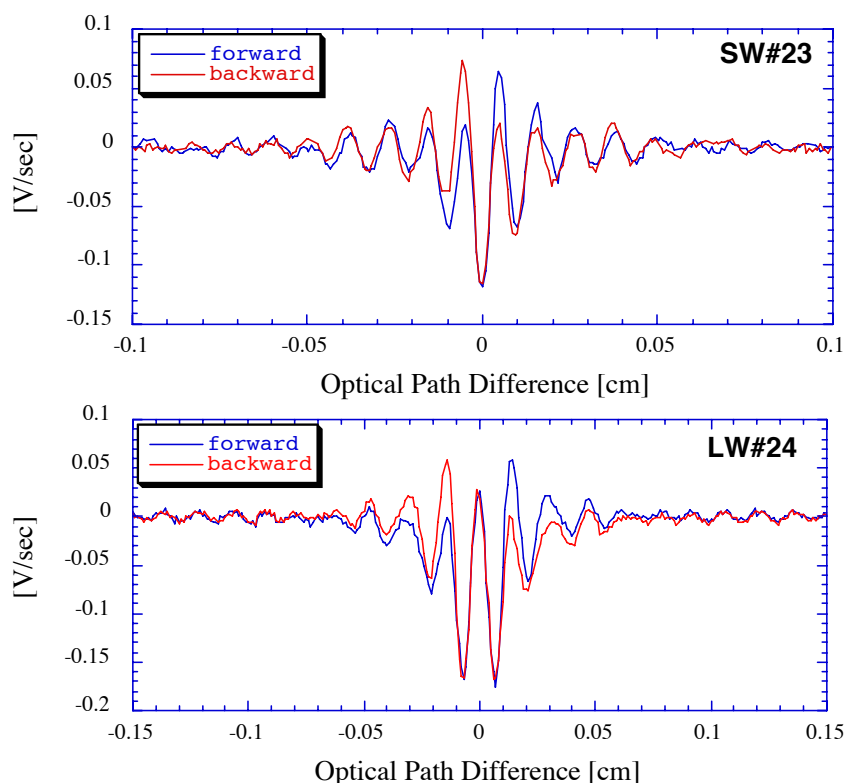
Figure 3.5.19: Comparison of forward (blue) and backward (red) interferograms. The difference between the two interferograms is thought to be due to detector transients.

3.5.2   Detector Response Inhomogeneity

As described above, pixels in the detector arrays do not have a uniform responsivity. Figure 3.5.20 indicates the relative responsivity variation of the detector pixels in the FTS mode integrated over an effective wave number range of 85-160 cm^{-1} for the SW array and 65-85 cm^{-1} for the LW array. The relative responsivity of most of the pixels are within 40% for the SW array however the pixels of the LW array have larger variation. There are several pixels with extremely high responsivity, e.g. SW pixel 23 and LW pixel 31.

The wavenumber dependence of the responsivity also differs from pixel to pixel, which should be calibrated as the spectral correction factor in the analysis tools (see section 4.3). In the LW detectors, there is also a variation in the wavelength profile (long wavelength cut-off).
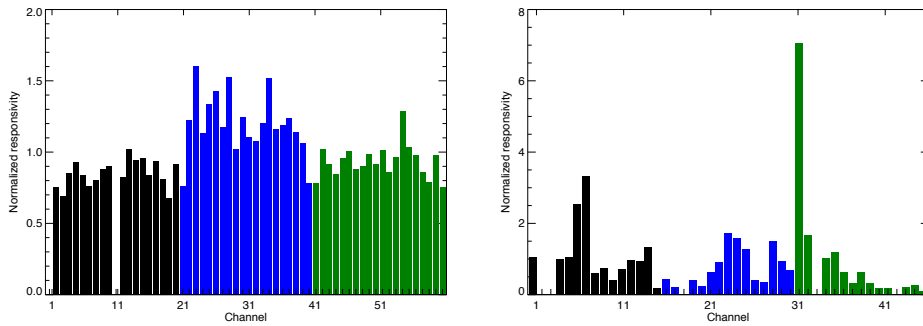
Figure 3.5.20: The relative responsivity variation of the detector pixels in the FTS mode integrated over effective wave numbers of 85-160 cm^{-1} for the SW array (left) and 65-85 cm^{-1} for the LW array (right). These data are obtained from the internal calibration source.

3.5.3 Spectrum Reproductivity

In order to evaluate the stability of the spectroscopic data, three spectra were taken during the laboratory tests. The first two were taken with a one hour interval, then the third one was obtained after three hours. The derived three spectra are almost equivalent to each other within about 10%.
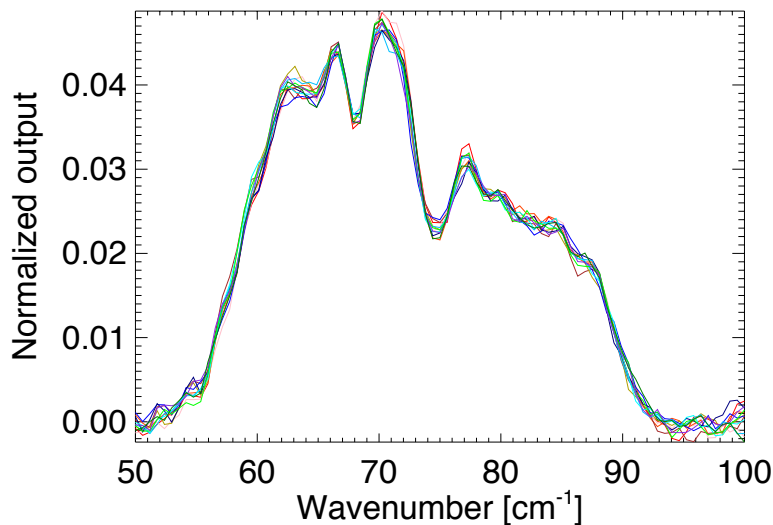
Figure 3.5.21: The internal calibration source spectra of LW pixel 7 obtained over the first year of the AKARI mission. They are normalized by the integration over the effective wavenumber of 65-85 cm^{-1}.

In orbit, the reproductivity of spectra from the internal calibration lamp was examined. Figure 3.5.21 shows the spectra over the first year of the mission. The spectra are consistent with each other within 10% after scaling with the integration over the effective wavenumber. For most LW pixels, it has been confirmed that the spectra can be reproduced to within 10%. Although the spectra of the SW channel show large amplitude fringes, the spectra of most pixels can also be reproduced to within 10% in wavenumber for those pixels less affected by fringes.

3.5.4 Fringes

The SW channel suffers from strong fringes in the spectra. Figure 3.5.22 shows an enlargement of the fringe patterns in the Full-Resolution mode and the SED mode respectively. The cause of the fringes is thought to be a reflection within the detector element, by the parallel surface of the chip (therefore it should also present in the photometric mode). Throughout the laboratory measurements, the fringe pattern remains at the same position, implying that it can be easily removed. The fringe pattern looks quite similar for different in-flight observations. The largest fringe component can be significantly reduced by applying a predefined model pattern. Further investigation is ongoing to remove the residual fringes. However, observations of sharp lines on the fringe shoulders will require special care.
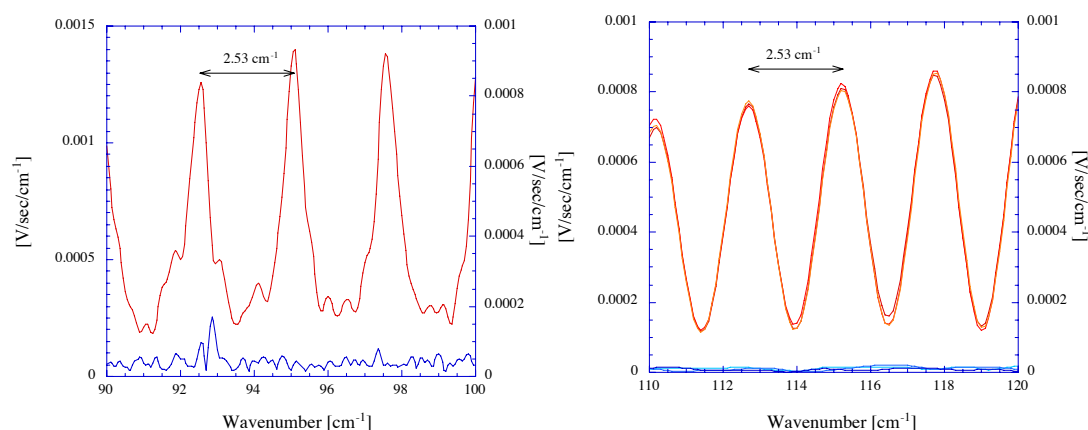
Figure 3.5.22: Fringe pattern of the FTS spectra in Full-Resolution mode (left) and SED mode (right). In Full-Resolution mode, the fringe pattern is resolved out and an "Airy pattern" of the Fabry-Perot interference is clearly seen.The blue lines in the bottom panel are the rms noise level. The three lines in the right panel are different measurements, and match each other well, indicating that the fringe pattern is reproducible.

3.5.5 Interference from the Cryocooler

It is known that the vibration from the cryocooler interferes with the FTS mirror drive. The vibration appears as a change of the mirror scan speed of up to 30%, periodically with a frequency of 15 Hz. As the detector readout is at a constant frequency, this means that the sampling of the interferogram is at inhomogeneous intervals of the optical path. As a result, the FFT technique cannot be applied. The frequency of 15 Hz corresponds to 196 cm^{-1} = 51 μm, which is outside the wavelength coverage of the FTS. Therefore it is expected that the effects of interference will not appear in the observed spectra. No clear influence on the resultant spectra has been observed at this stage of the data analysis.

3.5.6 Detector position

In-flight measurements of the relative positions of the SW and LW detectors indicate that the two detectors are not aligned as expected from the pre-flight design. Three reference positions are newly introduced as an AOT parameter (See section 2.2.5 and Figure 2.1.6). Note that the positions for the SW detector (Position 1) is not centered on a SW pixel for historical reasons, although the absolute pointing accuracy may be is as large as the pixel size.

Chapter 4

Data processing

FIS observations taken in (All-Sky) Survey Mode are processed by means of the AKARI/FIS Survey Data Reduction Pipeline. For the Pointed Observations (Slow-Scan mode) a dedicated toolkit is provided to the users. The toolkit is still evolving and users are recommended to check the updates.

Currently the distributed files contain the raw data and example reduction results (jpeg image) to give users a first impression of the data. Although they are fully reduced data, it must be emphasised that the processing is done in an automatic way (using the default options of the Slow-Scan tools) which does not involve any scientific judgment.

Instructions of how to use the FIS Slow-Scan tool (Cookbook) are given in Appendix A.

4.1 AKARI All-Sky Survey (ASS) Pipeline

The AKARI All-Sky Survey Pipeline can be divided into three steps; (1) construction of FITS datasets from telemetry data, (2) the scan processing and calibration (*Green Box*), and (3) confirmation, source extraction, and catalog production (ASTRO-F/FIS Data Reduction Team 2001 Sept. 4, "The ASTRO-F/FIS survey data reduction – The Pipeline Design and the Calibration Strategy –").

4.1.1 Out-line of the data flow

The pipeline *Green Box* modules process and calibrate the time series data (TSD; see Section 6.1). The procedures included are (see Figure 4.1.1); 1. flagging of the bad data, 2. correction of non-linearity arising from cryogenic readout electronics (CRE), 3. differentiation of the signal ramps, 4. detection of cosmic-ray glitches, 5. correction of transient and cross-talk effects, 6. subtraction of dark current level, 7. correction of DC-responsivity, and 8. flux calibration.
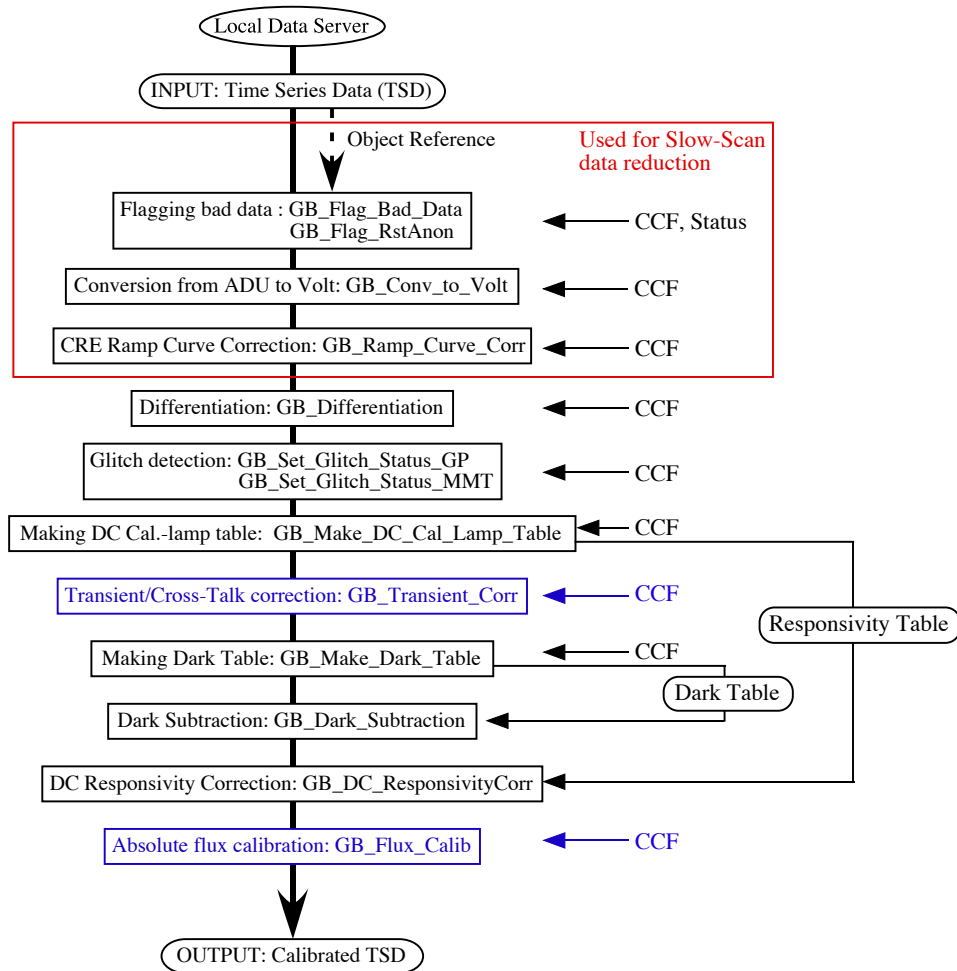
Figure 4.1.1: Outline of the flow of the time series data through the Green Box pipeline modules. TSD refers to Time Series Data, and CCF for Calibration Constants Files. The input and output of each procedure are TSD object reference. Blue boxes (Transient/Cross-talk correction, absolute Flux Calibration are not yet implemented in the pipeline structure)

The input and output of each procedure are `TSD object references` on memory within

IDL. Physical TSD files are not created by default until the end of the pipeline. Parameters are provided in an appropriate calibration constants file (CCF; see Section 6.2).

Four of these GB modules (flag bad data, flag anomaly after reset, conversion to voltage units and ramp curve correction) are also part of the Slow-Scan pointed observation data reduction tools and are described in the next section.

4.1.2   Green Box Modules used in the Slow-Scan data reduction process

These GB modules are automatically called from the Slow-Scan toolkit. At present, there are little or no options available,therefore users do not need to pay special attention to them. They are described here only for information and clarity.

Setting the flags to bad data (GB_Flag_Bad_Data)

This function sets flags in the data with the following conditions:

Frame condition	; blank frame
	; in SAA
	; near moon
Each pixel condition	; dead pixel
	; saturated pixel
	; reset position

These flags are applied to each frame (sampling) and each pixel. The output is stored in the branch FIS_OBS (under Flags) of the TSD file (see Section 6.1)

Besides this specific module for flagging data, all the Green Box modules of the All-Sky Survey pipeline set frame/pixel flags in the case where the particular module fails to process data properly or when any data have an anomaly. In addition, the BAD flag is an OR operation of the other flags (see Section 6.1). Therefore, the BAD flag can be used for a quick check of data quality. For more detailed analysis the individual flags should be inspected.

Digits to Volt conversion (GB_Conv_to_Volt)

This procedure converts from ADU to a signal in Voltage units. The output is stored in the branch FIS_OBS (under Detector data: Flux) of the TSD file (see Section 6.1)

CRE non-linearity correction (GB_Ramp_Curve_Corr)

The output of the cryogenic readout electronics (CRE) has non-linearity characteristics depending on the output voltage. This function corrects this non-linearity, assuming that the degree of deviation from an ideal integration ramp curve is a function of output voltage.

4.2 Slow-Scan processing and calibration: FIS01 and FIS02

4.2.1 Detecting glitches of cosmic ray-hits

Glitches are caused by the effects of cosmic ray particles on the detectors. A radiation hit or glitch shows up in the Slow-Scan data as an abrupt change of signal ($\sim$0.1s) while celestial sources exhibit a slower time profile ($\sim$1s). Thus, in principle, it is straight-forward to discriminate glitches from a source signal in the time domain.
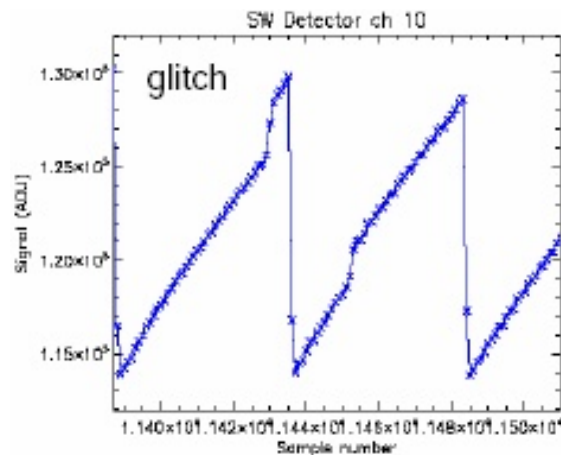
Figure 4.2.2: Glitch example

Glitch events are detected by taking the 1st and 2nd differential of the data and comparing the differential signal with the RMS noise. Then a glitch event is flagged for each pixel. There are more complex glitch detection algorithms prepared for the All-Sky Survey data. However, for Slow-Scan data this algorithm is sufficient and faster.

4.2.2 Calculation of signal current

The slope of an integration ramp (or signal in V/s) is proportional to the photo-current which in turn is a measure of the number of photons falling on the detector per unit time. The signal current is calculated by a linear fit to the ramps. In the case that glitches are detected in a single ramp, the ramp is divided into (number of glitches + 1) and a linear fit is made for each segment of the divided ramp. The weighted average flux of each segment is calculated as the mean flux for the ramp concerned. The uncertainty or fluctuation of the slope is the RMS of the fit residuals. The RMS noise of the LW detectors is very similar between shutter-close (dark signal) and shutter-open (sky signal). For the SW detectors, the shutter-open noise is slightly higher than that with shutter-close (see Fig 4.2.3).

The noise spectrum is under investigation. Preliminary results shows no clear difference in the noise spectra between shutter open/close signals, as shown in Fig 4.2.4.

4.2.3 Dark signal subtraction and flat-fielding

Shutter-close data is used for dark current subtraction. Currently, the Slow-Scan tool uses an average value of the data before the calibration lamp (CalA; see Section 2.1.2) is turned on for 2 minutes during shutter close.

For the responsivity correction and flat-fielding the Slow-Scan tool uses by default a flat-field built from the PV observations of zodiacal light and cirrus emission. The average flux of the 2
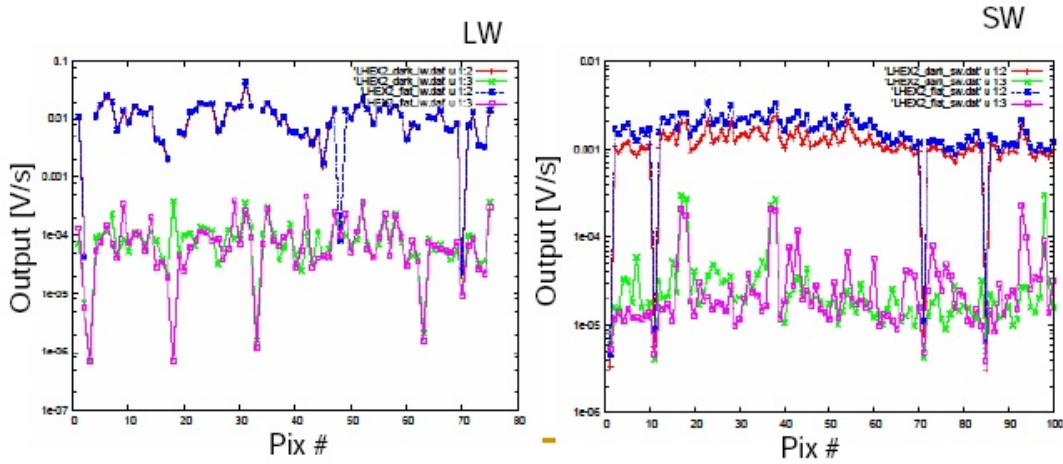
Figure 4.2.3: Comparison of the RMS noise for LW and SW detectors when the shutter is open (flat) and closed (dark)
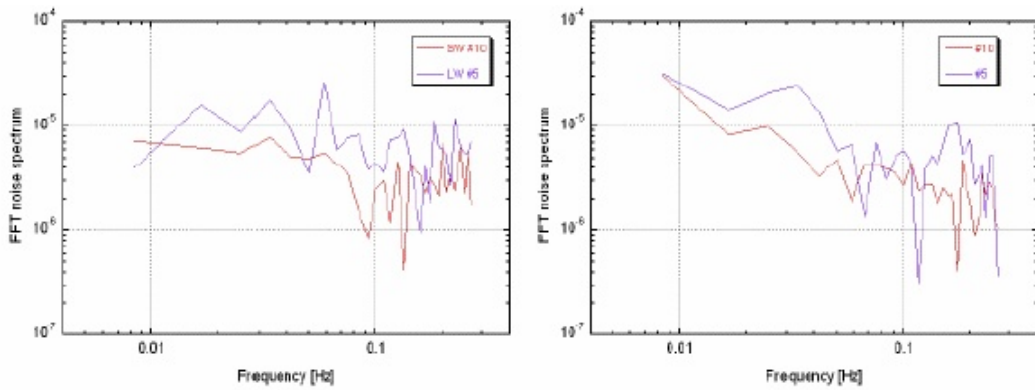
Figure 4.2.4: FFT noise spectra for a 2s integration data of shutter-open (left) and shutter-close (right)

minutes calibration lamp in that observations are used.

In Figure 4.2.5 the data intervals used for the dark subtraction and flat-fielding are shown. Examples of dark and flat-field tables are shown in Figure 4.2.6.

Flat-fielding with the observation (sky) data is attempted in the Slow-Scan tool (option LOCAL_FLAT) and often works successfully for flat (quiet) skies. An average responsivity for each wavelength band is corrected with the 2 minutes calibration lamp and the flat-field is built from the observed sky.

4.2.4   Conversion to surface brightness

The conversion from the slope of the integration ramp (V/s) to surface brightness (MJy/sr) is made by using the responsivity correction table.

The responsivity correction table is calculated as the ratio between the calibration lamp signal and the signal of celestial "flat" sources comprised of the zodiacal light and cirrus emission observed during the PV phase (see Section 4.2.8 for details).
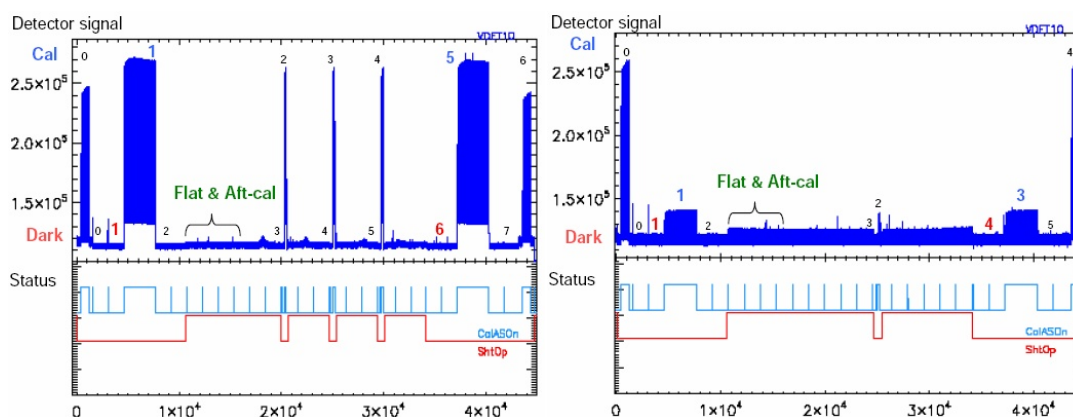
Figure 4.2.5: Sequence of FIS01 and FIS02 observations with the corresponding flags for shutter-close (red) and CalA on (blue). In bold red numbers, the average value during shutter-close used as the dark measurement is shown. In bold blue numbers the average value used for responsivity correction when the calibration lamp is on (CAL). Note that CalASOn status turned on every minute (pulses) but there is no signal on the detectors, as the current of the calibration lamp is set to 0.
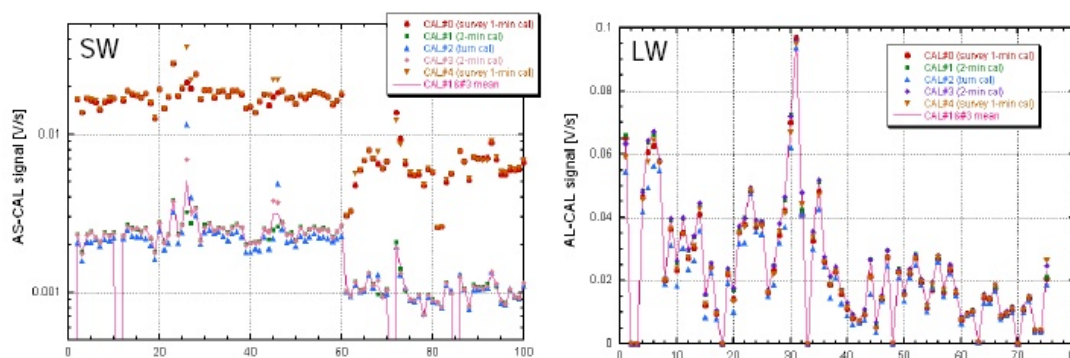
Figure 4.2.6: Examples of dark and responsivity tables.

4.2.5 Background offset subtraction

Only the instrumental (thermal) background inside the FIS entrance shutter is subtracted during the default processing. Stray light due to Earth shine reflected at the telescope baffle is then the major internal contribution to the observational background (see Section 3.1.6).

For point sources, the background subtraction can be performed by median filtering (option /MEDIAN_FILTER) in the time domain with a default window size of 10 data points (= 10 ramps). The stray light is also removed by this DC-rejection filter (see Figure 4.2.7).

However, diffuse sources with a size comparable to the median filter width will be also filtered out by this procedure. For this case, a different routine to model and subtract the stray light (/SL_RMV) is under construction (see Figure 4.2.8).

In the model, the baffle function is assumed to follow an exponential law:

$I = B + A \times \exp[-(\Theta/C)^2]$

where I is the signal, B is the sky background, A is a fitting constant, Θ is the Earth avoidance angle and C is a scale angle (~ 0.4 rad).

In addition, the option /SKY_SUB is also provided in the Slow-scan toolkit to subtract the mean sky level determined from the data before the Slow-Scan (during the stabilization).
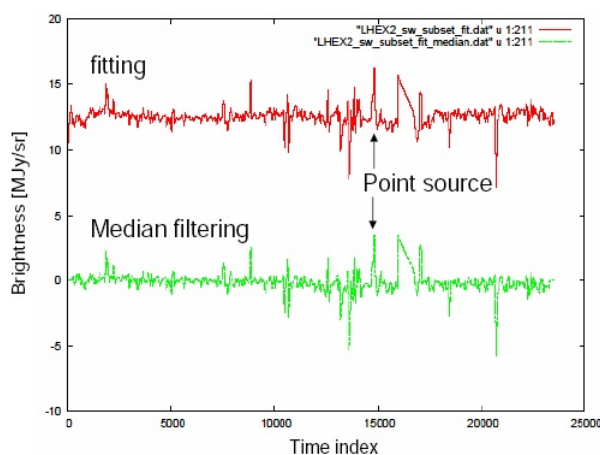
Figure 4.2.7: Background subtraction for point sources and small scale structures.
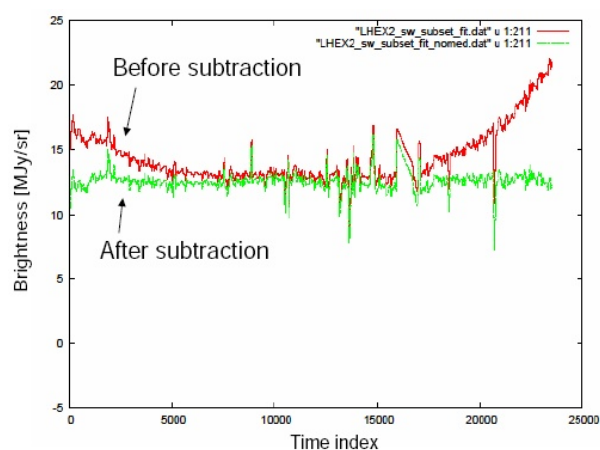
Figure 4.2.8: Baseline fitting with a stray light model.

4.2.6   Making images by co-adding multi-pixel data

Co-add images are created from the scan data. The positions of every pixel at every data point in the scan data are calculated from the boresight position given in the data file and the offset between the boresight and the detector pixels. Optical distortion of the detector arrays from the pre-flight simulation is taking into account in the pixel position table. Fine tuning of the alignment between the boresight to the arrays are carried out from the observation data.

An image plane of appropriate grid size is prepared and signals from the data points are summed up and then averaged over the number of data points per pixel. By default a pixel size of 15 arcsec and 30 arcsec are adopted for the SW and LW data in the FIS01 mode. The pixel size is doubled for the FIS02 mode.

The image grid positions are of simple equal pitch in local sky. Currently no projection to the world coordinate system (WCS) is considered. Therefore the FITS format output of the resultant image has a deviation from the real position towards the periphery of the images. It is recommended to use the image and coordinate information packed into the provided IDL `.sav` file for further analysis. Proper projection will be considered in a near future version of the toolkit.

By default all available data are accumulated on the image plane. An option `/SCUT` produces

images per individual (one-way) scan. See the Cookbook (Appendix A) for more details.

4.2.7   Image processing for multiple pointings

A tool is provided within the Slow-Scan data reduction toolkit to co-add/mosaic multiple pointings together. The tool may be used for both the co-addition of multiple pointings to improve redundancy or to make small maps from multiple FIS AOTs. See Cookbook (Appendix A) for details.

4.2.8   Photometric calibration

Calibration of scan data

The absolute calibration of the FIS Slow-Scan data is based on the measurements of the diffuse sky emission from zodiacal light and interstellar cirrus averaged over areas of several Slow-Scan observations. The absolute brightness is derived from COBE/DIRBE measurements.

The conversion factor from the detector signal I (V/s) to the sky brightness B (MJy/sr) for each pixel is derived as the ratio between the averaged sky brightness level and the averaged detector signal while the calibration lamp is continuously turned on (in the calibration sequence data at the beginning and end of each pointed observation). The conversion factor is given for different signal levels of the calibration lamp (corresponding to selected reset interval).

$$R[(\text{V/s})/(\text{MJy/sr})] = \frac{(I_{\text{sky}} - I_{\text{dark}})_{\text{flat}}}{B_{\text{flat}}} \tag{4.2.1}$$

In the data reduction, observation data is first flat-fielded by the signal of the calibration lamp, assuming that the variation of the detector responsivity is slower than the duration of the observation, then the conversion factor is adopted.

$$CTOF = \frac{I_{\text{cal}} - I_{\text{dark}}}{I_{\text{sky}} - I_{\text{dark}}} \tag{4.2.2}$$

$$B_{\text{obs}}[\text{MJy/sr}] = \frac{(I_{\text{cal}} - I_{\text{dark}})_{\text{obs}}}{CTOF \cdot R} \tag{4.2.3}$$

So far for the limited number of regions tested, this calibration is consistent with COBE/DIRBE even in very dark sky areas.

Point source photometry (based on preliminary initial results)

Images generated by the standard Slow-Scan data reduction tool are in brightness scale units of MJy/sr. Aperture photometry on these images should give the flux of the sources in Jy. Results of aperture photometry often depend on the size of the aperture and the sky area. This effect is significant in the FIS observations, especially in the LW channels. In the following we give an example photometry analysis using the calibration standard stars. Preliminary conclusions are:

- There are systematic differences between the measured flux and the expected flux from the model.

- The ratio of two fluxes seems to be constant within $\sim$20% (1σ) for the examined sources brighter than about 2 Jy.

The procedures are explained below. Photometry following this method should in essence provide consistent results. Note that this is *not* the definitive solution that will eventually be provided.

1. All data were taken in FIS01 with 8 arcsec/sec scan speed and 70 arcsec shift length. Data taken with other scan speeds or with FIS02 need further consideration (Section 5.3.1).

2. Images are generated using a local flat-field, with a sigma clipping threshold of 1.5 and a grid size of 7.5 arcsec for SW and 15 arcsec for LW. Note that the grid size is half of the nominal value used by the Slow-Scan tool for AOT FIS01 (see Appendix A). Such a small grid size produces many void pixels and therefore, it is not recommended for general purposes.

3. Following aperture and sky region are adopted:

Channel	Signal [arcmin]	Sky [arcmin]
SW	2.25	2.25–3.25
LW	3.0	3.0–4.0

   Sky level is determined by taking the average of all the available pixels.

4. For faint sources these aperture sizes are too large and may introduce contamination from the background. Smaller aperture sizes improve the S/N of the photometry. The aperture correction factor is derived from the 'curve of growth' analysis of the objects as follows.

Band	Aperture [arcmin]	Correction factor
N60	0.625	1.58
WIDE-S	0.625	1.74
WIDE-L	0.750	1.71
N160	0.750	2.03

5. The measured flux is compared with the expected flux of the sources. Asteroids and a star (α Boo) is used as the primary calibrators. Expected fluxes are derived from the TPM model (Müller and Lagerros 2002, A&A 381, 324) or stellar SED templates by M. Cohen for the Spectral Response of the FIS instrument. A colour correction is adopted to convert them to a flat spectrum ($\nu F_\nu = $ const.). In addition, several infrared luminous galaxies are included in the sample. Their fluxes are estimated from ISO observations or their IRAS flux.

6. The ratio of the measured flux to the expected flux is fairly constant among the samples and is tabulated below. These numbers are regarded as 'correction factor' from the measured flux to the real flux of the sources.

Band	Factor
N60	1.7
WIDE-S	1.7
WIDE-L	1.9
N160	3.8

For the moment, there is no clear explanation of the discrepancy between the expected flux and measured flux. The uncertainty of the photometry using the above method is crudely estimated as 20% in SW and 30% in LW. Especially the number for the N160 band needs special care to use, as only three objects were available for the analysis.

Colour correction

(Based on internal report by Y. Hibi 2006 Dec. 25)

The FIS photometric flux is defined for a flat spectrum ($\nu F_\nu = $ const.) at the defined *Central Wavelength (Frequency)* of each band (Table 2.1.1). Colour correction factor K is given by;

$$K = \int (F_\nu(\nu)_{\mathrm{flat}}/F_n u(\nu c)_{\mathrm{flat}})R(\nu)d\nu, \qquad (4.2.4)$$

where $F_{\nu\text{obs}}$ is the flux of the object, $F_{\nu\text{flat}}$ is the flux of the flat spectrum, $R(\nu)$ is the Relative Spectral Responsivity Function (RSRF; Figure 3.2.17) normalized at the Central Frequency.

Colour correction is applied as:

$$F_{\text{real}} = \frac{F_{\text{obs}}}{K} \tag{4.2.5}$$

Correction factors for typical cases are tabulated in Table 4.2.1 and 4.2.2.

Table 4.2.1: Colour correction factor K for a spectrum $F(\nu) \propto \nu^{\alpha}$

Band	α -4	-2	0	2	4
N60	1.08	1.01	1.00	1.05	1.17
WIDE-S	0.97	0.96	1.08	1.41	2.20
WIDE-L	1.23	1.05	0.96	0.94	0.97
N160	1.06	1.01	0.99	0.99	1.01

Table 4.2.2: Colour correction factor K for a black body

Band	Temperature [K] 10	30	100	300	1000	3000	10000
N60	3.38	1.05	0.99	1.03	1.04	1.05	1.05
WIDE-S	1.84	0.89	1.15	1.32	1.38	1.40	1.40
WIDE-L	1.55	0.96	0.93	0.94	0.94	0.94	0.94
N160	1.10	0.99	0.99	0.99	0.99	0.99	0.99

4.3   FTS spectroscopy processing: FIS03

FTS analysis toolkit is expected to be available very soon. Reduction of the FTS mode observations will consist of many iterative procedures and trial processing. There are various instrument anomalies that have to be settled and corrected, for example, distortion of the interferogram due to the transient response of detectors, Fabry-Perot like fringes in the SW spectra due to interferences in the detector, etc...

The current version of the FTS analysis toolkit can not yet be applied to all the FTS observations. There remain instrument anomalies which are not considered in the current toolkit, and the present calibration is only applicable to a limited subset of the observations. In addition, the absolute flux is also yet to be calibrated. **Therefore, users are urged to contact the FTS team in Japan via the Helpdesk in order to use the FTS analysis tools. Note that, without following this route, the output of the toolkit may result in incorrect scientific results.** Joining the FTS team for establishing the analysis toolkit is highly welcomed.

4.3.1   Overview

The FTS analysis toolkit consist of two pipelines, named *fts_part1.pro* and *fts_part2.pro*. The former reduces the Time Series Data (TSD) and provides raw spectra, and the latter applies flux & spectral calibrations and reduces the fringes. The processes contained within these two pipelines are listed below.

[**raw data (TSD)**]

1. Flag bad data : gb_flag_bad_data, gb_set_flag_rstanom

2. Convert to voltage units : gb_conv_to_volt

3. Ramp curve correction : gb_ramp_curve_corr

4. Differentiate data : gb_differentiation

   [**Interferogram + DC component**]

5. Separate into individual scans

6. Remove reset anomaly and glitches

7. Subtract DC component

8. Interpolate bad data

9. Determine the position of the center burst

10. Discrete Fourier transform

11. Average the spectra

   [**Raw spectra**]
(end of fts_part1)

12. Apply spectral correction factor and flux calibration

13. Remove fringes

   [**Spectra**]
(end of fts_part2)

4.3.2 Brief description of each process

Ramp curve correction

The standard Green Box module is used to correct for any non-linearity of the ramp curve (see section 4.1.2). The correction table is made from the interferogram far from the center burst using observations of targets of various brightnesses. (N.B. For very bright targets whose brightness exceeds the range of the correction table, you have to make a correction table from your data itself. In the present toolkit, the calibration will be incorrect in this case.)

Determination of the position of the center burst

Since the value of the position sensor is correct only relatively, the center of the optical path must be determined. In fact, the center depends on the wave number so a wavenumber-dependent phase correction is needed. However, the present toolkit determines the position of the center that minimizes the imaginary part integrated over the effective wavenumber. The determination is a two step process. First, the deviation of the center position between different scans is estimated. For this purpose, the most sensitive pixel (SW pixel 23 and LW pixel 31, see Fig. 3.5.20) is used, or alternatively, a pixel detecting a point source. It is then assumed that the relative deviation of the center position between different scans is the same for all pixels. Next, the deviation of the center position between different pixels is estimated.

Interpolation of bad data

We replace any bad data by the median of other scans. Since the first scan in the SED mode is affected by an irregular drive pattern at the starting point, we ignore the first scan when calculating the median in the SED mode.

Fourier Transform

After applying Fourier transforms to the interferogram of each and every scan, a correction for the slight variation of the responsivity within one pointed observation is made by scaling with the integration of the effective wavenumber, 85-160 cm^{-1} for SW and 65-85 cm^{-1} for LW (except for the first scan in the SED mode). The average spectrum is then taken.

Spectral correction factor and flux calibration

The spectral correction factors are primarily made from the spectra of the internal calibration source. These include the correction for the wavenumber-dependent response and the relative sensitivity of the pixels. At present, celestial calibration sources have not been taken into account, thus the difference between the spectra of the internal sources and external sources is not taken into account and thus absolute flux calibration is not applied.

Removal of fringes

In the present toolkit, only fringes in the SW full-resolution mode are reduced using model calculations of an airy pattern with a period of 2.53 cm^{-1}. Since the spectral correction factors are made using data from the internal calibration source, which are in the SED mode, fringes in SED mode observations should be removed when the spectral correction factors have been applied. For Full-Resolution mode observations, the fringes are removed from both the observed data and the spectral correction factor using an airly pattern of the corresponding wavenumber resolution. Residual fringes and LW fringes are not reduced in the present version of the toolkit.

4.3.3   Further limitations in the functionality of the current version of the FTS toolkit

- Transient correction.

- Wavenumber calibration.

- Apodization.

- Wavenumber-dependent phase correction.

- Difference between the internal source and the external source.

- Absolute flux calibration.

Chapter 5

Caveats in the Data Processing

The reduction software and calibration for the FIS Slow-Scan observation is still at a rather preliminary stage. As the analysis is progressing new complicated problems of the data will inevitably become apparent. We try to describe the current limitation of the calibration to avoid user over-interpretation of the data. Up-to-date information about the calibration and data reduction will be included in this document and displayed on the observer support web page. You are also welcome to contact the Helpdesk for any queries regarding the data reduction.

5.1 Treatment for transient effects

At present, there is no formal treatment of transients in the Slow-Scan data reduction tool. Only after-effects induced by calibration light pulses are considered, and this only affects observations taken during the PV phase as the periodic pulse flashes were stopped for pointed observations in Phase-1 (see Section 2.1.2).

5.2 Straylight correction

For point sources, the stray light caused by the Earth shine reflected at the telescope baffle can be removed by the median filtering used for the background subtraction. However, diffuse sources with a size comparable to the median filter width are also filtered out by this median filtering. The modelling and correction by stray light is still being analysed (see Section 4.2.5).

5.3 Photometric calibration

5.3.1 Scan speed

Most observations of the flux calibration targets are carried out in FIS01 with a scan speed of 8 arcsec/sec. If your observation uses a higher scan speed, 15 arcsec/sec or 30 arcsec/sec, the observed signal would be reduced due to detector transient effects and will result in an underestimation of the source flux. An investigation into these effects has recently begun. The initial report implies that the measured flux from the aperture photometry for the 15 and 30 arcsec/sec data are ~10-20% fainter than that from the 8 arcsec/sec case. Reliable calibration information for all scan speeds will be given as soon as this analysis has been concluded.

5.3.2 Calibrators

Correction factors are derived for all detectors from the different calibrators (see Section 4.2.8). The photometry uncertainty is estimated to be ~20% (SW) and ~30% (LW). However, for the

N160 band, special care is needed as only three objects were available for calibration measurements.

5.4   Attitude Determination During the Pointed Observations

The attitude information for the FIS pointed observations is provided from two sources. The on board computer `AOCU` (Attitude and Orbit Control Unit) calculates the satellite attitude and these results are downlinked to the ground as telemetry data together with the data from the on board sensors. The Ground-based Attitude Determination System (`G-ADS`) re-calculates the attitude with a greater degree of care. Both data are recorded in the observation data file.

Both systems use the same input data from the on board Attitude Control System sensors and there should only be minor differences in the absolute positional accuracy. Nevertheless, the `G-ADS` is expected to provide more reliable information than the `AOCU` since this data includes fine tuning of the algorithm and software system to the input data. The Slow-Scan data reduction tool uses `G-ADS` information by default. However, as of February 2007, the tuning of the `G-ADS` system has not been completed and the results are not accurate enough under some conditions. Such inaccuracies may appear in the reduced images as an unexpected elongation of the images. It is recommended to run the software with the `/AOCU_ADS` option and to compare the results with the default (`G-ADS`) processing.

The `G-ADS` is expected to be improved in around a months time. Note that the Pointing Reconstruction processing is carried out with the data from the Focal-Plane sensors for the All-Sky Survey by ESAC/ESA, which will provide better than a few arcsec accuracy.

Positional error has been crudely evaluated using around 40 (SW) and 20 (LW) point-like sources reduced by the Slow-Scan tool in the standard manner. The deviation of the centroid position on the image maps from the catalogued positions scatters with a 1σ dispersion of $\sim$6 and $\sim$11 arcsec in the in-scan and cross-scan directions respectively. SW positions and LW positions are consistent to within $\sim$11 arcsec (in-scan) and $\sim$23 arcsec(cross-scan) respectively for bright sources.

5.5   Pixel position table

The current pixel position table is based on simulations. Corrections based on in-flight data are being analysed.

5.6   Projection

Currently, the FIS images in FITS format have a known problem with projection and the coordinates of the image may deviate from the real position; from the image center to the edge. This deviation is typically a few arcmin at the corner. It is recommended to use the data in the IDL `.sav` file for further analysis of the image data.

Chapter 6

Instrument Related Data Products

In this Chapter we describe the internal structure of the AKARI/FIS observation data. A set of IDL data interface routines is provided as a part of the data reduction toolkit. Those who are interested in modifying or developing data reduction tools are welcome to contact the data reduction team in Japan via Helpdesk for more detailed information.

6.1 Time Series Data (TSD): Overview and structure

(H. Baba, I. Yamamura, A. Kawamura, S. Makiuti, H. Kaneda, T. Nakagawa and C. Yamauchi 2006, "ASTRO-F FIS/Survey Data Structure")

6.1.1 Overview

The data consists of header parts and arrays of data record. A record (corresponds to a sampling of the detector) consists of the instrument data and necessary information from other house keeping (HK) instruments, as well as positional information given by the ground station. Usually the sampling rate of HK-data is much slower than that of instrument data. These information are regridded by a suitable method (e.g. interpolation) to synchronize with the clock of the target instrument.

The data for individual instruments (or source of information) are each maintained in a separate unit known as a 'branch'. TSD data are examples of these branches. In the TSD data structure, all data are related to each other by a time stamp. The reference time stamp throughout the data is called the "Key Time", and is given by the main instrument (FIS detector readout timing). The Key Time is copied to other branches and data from the instruments are regridded to it.

All information from the main instrument is included in the TSD dataset, while only the subset of any information that is needed for the data reduction is provided from other instruments.

6.1.2 Physical file format of TSD

The physical file format of the TSD to exchange the data is the *FITS Binary Table Extension*. In the table, each row corresponds to a sampling which is identified by PIM-TI, the clock counter provided by the DHU (Data Handling Unit) of the spacecraft.

For the detailed information about FITS Binary Table Extension, see "section 8.3 Binary Table Extension" in "Definition of Current FITS Standard - NOST 100-2.0" [1].

Size of one TSD file for a single pointed observation is 100–200 MB.

---

[1] http://fits.gsfc.nasa.gov/

TSD Branch	Time	Status (boolean)	Telemetry (analog)	Detector Data (analog)	Flags (boolean)		Quality	Counter
		Non-Editable			Editable			
FIS_OBS				det	flux ferr	frame flags pixel flags		
FIS_HK								
IRC_HK								
HK_2								
AOCU								
GADS								
PR								
SE								

Figure 6.1.1: An overview of Time Series Data (TSD) structure.

6.1.3   Nomenclature of Data Type

Data type are expressed in C-like notation in the following descriptions.

```
bit             : 1 bit   0 or 1
byte            : 1 byte  unsigned byte ( >= 0)
short           : 2 bytes integer
long            : 4 bytes integer
longlong        : 8 bytes integer
float           : 4 bytes single precision floating point
double          : 8 bytes double precision floating point
```

We express the elements of status column 'n:' where n is the element index defined in the FITS.

6.1.4   Time stamp

- The main purpose of time stamp in the data reduction system is to synchronize the information taken with different instruments and other information sources (e.g. for pointing reconstruction).

- For this purpose, time information maintained in TSD is that already corrected various delays. It is the time when the data is sampled by the instruments.

- Time in the on board clock is 36 bits with LSB of 1/512 sec. Practically 32 bits data either with 1/32 sec or 1/512 sec are stored in the packet depending on the instruments. Internally we use a 64 bits integer (long64 in IDL) for time field.

- The original point of the time for the AKARI project is 2000 January 1st, 00:00:00 UTC.

6.1.5   Status

The 'Status', 'Flags' and 'Quality' of TSD columns are composed of multiple elements of the TBIT type (i.e., the TFORM definitions of FITS standard are '8X', '16X', etc.).

Figure 6.1.2 shows an example of the status section of this document. The left hand number shows the element index. The 'fv' displays this index when we click the 'expand' button. The first element (index=1) corresponds to the MSB (bit31) in the binary. The next is the element name, which cannot be defined in the FITS standard. However, we define the element name and write them to each header of the HDU. For example, the element names of status in FIS_OBS extension are written in the header of its HDU as follows:

TELEM6 = 'CREON,SHTOP,FWPOSON,FWPOS_B1,FWPOS_B0,MPOSON,MPOS_B1,MPOS_B0, ...

The user should use the element name to access the status bits, rather than element index.

Figure 6.1.2: An example of status section.

6.1.6   TSD: detailed description

Primary Header

```
string  FMTTYPE          ; Type of Format in FITS file
integer FTYPEVER         ; Version of FMTTYPE
string  CNTTYPE          ; Type of data content
string  DATE             ; File Creation Date
string  CREATOR          ; Data generator program name
```

```
string   CRTRVER         ; Version of CREATOR
string   PIPELINE        ; Data Processing Pipeline name
string   DATASTAT        ; Data status
string   ORIGIN          ; Organization creating FITS file
string   TELESCOP        ; AKARI mission
string   INSTRUME        ; Identifier of the instrument
string   DETECTOR        ; Detector name
string   OBSERVER        ; PI Name (Observer's ID)
string   PROPOSAL        ; Proposal ID
string   OBS-CAT         ; Observation Category
integer PNTNG-ID         ; Pointing ID
integer TARGETID         ; Target ID
integer SUBID            ; Sub ID
string   OBJECT          ; Object name
double   OBJ-RA          ; [degree] Target position
double   OBJ-DEC         ; [degree] Target position
string   AOT             ; Observation AOT
string   AOTPARAM        ; AOT Parameter
string   INSTMODE        ; Instrument operation mode
string   TIMESYS         ; Explicit time scale specification
string   DATE-OBS        ; Observation start date+time
string   DATE-END        ; Observation end date+time
string   DATE-REF        ; Reference time in the Observation
double   AFTM-OBS        ; DATE-OBS in ASTRO-F Time
double   AFTM-END        ; DATE-END in ASTRO-F Time
double   AFTM-REF        ; DATE-REF in ASTRO-F Time
string   PIMTIOBS        ; DATE-OBS in PIM-TI (36bits DHUTI)
string   PIMTIEND        ; DATE-END in PIM-TI (36bits DHUTI)
string   PIMTIREF        ; DATE-REF in PIM-TI (36bits DHUTI)
double   EQUINOX         ; Epoch of Coordinate
double   RA              ; [degree] Target position at DATE-REF
double   DEC             ; [degree] Target position at DATE-REF
double   ROLL            ; [degree] Roll Angle at DATE-REF
double   AA-SOL          ; [degree] Solar avoidance angle at DATE-REF
double   AA-EAR          ; [degree] Earth avoidance angle at DATE-REF
double   AA-LUN          ; [degree] Lunar avoidance angle at DATE-REF
double   TM-SAA          ; [sec] Duration since last SAA passage at DATE-REF
double   SAT-POSX        ; [km] Satellite position at DATE-REF
double   SAT-POSY        ; [km] Satellite position at DATE-REF
double   SAT-POSZ        ; [km] Satellite position at DATE-REF
string   DAYNIGHT        ; day/night status at DATE-REF
integer STTA-NUM         ; number of stars in STT-A at DATE-REF
integer STTB-NUM         ; number of stars in STT-B at DATE-REF
string   STTA-MOD        ; STT-A Mode status at DATE-REF
string   STTB-MOD        ; STT-B Mode status at DATE-REF
string   HISTORY         ; Processing History. Any length text.
```

Description

```
##### FITS basic information, data size information
SIMPLE  =                     T / Standard FITS format
# Fixed

BITPIX  =                    16 / number of bits per data pixel
# FIS (Binary table) :  8 (Fixed)

NAXIS   =                     0 / Number of axes
# FIS : 0 (Fixed)

EXTEND  =                     T / Extension may be present
# 'T' Fixed

##### Data type, Data creation / processing program information
FMTTYPE = 'ASTRO-F TSD FIS_SW' / Type of File Format in FITS file
# Unique name of the data format
# Keep 'ASTRO-F' by historical reason
# One of: 'FIS_SW TSD', 'FIS_LW TSD'

FTYPEVER=                     4 / Version of FMTTYPE
# Version of the file format described in FMTTYPE

CNTTYPE = 'FIS_SW  '           / Type of data content
# Data content
# One of: 'FIS_SW', 'FIS_LW'

DATE    = '2006-09-25T09:45:24'/ File Creation Date
# File Creation Date

CREATOR = 'tsd_bin2dat'        / Data generator program name
CRTRVER = '1.0     '           / Version of CREATOR
# Name and version of the program that creates this file
# FIS: tsd_bin2dat

PIPELINE= 'fispl ver. 1.0 '    / Data Processing Pipeline name
# name and version of the pipeline program

DATASTAT= 'GOOD    '           / Data status
# Describes data status mainly from completeness of telemetry data.
# This does not tell detailed scientific quality of the data
# All appropriate error status are listed, otherwise GOOD is given
#  GOOD: No problem
#  INCOMPLETE: (Scientific data) incomplete due to telemetry loss etc.
#  NOHK: HK Status not available
#  NOADS: Attitude information not available
#  STTINI: STT did not work properly
# More status may be added as analysis progresses
# Data other than GOOD may not be in the archive at the first stage.
```

```
##### Instrument information
ORIGIN  = 'ISAS/JAXA'           / Organization creating FITS file
# Fixed


TELESCOP= 'AKARI   '            / AKARI mission [Satellite Name]
# Fixed


INSTRUME= 'FIS     '            / Identifier of the instrument
# One of 'FIS', 'IRC', 'FSTS', 'G-ADS'


DETECTOR= 'SW      '            / Detector name
# Detector name
# One of 'SW', 'LW'


##### Observation details
# following information is taken from Observation Database


OBSERVER= 'PI Name '            / PI Name (Observer's ID)
PROPOSAL= 'PRPID   '            / Proposal ID
# information about observation programme
# e.g., LSNEP, LSLMC, AGBGA, ...


OBS-CAT = 'MP      '            / Observation Category
# Observation category
# One of 'LS', 'MP', 'OT', 'DT', 'CAL', 'ENG'


PNTNG-ID=              1234567 / Pointing ID
# Identification of the pointing observation. Usually it is identical
# with the Target ID, but is different for 'parallel mode' observations.


TARGETID=              1234567 / Target ID
SUBID   =                    1 / Sub ID
# Unique number to specify the observation


OBJECT  = 'target  '            / Object name
# Object name
# 'SURVEY' for survey mode observations


OBJ-RA  =            320.5533 / [degree] Target position
OBJ-DEC =            -23.3325 / [degree] Target position
# Target position recorded in observation database
# Only for pointed observations.
# Values are in double precision


AOT     = 'FIS01   '            / Observation AOT
# AOT Used for the information
# 'FIS01', 'FIS02', ...., 'IRC04', 'IRC11', 'SURVEY', ...
```

```
AOTPARAM= '8;0.5;70'               / AOT Parameter
# Parameters for each AOT

INSTMODE=                          / Instrument operation mode
# Detailed instrument setup not described in AOT / AOTPAR
# FIS: readout mode (Telemetry name: PACKETID)

TIMESYS = 'UTC      '              / Explicit time scale specification
# Time system used in this file

DATE-OBS= YYYY-MM-DDTHH:MM:SS  / Observation start date+time
DATE-END= YYYY-MM-DDTHH:MM:SS  / Observation end date+time
DATE-REF= YYYY-MM-DDTHH:MM:SS  / Reference time in the Observation
AFTM-OBS= [double]                 / DATE-OBS in ASTRO-F Time
AFTM-END= [double]                 / DATE-END in ASTRO-F Time
AFTM-REF= [double]                 / DATE-REF in ASTRO-F Time
PIMTIOBS= '0xXXXXX '               / DATE-OBS in PIM-TI (40 bits)
PIMTIEND= '0xXXXXX '               / DATE-END in PIM-TI (40 bits)
PIMTIREF= '0xXXXXX '               / DATE-REF in PIM-TI (40 bits)
#
# [FIS]
# ????_OBS: Time stamp/PIMTI of the first frame in the file
# ????_END: Time stamp/PIMTI of the last frame in the file
# ????_REF: On-target observation start: 690 sec from the
#           observation start (file top)
#
# Note: PIMTI is the primary information directly from telemetry.
#       AFTI- and DATE- are from the timing correction based on PIMTI
#

##### Attitude Information (at DATE-OBS)

EQUINOX =             2000.0000 / Epoch of Coordinate
RA      =              320.5533 / [degree] Target position at DATE-OBS
DEC     =              -23.3325 / [degree] Target position at DATE-OBS
ROLL    =               -30.553 / [degree] Roll Angle at DATE-OBS
AA-SOL  =               90.0021 / [degree] Solar avoidance Angle at DATE-REF
AA-EAR  =              180.2083 / [degree] Earth avoidance Angle at DATE-REF
AA-LUN  =              210.6821 / [degree] Lunar avoidance Angle at DATE-REF
TM-SAA  =                 1829. / [sec] Duration since last SAA at DATE-REF
# Definition of SAA is different for different detectors. SAA region
# is defined by the glitch rate map observed by the Star Tracker with
# arbitrary threshold level. IRC follows this threshold. Shifts of 30
# and 60 seconds are applied to FIS SW and LW, respectively.
```

```
SAT-POSX=              2903.5528 / [km] Satellite position at DATE-OBS
SAT-POSY=              1704.3092 / [km] Satellite position at DATE-OBS
SAT-POSZ=              1968.4286 / [km] Satellite position at DATE-OBS
DAYNIGHT= 'DAY     '             / Day/night status at DATE-REF
# These files are updated as pointing analysis goes on from
# On-board AOCS -> G-ADS (-> Pointing reconstruction for Survey mode)

STTA-NUM=                      4 / number of tracked stars in STT-A at DATE-REF
STTB-NUM=                      4 / number of tracked stars in STT-B at DATE-REF
# number of tracked stars in the two STT field at DATE-OBS

STTA-MOD= 'TRK     '             / STT-A Mode status at DATE-REF
STTB-MOD= 'TRK     '             / STT-B Mode status at DATE-REF
# Status of the STT
# one of 'TRK', 'ACQ', 'STB', 'INI_R', 'INI_N'


COMMENT                          / Any strings
HISTORY                          / Any strings
END
```

FIS_OBS extension

Here we show the data structure for FIS data.

(1) Time

```
double aftime           ; ASTRO-F (AKARI) Satellite Time (calibrated)
                        ; which is the seconds since 2000/January/1 00:00 (UTC)
longlong pimtiorg       ; PIMTI counter (from original packet)
longlong fistiorg       ; FISTI counter (from original packet)
longlong pimti          ; PIMTI counter (interpolated)
longlong fisti          ; FISTI counter (interpolated)
```

(2) Status

Status information is provided in the telemetry packet. Each status is copied from the corresponding bit in FIS_OBS packet. All four band's status are included considering possible interference.

```
bit status[32]          ; FIS instrument status
   1: creon             ; CRE on:1 / off:0                % 0x09:1
   2: shtop             ; Shutter open:1 / close:0        % 0x09:1
   3: fwposon           ; FW Position sensor on:1 / off:0 % 0x09:1
   4: fwpos_b1          ; Filter Wheel Position bit #1    % 0x09:1
   5: fwpos_b0          ; Filter Wheel Position bit #0    % 0x09:1
   6: mposon            ; Mirror Position sensor on:1 / off:0% 0x09:1
   7: mpos_b1           ; Mirror Position bit #1          % 0x09:1
   8: mpos_b0           ; Mirror Position bit #0          % 0x09:1

   9: rstwidelon        ; Reset Wide-L on:1 / off:0       % 0x0C:1
  10: rstwideson        ; Reset Wide-S on:1 / off:0       % 0x0C:1
  11: rstn170on         ; Reset N160   on:1 / off:0       % 0x0C:1
  12: rstn60on          ; Reset N60    on:1 / off:0       % 0x0C:1
  13: lwbooston         ; LW BIAS Boost on:1 / off:0      % 0x0E:1
  14: swbooston         ; SW BIAS Boost on:1 / off:0      % 0x0E:1
  15: lwbiason          ; LW BIAS on:1 / off:0            % 0x0E:1
  16: swbiason          ; SW BIAS on:1 / off:0            % 0x0E:1

  17: calalon           ; CAL AL (LW) on:1 / off:0        % 0x0F:1
  18: calason           ; CAL AS (SW) on:1 / off:0        % 0x0F:1
  19: calbon            ; CAL B  (BG) on:1 / off:0        % 0x0F:1
  20: sinalon           ; CAL sin-conv. AL on:1 / off:0   % 0x0F:1
  21: sinason           ; CAL sin-conv. AS on:1 / off:0   % 0x0F:1
  (22-32: reserved)
```

The 'rstn170on' should be renamed to 'rstn160on'. However, we do not change it for historical reasons.

(3) Analog Telemetry

```
byte packetid           ; PacketID (FIS obsmode)         % 0x00:8
```

```
    byte rstcntwidel        ; Reset counter Wide-L        % 0x0A:4
    byte rstcntwides        ; Reset counter Wide-S        % 0x0A:4
    byte rstcntn170         ; Reset counter N160          % 0x0B:4
    byte rstcntn60          ; Reset counter N60           % 0x0B:4

    byte calplscntal        ; CAL pulse counter AL        % 0x0C:4
    byte calplscntas        ; CAL pulse counter AS        % 0x0D:4
    byte calplscntb         ; CAL pulse counter B         % 0x0D:4
    byte aderrcntsw         ; SW A/D error counter        % 0x19:4
    byte aderrcntlw         ; LW A/D error counter        % 0x19:4
    long mposcnt            ; Assigned mirror position    % 0x1A-0x2F
                            ; Assigned/interpolated frame
                            ; counter in the survey mode

    byte dacbiaswides       ; DAC BIAS Wide-S level       % 0x10:8
    byte dacbiasn60         ; DAC BIAS N60    level       % 0x11:8
    byte dacbiaswidel       ; DAC BIAS Wide-L level       % 0x12:8
    byte dacbiasn170        ; DAC BIAS N160   level       % 0x13:8

    byte daccalas           ; DAC CAL AS level            % 0x14:8
    byte daccalal           ; DAC CAL AL level            % 0x15:8
    byte daccalb            ; DAC CAL B level             % 0x16:8
    byte dacsinas           ; DAC CAL sin-conv. AS level  % 0x17:8
    byte dacsinal           ; DAC CAL sin-conv. AL level  % 0x18:8

    short tpbody            ; FIS body temperature        % 0x3E-3F
    short tpsw              ; SW Detector temperature     % 0x40-41
    short tplw              ; LW Detector temperature     % 0x42-43
    short tpcalft           ; CAL FT temperature          % 0x44-45
```

The 'rstcntn170' and 'dacbiasn170' should be renamed to 'rstcntn160' and 'dacbiasn160' respectively. For historical reasons, we keep the original name of the narrow LW band (N160) as 'rstcntn170' and 'dacbiasn170' in the data structure.

(4) Detector data

Either SW(NDET=100) or LW (NDET=75) data are included in one data set.

```
    long det[NDET]          ; Detector signal [ADU]
    float flux[NDET]        ; Detector data in physical unit
    float ferr[NDET]        ; Flux uncertaintity
```

(5) Flags

Flags are those set in the reduction software. These flags are set for each frame (sampling).

```
    bit flag[8]             ; Flag for detector condition
      1: bad_frame          ; set at all the unrecoverable frames
```

```
                                ; described by the other flags:1
  2: undef_anom_frame          ; unusable data but the anomaly cannot
                                ; be described by the existing flags.
  3: blank                     ; blank:1
  4: in_saa                    ; in SAA:1
  5: near_moon                 ; near moon:1
                                ; "aa_lun" is used for lunar avoidance
                                ; angle in GADS extension.
  6: untrusted_frame           ; incomplete restitution of higher-order bits of DET.
  (7-8: reserved)
```

These flags are set for each frame (sampling) and each pixel.

```
bit pix_flag[32*NDET]         ; Flag for each pixel condition
  1: bad                       ; bad pixel:1
  2: undef_anom                ; unusable data but the anomaly is not
                                ; described by any other flags.
  3: arith_err                 ; special values for undefined results;
                                ; NaN and INFINITY
  4: dead                      ; dead pixel:1
  5: saturate                  ; saturated pixel:1
  6: reset                     ; data taken just after reset:1
  7: rstanom                   ; anomaly seen in a few certain
                                ; samplings just after reset.
  8: no_diff                   ; No differentiation enable:1
  9: no_rp_corr                ; impossible to carry out ramp curve correction
  10: no_dk_corr               ; dark has not been subtracted successfully.
  11: no_dccal_corr            ; DC responsivity correction has not been
                                ; corrected successfully.
  12: no_tr_corr               ; transient effect has not been corrected successfully.
  13: no_flat_field            ; flat fielding has not been carried out successfully.
  14: no_gpgl                  ; unable to search/correct for glitch
  15: no_mtgl                  ; unable to search/correct for glitch
  16: no_abscal                ; abs. flux calibration has not been done successfully.

  ; For glitch detection using Gaussian Processing method(Kester)
  17: gpgl_type1               ; Glitch Type 1
  18: gpgl_type2               ; Glitch Type 2
  19: gpgl_type3               ; Glitch Type 3
  20: gpgl_type4               ; Glitch Type 4
  21: gpgl_tail                ; Glitch Tail

  ; For glitch detection using Median Transformation method (Serjeant)
  22: mtgl_type1               ; Glitch Type 1
  23: mtgl_type2               ; Glitch Type 2
  24: mtgl_type3               ; Glitch Type 3
  25: mtgl_type4               ; Glitch Type 4
  26: mtgl_tail                ; Glitch Bad

  27: no_peri_corr             ; No periodic noise correction available
```

```
;; For SUSSEXtractor
28: sx_peak            ; threshold detection
29: sx_source          ; source detected:1
30: sx_obj             ; anomalous detected
(31-32: reserved)
```

(6) Quality

```
bit quality[40*NDET]   ; Quality Flag for each pixel condition

  ;; gb_conv_to_volt ;;
  1-2: qual_cv_param   ; conversion quality from ADU to Volts.

  ;; gb_ramp_curve_corr ;;
  3-4: qual_rc_param   ; accuracy of correction parameters
  5-6: qual_rc_cf      ; correction factor (difference between
                       ; corrected and the original data)

  ;; gb_differentiation ;;
  7-8: qual_df_eq      ; order of polynomials/number of points used.

  ;; gb_dc_responsivity_corr / make_DC_cal_lamp_table ;;
  9-10: qual_rp_data   ; accuracy of the derived cal. lamp intensity
                       ; from data in a "cal. lamp on."
  11-12: qual_rp_param ; availability of "cal. lamp on" to derive
                       ; a correction factor
  13-14: qual_rp_table ; quality of the correction table (fluctuation etc.)

  ;; "correction for flat fielding" ;;
  15-16: qual_ff_param ; quality of the parameters for flat fielding
  17-18: qual_ff_cf    ; correction factor (difference between
                       ; corrected and the original data)

  ;; gb_set_glitch_status_gp & gb_set_glitch_status_gp ;;
  ;; -> correction after glitch detection
  19-20: qual_gpgl_corr; correction of glitch tails for Gaussian
                       ; processing method
  21-22: qual_mtgl_corr; correction of glitch tails for Median
                       ; transformation method

  ;; gb_transient_corr ;;
  23-24: quql_tr_hist  ; history information availability
  25-26: qual_tr_param ; correction parameter availability

  ;; gb_dark_subtraction/ make_dark_table ;;
  27-28: qual_dk_data  ; quality of the dark data in one "shutter-close".
  29-30: qual_dk_param ; availability of the data of a "shutter-close"
                       ; to derive a dark value.
  31-32: qual_dk_table ; quality of the dark values of the correction
```

```
                             ;  table (fluctuation etc.)

  ;; gb_flux_calib ;;
  33-34: qual_fx_corr  ; availability of calibration parameters
  35-36: qual_fx_param ; error in calibration factors
  (37-40: reserved)
```

(7) Counter

```
  short cnt_saa[NDET]       ; time in seconds since the last SAA passage
                            ; # "tm_saa" is used in SE extension
  short cnt_glitch_gp[NDET] ; duration since the last corresponding glitch(GP).
  short cnt_glitch_mt[NDET] ; duration since the last corresponding glitch(MMT).
```

FIS_HK extension

Outputs of APID='FIS_HK' (which contains some minor status of FIS) are stored in this extension.

(1) Time

```
double aftime           ; ASTRO-F (AKARI) Satellite Time (calibrated)
                        ; which is the time since 2000/January/1 00:00 (UTC)
longlong pimtiorg       ; PIMTI counter (from original packet)
```

(2) Status

```
bit status[8]           ; Satellite attitude status
   1: blank             ; blank:1
   2: blank_subcom_data ; blank bit for subcom data (for sw_heater_tmp)
   (3-8:reserved)
```

Note that some FIS status are stored in the HK_2 extension.

(3) Analog data

```
byte fis_fw_f_pul       ; Filter wheel pulse counter (Forward)
byte fis_fw_r_pul       ; Filter wheel pulse counter (Rewind)
byte fis_lw_wire_light  ; LW wire light DAC set value
byte fis_run_mode       ; RUN mode
byte fis_obs_mode       ; Observation mode
byte fis_asq_pattern    ; ASQ pattern
long fis_asq_step       ; ASQ step
byte sw_heater_tmp      ; SW heater temperature
```

IRC_HK extension

Outputs of APID='IRC_HK' (which contains status of temperature of the focal plane instruments) are stored in this extension.

(1) Time

```
double aftime            ; ASTRO-F (AKARI) Satellite Time (calibrated)
                         ; which is the time since 2000/January/1 00:00 (UTC)
longlong pimtiorg        ; PIMTI counter (from original packet)
```

(2) IRC status

```
bit status[8]            ; Status of IRC functions which may cause
                         ; interference
   1: blank              ; Data blank:
   (2-8:reserved)        ; Details TBD with IRC team
```

(3) Analog data

```
TBD
```

HK_2 extension

Outputs of APID='HK_2' (which contains basic data of Cryostat, FIS and IRC) should be stored
in this extension.

(1) Time

```
double aftime            ; ASTRO-F (AKARI) Satellite Time (calibrated)
                         ; which is the time since 2000/January/1 00:00 (UTC)
longlong pimtiorg        ; PIMTI counter (from original packet)
```

(2) Cryostat/FIS/IRC status

```
bit status[16]           ; CRYO/FIS status
   1: blank              ; blank:1
   2: blank_cryo_temp_data; blank bit for Cryo temperature data
   (3-4:reserved)
   5: cryo_temp_data_en_ds; Cryo temperature data enabled/disabled
   (6:reserved)
   7: fis_cpu_run_rst    ; FIS CPU run/reset
   8: fis_fis_on_off     ; FIS on/off
   9: fis_tmp_pol_pos_neg; Thermometer polarity
   10: fis_obs_seq       ; Observation sequence start/stop
   11: fis_rsw_auto_cmnd; Auto (periodic) reset mode on/off
   12: fis_fcal_frq_b1   ; CAL overlay sine wave frequency B1 bit #1
   13: fis_fcal_frq_b0   ; CAL overlay sine wave frequency B1 bit #0
   (14:reserved)
   15: irc_cpu_ru_rs     ; IRC CPU run/reset
   16: irc_irc_on_of     ; IRC on/off
```

(3) Cryostat temperature

```
float cryo_he_tank_1     ; He tank 1 temperature[K] (one close to heat strap)
float cryo_baffle_1      ; Baffle 1 temperature[K] (one close to the tel.?)
float cryo_baffle_2      ; Baffle 2 temperature[K]
```

(4) Cryostat current

```
float cryo_cold_hd_a_dr_i; Cold head A driving current[A]
float cryo_cold_hd_b_dr_i; Cold head B driving current[A]
float cryo_comp_a_dr_i   ; Compressor A driving current[A]
float cryo_comp_b_dr_i   ; Compressor B driving current[A]
```

(5) IRC Analog data

```
float irc_mainref_tmp1   ; Primary mirror temperature[K] (IRC)
float irc_subref_tmp     ; Secondary mirror temperature[K] (IRC)
float irc_fpip_tmp1      ; FPI plate[K] (IRC)
```

Attitude and Orbit Control Unit (AOCU) extension

Outputs of APID='AOCU' (Attitude and Orbit Control Unit) is stored in this extension.

(1) Time

```
    double aftime          ; ASTRO-F Satellite Time (calibrated)
                           ; which is the time since 2000/January/1 00:00 (UTC)
    longlong pimtiorg      ; PIMTI counter (from original packet)
```

(2) AOCU Status

```
    bit status[8]          ; AOCS operation status
       1: blank            ; blank:1
       2: ao_rom_ram       ; ROM mode:1 / RAM mode:0
                             i.e., the blank bit for the ads_mode_b1,
                             ads_mode_b0 and aodu_ads_q.
       3: ads_mode_b1      ; Attitude determination mode (AOCU_ADS_MODE) bit #1
       4: ads_mode_b0      ; Attitude determination mode (AOCU_ADS_MODE) bit #0
       (5-8:reserved)
```

(3) Analog telemetry

```
    double aocu_ads_q[4]    ; Quaternion at boresight
    double aocu_body_rate[3]; Body rate (Angular velocity[deg/s]) at boresight

    byte aocu_saab_mode    ; STT-A operation mode
    byte aocu_sbab_mode    ; STT-B operation mode
    byte aocu_saab_win_num ; Number of stars in STT-A
    byte aocu_sbab_win_num ; Number of stars in STT-B

    double ra              ; J2000 R.A. (deg) at boresight
    double dec             ; J2000 Dec. (deg) at boresight
    double roll            ; Roll angle at boresight (deg)
    double d_ra            ; Scan rate in J2000 R.A.
    double d_dec           ; Scan rate in J2000 Dec.
    double d_roll          ; Scan rate in roll angle

    double crs_off         ; Offset in cross-scan direction from
                           ; Nominal scan path
```

(4) Quality

```
    bit quality[8]         ; Quality Flag for condition
```

Ground-based Attitude Determination System (GADS) extension

Results of ground-based attitude determination are stored in this extension.

(1) Time

```
double aftime            ; ASTRO-F (AKARI) Satellite Time (calibrated)
                         ; which is the time since 2000/January/1 00:00 (UTC)
longlong pimtiorg        ; PIMTI counter (from original packet)
```

(2) Status

```
bit status[8]            ; Satellite attitude status
   1: blank              ; blank: 1
   (2-8:reserved)
```

(3) Analog telemetry

```
double attitude[4]       ; Quaternion at boresight
double attitude_er[3]    ; Estimated error of position
double angl_vel[3]       ; Body rate (Angular velocity) at boresight

double ra                ; J2000 R.A. (deg) at boresight
double dec               ; J2000 Dec. (deg) at boresight
double roll              ; Roll angle at boresight (deg)
double d_ra              ; Scan rate in J2000 R.A.
double d_dec             ; Scan rate in J2000 Dec.
double d_roll            ; Scan rate in roll angle

double el_sol            ; Solar elongation
double aa_sol            ; Solar Avoidance Angle
double aa_ear            ; Earth Avoidance Angle
double aa_lun            ; Lunar Avoidance Angle

double crs_off           ; Offset in cross-scan direction from
                         ; Nominal scan path
```

(4) Quality

```
bit quality[8]           ; Quality Flag for condition
```

Pointing Reconstruction (PR) extension

Results of pointing reconstruction is stored in this extension.

(1) Time

```
double aftime            ; ASTRO-F (AKARI) Satellite Time (calibrated)
                         ; which is the time since 2000/January/1 00:00 (UTC)
longlong pimtiorg        ; PIMTI counter (from original packet)
```

(2) Status

```
bit status[8]            ; Satellite attitude status
   1: blank              ; blank: 1
   (2-8:reserved)        ; Details will be discussed with ESA.
```

(3) Analog telemetry

```
double quaternion[4]     ; Quaternion at boresight
double pos_err[3]        ; Estimated error of position
double body_rate[3]      ; Body rate (Angular velocity) at boresight

double ra                ; J2000 R.A. (deg) at boresight
double dec               ; J2000 Dec. (deg) at boresight
double roll              ; Roll angle at boresight (deg)
double d_ra              ; Scan rate in J2000 R.A.
double d_dec             ; Scan rate in J2000 Dec.
double d_roll            ; Scan rate in roll angle

double el_sol            ; Solar elongation
double aa_sol            ; Solar Avoidance Angle
double aa_ear            ; Earth Avoidance Angle
double aa_lun            ; Lunar Avoidance Angle

double crs_off           ; Offset in cross-scan direction from
                         ; Nominal scan path
```

(4) Quality

```
bit quality[8]           ; Quality Flag for condition
```

Satellite Ephemeris (SE) extension

The following information is calculated from the satellite orbital parameters provided three times a week.

(1) Time

```
    double aftime            ; ASTRO-F (AKARI) Satellite Time (calibrated)
                             ; which is the time since 2000/January/1 00:00 (UTC)
    longlong pimtiorg        ; PIMTI counter (from original packet)
```

(2) Status

```
    bit status[8]            ; Satellite attitude status
       1: blank              ; blank:1
       2: type               ; Data type (Prediction/Determinated)
       3: daynight           ; Day / Night
       4: in_saa             ; in SAA region
       5: in_polar           ; in Polar region
       (6-8:reserved)
```

(3) Analog value

```
    double tm_saa            ; seconds since last SAA passage.
                             ; < 0 during the passage
                             ; Clock start at end of Bias Boost ?

    double sat_posx          ; Satellite position in Earth reference frame
    double sat_posy          ; Satellite position in Earth reference frame
    double sat_posz          ; Satellite position in Earth reference frame
```

6.2 Calibration Constant Files (CCF)

Calibration Constant Files (CCF) contain either correction factors or instrumental parameters necessary to:

- steer the processing

- to remove or to correct for instrumental effects in the data, and

- to carry out the flux calibration

In this section detailed descriptions are given of the structure and contents of the CCF files. Note that users do not have to deal with the CCF files directly unless they explicitly wish to change the calibration.

6.2.1 CCF Structure

A CCF file contains one set of parameter(s), i.e. a constant, an array, or a structure variable. Multiple values are packed in IDL type structures.

A CCF file consist of a header part, a data definition part, and one or more data body part(s).

Header starts with "#HEADER" and end at "#ENDHEADER".

Data type definition starts with "#DEFINE" and end at "#ENDDEFINE".

Data body starts with "#DATA" and end at "#ENDDATA".

The data definition appears before the data body.

The definition part contains a line starting with one of 'C' (constant), 'A' (array), or 'S' (structure) followed by variable type and array dimension. Structure definition also includes description of the structure in a similar style. Detailed explanation with examples are given below.

Data body part contains actual value(s) corresponding to the data type and dimension in the definition part. In case of array or structure they are read in the order of the definition.

Header

The header contains information about the CCF file which is used to maintain it.

Syntax:

```
#HEADER
NAME     CCF name
SET_NO   CCF set number
REV_NO   Revision of the data
STATUS   Validated or test version
RANGE    Applicable data range in AFTIME
CREATOR  Creator of the CCF
CDATE    Create date of the CCF
FMTVER   CCF Format version.
COMMENT  Comments
#ENDHEADER
```

```
Example:

#HEADER
NAME      C2VT_
SET_NO    001
REV_NO    001
STATUS    TEST
RANGE                 0.00000          0.00000
CREATOR   MAKIUTI
CDATE     2005-07-12T14:16:58
FMTVER    001
COMMENT   Threshold for conversion to Volt from ADU
#ENDHEADER
```

A constant parameter

The data definition contains only one line starting with 'C' that is followed by data type.

```
Syntax:

#DEFINE
C   type
#ENDDEFINE


#DATA
value
#ENDDATA


Example:

#DEFINE
C   double
#ENDDEFINE


#DATA
2.55837499234      ; this is an example of a constant.
#ENDDATA
```

An array parameter

The data definition part starts with an 'A' to indicate that the data is an array. Data type and array dimensions follow. Up to 8 dimensions (IDL limit) can be specified. Note that the left-most index changes first (IDL standard) in the multi-dimensional arrays (an array of [dim1, dim2] is created in the example below). The array values are given in the data body part. Any blank space, tabs or new lines are recognized as a delimiter, i.e., the values can be split over multiple lines.

```
Syntax:

#define
A double dim1 dim2 .....
#enddefine

#data
value1 value2 value3 .... value[dim1xdim2x...]
#enddata

Example:

#define
A double 2 3
#enddefine

#data
1 2
3                          ; comment1
5.5 3E-10
                           ; comment2
 6.5
#enddata
```

A structure parameter

The definition part of the structure CCF begins with a 'S' and the dimension size of the structure. Components of the structure ('Tag') are specified in the following lines. A tag definition starts with a 'T' and a structure tag name, then data definition (constant or array, see below).

The data body is included for each tag. Therefore there are the same number of pairs of '#DATA' and '#ENDDATA' as the number of tags in the definition. In order to identify each data body with the data tag, the data body starts with a 'T' and the tag_name before the values. A data body is present for each data tag. In case of an array of structures, the corresponding number of values are in the data body. For example, if the parameter is a 100 element array of structures, and one of the tags in the structure is an array of 3 elements, the data body will have 300 values, first the tag array for the 1st element of the structure, then for the 2nd structure...(see example).

```
Syntax:

#define
S dimS
   T tagname {C|A} datatype [dimension]
#enddefine

#data
T tagname
value
#enddata
```

```
Example:

#define
S 2
   T tag_cst C uint
   T tag_arr A double 2 3
#enddefine

#data
T tag_cst
100  ;  for the 1st structure element
200  ;  for the 2nd structure element
#enddata
#data
T tag_arr
0.1 0.2  ; they are for the 1st structure element
3
5.5 3E-10
 6.5     ; followings are for the 2nd structure element 1e2 1e2 1e2 2e3 2e3 2e3
#enddata
```

6.2.2   List of CCFs

Detector properties

BADPL	; Bad Pixel for the LW band.
BADPS	; Bad Pixel for the SW band.
DEADL	; Dead Pixel for the LW band.
DEADS	; Dead Pixel for the SW band.
CRNRL	; Detector corners for the LW band, wide resp narrow.
CRNRS	; Detector corners for the SW band, wide resp narrow.
OFSTL	; Detector offsets for the LW band, wide resp narrow.
OFSTS	; Detector offsets for the SW band, wide resp narrow.
RSTAL	; Reset anomaly for the LW band.
RSTAS	; Reset anomaly for the SW band.
SATUL	; Saturation level in Volt for the LW band.
SATUS	; Saturation level in Volt for the SW band.

Calibration

C2VT	; Threshold for conversion to Volt from ADU.
FLATL	; Ratio of A-Cal/(flat source) and error for the LW band.
FLATS	; Ratio of A-Cal/(flat source) and error for the SW band.
RCTBL	; Ramp curve correction table (flight preliminary)for the LW band.
RCTBS	; Ramp curve correction table (flight preliminary)for the SW band.
SIGJL	; sigma_j estimated from fis20050219_031354_04_lw.
SIGJS	; sigma_j estimated from fis20050219_031354_04_sw.
V2FL	; Scaling factor from Volt to Flux.

Constants

GLGP	; Parameters for various Glitch Processing modules.

Appendix A

FIS Slow-Scan Toolkit Cookbook

In this section we describe how to use the FIS Slow-Scan data reduction toolkit provided from the project team. This software tools are often globally referred to as the **fisdr** system.

A.1 Installation

A.1.1 Prerequisites

The toolkit is currently developed under IDL[1] version 6.3/6.4. It may work with IDL versions as early as 6.0 but it is not guaranteed. The toolkit does not support earlier versions of IDL. It has been reported that the software works under the Linux (Redhat/Fedora/CentOS/Vine), MacOS 10.4 and Windows XP environments. At least 512 MB of free memory space is required to process the Slow-Scan data. A computer with 1 GB or more memory is recommended.

The toolkit uses the IDL Astronomy Library (`http://idlastro.gsfc.nasa.gov/`). The routines contained in this library are often updated. Therefore, they are included in the distribution package in order to avoid compatibility problems. It is highly recommended to keep and use the distributed IDL Astronomy libraries and please be sure that your IDL set up will not cause version conflict with the package. The standard set up, as instructed in this cookbook, should not cause such a problem.

A.1.2 Distribution package

The **fisdr** software package is obtained from the Observation Support web page, as a tar+gzipped file. The file is named as `fisdr_YYYYMMDD.tar.gz`, where `YYYYMMDD` indicates the version.

The package is composed of several directories containing:

- All the Slow-Scan tool programs and calibration parameter files

- *GreenBox* modules from the All-Sky Survey Pipeline including the Calibration Constant Files (CCF) (see Chapter 4)

- The IDL Astronomy Library

- The FIS Data Visualizer (FISv; see Section A.3)

The distribution package also includes the startup directory which contains the initialization files of the FIS data reduction environment. They start-up IDL and set up the appropriate environment variables.

---

[1]IDL is a product of IIT Corporation (`http://www.ittvis.com/idl/`).

A.1.3   Setting and Starting up fisdr under Unix environment

The setup procedure described here is for Unix (including Linux/MacOS).

File extraction

Extracting the FIS reduction package file will create a directory `reduction_YYYYMMDD/` and will put all files in it. It is recommended to put this directory under the default location: `${your_home_directory}/ASTRO-F/`.

```
% cd ~
% mkdir ASTRO-F
% cd ASTRO-F

% tar xzvf fisdr_YYYYMMDD.tar.gz
        or
% gunzip -c fisdr_YYYYMMDD.tar.gz | tar xvf -
```

Change the directory name

The system assumes that the files are under the `˜/ASTRO-F/reduction/` directory. You may want to do one of the following under `˜/ASTRO-F/`:

- Make a symbolic link (We recommend this method).

  ```
  % ln -s reduction_YYYYMMDD reduction
  ```

- Change the directory name.

  ```
  % mv reduction_YYYYMMDD reduction
  ```

Start up fisdr

```
% ~/ASTRO-F/reduction/startup/bin/fisdr
```

This will startup IDL and set up several internal variables/constants used in the system. You may want to add the above path to your default setup, or define an alias to the command in your `.cshrc` or `.bashrc` etc.

```
% set path=( ~/ASTRO-F/reduction/startup/bin/ $path)
```

```
% alias fisdr ~/ASTRO-F/reduction/startup/bin/fisdr
```

If you prefer idlde environment, you can call it with the '-de' option:

```
% fisdr -de
```

Environment variables

Two environment variables are defined for stating up the Slow-Scan tool.

FISDR_ROOT specifies the `fisdr` ROOT directory where all the package files are stored. The default (the value applied when this environment variable is not set) is `/ASTRO-F/reduction`.

```
setenv FISDR_ROOT my-reduction-directory/reduction/
# for csh, tsch etc. and

FISDR_ROOT=my-reduction-directory/reduction/
export FISDR_ROOT
# for sh etc.
```

FISDR_USER_SETUP Some users have their own IDL setup for example the display colour mode etc. They are often given in `/.idlrc`. An IDL batch script file specified in this environment variable is executed during the startup process and will set appropriate parameters. Note that the **fisdr** standard setup may over ride the user's setup.

```
setenv FISDR_USER_SETUP ~/.idlrc
# for csh, tsch etc. and

FISDR_USER_SETUP=~/.idlrc
export FISDR_USER_SETUP
# for sh etc.
```

Details of the startup procedure

When the `fisdr` command is executed it checks the FISDR_ROOT environment variable. If the environment variable is not set it assumes the default location (`~/ASTRO-F/reduction/`). Then it sets the IDL_STARTUP environment variable to the standard **fisdr** setup script ${FISDR_ROOT}/startup/pro/startup_fisdr. startup_fisdr is a simple IDL batch file that calls `fisdr.pro`, which actually sets the **fisdr** internal environment variables.

The startup script `fisdr` over rides the IDL_STARTUP variable originally set by the user. If users want to apply their own IDL setting, the FISDR_USER_SETUP should be used to specify a setup script. The file is actually executed in `fisdr.pro`. Note that the calling the script given by FISDR_USER_SETUP is before the main setup in `fisdr.pro`, and the users setup may be overrode. Also, it is not guaranteed that the **fisdr** system will work properly with the user's setup.

IDL 6.2 and later versions run the startup script every time the session is reset by the `.reset_session` command so that users can maintain the proper environment. In the earlier version you may be able to recover the environment with;

```
IDL> fisdr
```

command (though earlier versions are not officially supported).

A.1.4   Setting and Starting up fisdr under the Windows environment

The `fisdr` system should also work properly under the Windows environment although it is not thoroughly tested. Contributions from users are welcome.

File extraction

User should prepare file extraction tools for tar.gz file. The usage of such tools is dependent on the specific software so it is not explained here. The file can be located anywhere in the PC, but may be somewhere like
`ASTRO-F`
`reduction`
under the users home directory.

Change the directory name

Similarly to the Unix system, change the directory name from `reduction_YYMMDD` to `reduction`. Creating a shortcut is also possible.

Setting the startup script

We provide a Visual Basic Script for starting up the **fisdr** system on Windows. You need to edit the script for your personal environments.

The script file is `${HOME}/ASTRO-F/reduction/startup/bin/win_fisdr.vbs`. You can copy the file to Desktop or anywhere you like. Open the file with editor and set the `fisdr_root` variable to point the directory where you have the system.

```
' ===================================================================
'  Please edit the following line to point the directory where you
'  locate the toolkit.
' ===================================================================

fisdr_root = "C:\Documents and Settings\astrof\ASTRO-F\reduction\"

==> (for example)

fisdr_root = "C:\Documents and Settings\myhomedir\ASTRO-F\reduction\"
```

Start `win_fisdr.vbs`

Click the icon of `win_fisdr.vbs`. If the set up is correct and IDL is properly installed in the system you will see that IDL starts and says "FISDR: Environment setup done." In case of trouble, check the above setup or contact to Helpdesk.

A.2   The Slow-Scan tool

The Slow-Scan data reduction tools consist of a series of IDL procedures which are under the directory reduction/slowscan/. In principle, all processes can be controlled from the main routine `ss_run_ss.pro`. The processing of the FIS Slow-Scan data consists basically of two steps which are executed by `ss_run_ss` making use of two main routines:

- `ss_init_proc.pro`: Flagging bad data, measurement of sky signal, and production of dark and responsivity correction tables.

- `ss_make_map.pro`: Calibration, flat-fielding, and construction of co-added images.

The following people mainly contribute to the development of the Slow-Scan tool: S. Matsuura, M. Shirahata, S. Makiuti, I.Yamamura, T. Suzuki (ISAS).

A.2.1   Running `ss_run_ss`

First Look Processing

Consider an example set of pointed observation data in the directory
~/ASTRO-F/fisdata/AKARI_FIS_1234567_001/.

```
% cd ~/ASTRO-F/fisdata/
% ls AKARI_FIS_1234567_001/
FIS_LW_20061225081641_1770.fits.gz  FIS_SW_20061225081641_1770.fits.gz
FIS_LW_20061225081641_1770.jpg      FIS_SW_20061225081641_1770.jpg
README
```

(WARNING: You may want to preserve the jpeg files as they are overwritten during the processing).

Start up fisdr and run `ss_run_ss` with the default setup:

```
% fisdr
IDL> ss_run_ss, 'AKARI_FIS_1234567_001', /AOCU
```

The program will search for all the FIS data (`FIS_[SW|LW]_*.fits.gz`) in the specified directory and will attempt to process them.

The option '`/AOCU`' is needed if you want to compare your results with the sample jpeg files (see Section 5.4). See below for more details on the different running options.

You will see some plots and images in different plot windows. If the processing completes without error, the program will produce several output files in the directory:

```
[Input data]
FIS_[SW|LW]_20061225081641_1770.fits.gz

[Intermediate files]
FIS_[SW|LW]_20061225081641_1770_ar.sav
FIS_[SW|LW]_20061225081641_1770_pr.sav
FIS_[SW|LW]_20061225081641_1770_cal.sav
FIS_[SW|LW]_20061225081641_1770_dark.sav
FIS_[SW|LW]_20061225081641_1770_flat.sav
```

```
[Output result files]
FIS_[SW|LW]_20061225081641_1770_img.jpg
FIS_[SW|LW]_20061225081641_1770_img.sav
FIS_[SW|LW]_20061225081641_1770_img_[w|n].fits
FIS_[SW|LW]_20061225081641_1770_err_[w|n].fits
FIS_[SW|LW]_20061225081641_1770_num_[w|n].fits

(with /CUBE_FITS option the following files are created instead of
*_img, *_err, *_num files).
FIS_[SW|LW]_20061225081641_1770_cube_[w|n].fits
```

Compare the jpeg files with those attached in the package. If they look identical, the toolkit works as it is supposed to.

Note that the results may be different if the version of the toolkit is different. A file called "VERSION" included in the data distribution package contains the version of the toolkit used to generate the jpeg files.

Looking at Images

Several image data/files are created by ss_run_ss.pro:

```
*_img.jpg          : jpeg format image files
*_img.sav          : image data in IDL save set files
*_img_[w|n].fits   : image map of wide/narrow band data
*_err_[w|n].fits   : error map of wide/narrow band data
*_num_[w|n].fits   : density map of wide/narrow band data

*_cube_[w|n].fits  : image/error/density maps are in a cube fits file
```

The *_img.sav files contain the following data:

```
IDL> restore, 'AKARI_FIS_1234567_001/FIS_SW_20061225081641_1770_img.sav'
IDL> help
COAD_DET        DOUBLE    = Array[2, 144, 170]
   : Image of WIDE (coad_det[0, *, *]) and NARROW (coad_det[1, *, *])
   : detectors in MJy/sr.

COAD_STDERR     DOUBLE    = Array[2, 144, 170]
   : Error map of the WIDE/NARROW detectors.
   : (RMS of the data points per pixel).

COAD_NUM        DOUBLE    = Array[2, 144, 170]
   : Density map of the WIDE/NARROW detectors.

IM_LAT_COORD    DOUBLE    = Array[144, 170]
IM_LON_COORD    DOUBLE    = Array[144, 170]
   : Position of all pixels of the image array in degrees.

DATA_TYPE       STRING    = 'FIS_SW'
   : type of input data. Either 'FIS_SW' or 'FIS_LW'
```

```
GRID_SIZE       DOUBLE    =    0.0041666667
   : grid size of the image

MAP_MEAN        DOUBLE    = Array[2, 4]
   : Information of the image data
   : MAP_MEAN[0, *] : WIDE band
   : MAP_MEAN[1, *] : NARROW band
   : MAP_MEAN[*, 0] : Average sky level (3-sigma clipped)
   : MAP_MEAN[*, 1] : Standard deviation of sky level
   : MAP_MEAN[*, 2] : Number of sky data points

HDR             STRING    = Array[27]
   : FITS header strings
```

A.2.2   Available options for ss_run_ss

ss_run_ss has many options for selecting the data reduction/calibration methods, as well as to control its functions.

[**Process flow control**]

```
/INIT
   : Stop after ss_init_proc completed.

/MAP
   : Run only ss_make_map module. Data should have been processed by
   : ss_init_proc (with /INIT option). This allows different options of
   : ss_make_map to be tested without running ss_init_proc every time.

/SW, /LW
   : Process only SW / LW data.
```

[**Input / Output file names**]

```
TAG_NAME = tag_name
   : Add a specified string to the output file names. For example,
   : tag_name = '_new' will make the output file names as,
   : FIS_[SW|LW]_20061225081641_1770_new_img_[w|n].fits.

/FILE_INPUT
   : The first argument of ss_run_ss is a file name instead of
   : directory name.

/CUBE_FITS
   : Generate image cube fits containing image, error, and density
   : maps in a FITS file, instead of three independent files. The output
   : file names are *_cube_[w|n].fits.
```

[**Selection of positional information**]

```
/AOCU_ADS
   : Use the AOCU determined boresight position instead of
   : default G-ADS position data.
```

[Options for signal measurements]

The following options are passed to ss_init_proc.pro.

```
N_RAMP_DIV = n_ramp_div
   : By default a linear fit is applied to each integration ramp to derive
   : the signal level. If N_RAMP_DIV greater than 1 is given, A ramp
   : is divided into n_ramp_div's, and linear fitting is made for each
   : segment of the divided ramp. Taking n_ramp_div greater than 1 provides
   : higher spatial resolution in the in-scan direction at the cost of
   : noise level, as well as increased calibration uncertainty due to any
   : remaining non-linearity of the ramps after the correction.
```

```
/USE_BAD
   : In addition to automatic detection and flagging of the bad data by the
   : program, this option force the program to refer to PIXEL_BAD flag in
   : the input TSD and discard flagged data. This option is used to reflect
   : the results of manual flagging of data prior to use of the Slow-Scan tool
   : with the FISv data browser. Default is that PIXEL_BAD is not checked.
```

```
/LOCAL_FLAT
   : To use the 'blank' sky data in the observation for flat-fielding.
   : If T_FLAT_START and T_FLAT_END (as specified below) are not
   : provided, the data during attitude settling (approximately 420-630 sec
   : from the beginning of the data) are used for the correction.
   : Without this option flat-fielding is applied using 'the nominal flat'
   : built from the PV observations of zodiacal light and cirrus emission.
   : The usage of /LOCAL_FLAT may provide better flat-fielding results
   : for flat (quiet) skies.
```

```
T_FLAT_START = t_flat_start
T_FLAT_END = t_flat_end
   : They are only valid with the /LOCAL_FLAT option and specify the
   : data range used for local flat-fielding. They are in seconds
   : from the beginning of the TSD data. The defaults are:
   :              T_FLAT_START    T_FLAT_END
   : PV data        540 sec          750 sec
   : Phase 1&2      540 sec          630 sec
```

```
PLOT_PIXEL = plot_pixel
   : 'ss_init_proc' procedure displays several plots of data as
   : a function of time/index during the process. This option
   : specifies the detector pixel number(s) to be plotted.
   : The default setting is plot_pix=5.
```

```
/RAMP_COR_OFF
```

```
: Ramp curve correction (non-linearity correction) is not applied
: before the linear fitting process. Usually ramp curve correction
: is needed for all data sets.


/GLITCH_RMV_OFF
: Do not detect + mask glitches.
```

[Options for calibration and map making]

The following options are passed to ss_make_map.pro.

```
/PIX_MAPPING
: By default ss_make_map.pro creates so called "foot print map";
: each data point in the input time series data is placed on
: an image pixel closest to the data position. With this option
: convolution by a disk of a radius corresponds to the beamsize
: is applied. This fills void pixels often seen in some data.


/TRANS_COR
: A simple correction of the detector responsivity time variation
: caused by the calibration lamp, by iterpolating the signal
: level at before and well after the lamp. Default is OFF.


/MEDIAN_FILTER
: Apply a median filter to the time series data for removing
: remaining background offsets between the pixels as well as
: excess by stray light from the Earth shine. This median
: filtering is only applicable for point sources. Diffuse
: sources with a spatial scale comparable to the 'WIDTH\_FILTER'
: used (see below) would be also filtered out by this process.
: The default filter width is 40 seconds.


/SMOOTH_FILTER
: Similar to MEDIAN_FILTER but use boxcar smoothing to
: evaluate the background offsets instead of the median.
: The default filter width is 40 seconds.


WIDTH_FILTER
: (previously known as WIDTH_MEDIAN).
: The width of the MEDIAN_FILTER/SMOOTH_FILTER, in units of
: seconds. The default is 40 seconds.


SIGMA = sigma
: Sigma clipping threshold for the map making. Default is 2.0.
: Smaller values (e.g., 1.5) may improve the output quality
: with a risk of less data points used to make the maps.


T_START = t_start
T_END = t_end
```

```
    : Specify start and end of the data used to make the images.
    : Given in units of seconds counted from the beginning of the
    : TSD data. The defaults are:
    :            T_START      T_END
    : PV data      750 sec    1350 sec
    : Phase 1&2    630 sec    1350 sec


/GALACTIC
/ECLIPTIC
    : Specify the coordinate system of the output images.
    : The default coordinate system is Equatorial (J2000)


LON_CENTER = lon_center
LAT_CENTER = lon_center
    : Centre position of the image. By default centre position is
    : estimated from the input data. These options are useful when
    : one wants to compare the images from different data sets of nearby sky.
    : Units are in degree, in the corrdinate system specified.


LON_SIZE = lon_size
LAT_SIZE = lat_size
    : Image size in degrees. By default image size is automatically
    : determined to cover the input data. Useful to make consistent
    : set of images from different observational data sets.


GRID_SW = grid_sw
GRID_LW = grid_lw
    : Grid size of the resulting image map in arcsec. Default values are:
    :       AOT    FIS01        FIS02
    :       SW     15 arcsec    30 arcsec
    :       LW     30 arcsec    60 arcsec
    : Smaller grid sizes for low-redundancy data may result in
    : many void pixels in the image. Note that the grid size
    : has the lower limit given by the program automatically,
    : and too small values for the parameters are truncated to
    : the lower limits. The values are defined as;
    :    grid_limit = beam_size/3600D/n_int*(scan_speed/15["/s])
    : where beam_size is 40 and 60 arcsec for SW and LW detectors,


BAD_THRSHLD = bad_thrshld
    : Responsivity of each pixel derived from the observational data
    : is compared with the 'nominal' value in the responsivity table
    : and if the difference is larger than a factor specified by this
    : option the data of that pixel is not used throughout the observation.
    : The cause of responsivity change could be glitch after effects.
    : The default is 10 (practically no flagging).


/SCUT
    : Produce individual images per one way scan, i.e, four images
    : are produced for FIS01 observations (two roundtrips) and two
```

```
           : images for FIS02 observations (one roundtrip). This option is
           : useful to confirm source detections by comparing independent
           : scans. Normal coadded image (from all scans) is also created.
           : Output image files are labeled as;
           : *_img_[1,2,..].sav & *_img_[1,2,..]_[w|n].fits.

  /SL_RMV
           : When this keyword is set, the stray light caused by the Earth
           : shine reflected at the telescope baffle is subtracted. The
           : stray light component is evaluated by a boxcar filter of 90
           : seconds width, then subtracted from the data.

  /MASK_OFF
           : Normally, data in the state of Shutter close and CAL-ON are
           : masked and do not appear in the output data.
           : If this keyword is set, the masked data appears in the output
           : data file and the output image. For experts and debugging.

  /RESP_COR_OFF
           : If this keyword is set, the responsivity correction is not
           : performed  and the output is the slope of the ramp in units
           : of [V/s]. For experts.
```

[Image plot style options]

The following options are passed to ss_make_map.pro.

```
/COORD_GRID_ON
     : Display coordinate grid on a JPEG image.

/OUTLINE
     : Produce jpeg image with outline contour.

CONTOUR_NUM=contour_num
     : Number of contour lines drawn in the JPEG image map.
```

[Batch mode process control]

These options are prepared for batch processing at ISAS and are not relevant for the users.

```
/NO_DISPLAY
     : Running in batch process mode and do not display
     : any plots on the screen.

/MK_TXT_FILE
     : Create text file format intermediate files.
     : This option remains for compatibility with the older versions.
     : It is not recommended for the observers.
```

```
/DEL_FILES
   : Delete output files (*.txt, *.sav, *.fits) other than image jpeg files.

/VERSION_COPY
   : Copy the version file into the processed directory.
```

A.2.3   Tips and suggestions for Slow-Scan data reduction

Here we note some useful *recipes* for the Slow-Scan tools for several typical cases we have experienced. The Slow-Scan toolkit has been used with a relatively limited number of data sets by the developers. Comments and contributions from the users are welcome and will improve future versions of the pipeline.

/AOCU option
> As of September 2007 the default positional information from `G-ADS` is yet to be confirmed to be reliable. Therefore we recommend to use this option to apply `AOCU` position and compare the results.

Improving flat-fielding
> It is reported that the `/LOCAL_FLAT` option often improves the flat-fielding of the image. It is most effective if the background sky is relatively smooth. `/MEDIAN_FILTER` is another option to correct any remaining offset between the scans/pixels.

Very dark sky
> Give `T_FLAT_START` and `T_FLAT_END` to cover the entire observing region together with `/LOCAL_FLAT`. If the sources in the region give only minor contribution to the total flux from the region this could even further improve the flat-fielding. The data range in seconds from the beginning of the file can be obtained with FISv (See Section A.3) by selecting `aftime` in X-axis.

Measuring the sky brightness
> If absolute sky brightness of the diffuse radiation is important, try `/SL_RMV` and `/TRANS` options together.

Point sources / Small extended sources
> Try `/SL_RMV` + `/TRANS` + `/MEDIAN`, or `/TRANS` + `/MEDIAN_FILTER`. Applying `/MEDIAN_FILTER` option improves the RMS noise of the image and is useful to detect faint point sources.

/MEDIAN_FILTER and /SMOOTH_FILTER For the bright sources `/SMOOTH_FILTER` results in smaller "holes" next to the sources.

SIGMA option
> Try `SIGMA=1.5` which may remove more outlier data points resulting in better images.

Comparison between scans in an observation
> `/SCUT` option will produce separate images for each one-way scan in the observations. You can compare them for cross-checking of detections and consistency of the positions, etc...

Removing glitch effects
> If bright lines (stripes) are observed, try using a `BAD_THRSHLD` lower than the default (10). Often such stripes are responsivity jumps due to glitches. By giving a lower `BAD_THRSHLD`, pixels with a responsivity level higher than nominal can be discarded.

A.2.4   Behind `ss_run_ss`

In the following section we describe the two major steps in the Slow-Scan processing. They correspond to two separate programs: `ss_init_proc` and `ss_make_map`. These programs are executed from `ss_run_ss`. Note that the contents of the following sections are subject to continuous update without notification.

Dark and responsivity correction tables: `ss_init_proc.pro`

`ss_init_proc` generates dark and responsivity correction tables in [V/s], which are used by `ss_make_map` for further calibration and map making. This routine is called from the main program `ss_run_ss` with all available options. Therefore users are not required to apply this routine directly.

   `ss_init_proc` procedure makes use of the following routines:

`ss_flux_ave.pro` calculates mean flux of line fit data in a given time range.

`ss_aftcal_ave.pro` makes a template of CAL after effect signal and output data table (only for PV-phase observations).

`ss_q_to_radec` calculates equatorial coordinates of each pixel from quaternion in `GADS` or `AOCU` data.

   `ss_init_proc` produces several intermediate data files in the IDL save file format. These files will be used at the following steps in the processing. Users can ignore these files but those interested in the details and who would like to participate in the data reduction activity to improve the results, are advised to contact the data reduction team in Japan via the Helpdesk. The AKARI data reduction support team welcomes the users' participation.

```
FIS_[SW|LW]_20061225081641_1770_pr.sav
   : Time series calibrated detector signal and related information.
   : ({\tt "pr"} denotes Pre-Reduction).

FIS_[SW|LW]_20061225081641_1770_cal.sav
   : Information of calibration lamp signal strength.

FIS_[SW|LW]_20061225081641_1770_dark.sav
   : Information of dark measurement signal strength.

FIS_[SW|LW]_20061225081641_1770_flat.sav
   : Information of flat-fielding measurements.
```

   `FIS_[SW|LW]_*_pr.sav` contains the following information. The data are time sequential 3542 data points of the SW (=100 pixels) detector. `*_cal.sav`, `*_dark.sav`, and `*_flat.sav` files are also explained.

```
FISDR> restore, 'FIS_SW_20070705213613_1770_pr.sav'
FISDR> help
RCOUNT          LONG      =          3542
   : Number of data points (number of ramps used)
```

```
X_AVE            DOUBLE    = Array[3542]
   : Data sampling index averaged over each ramp.

COEFF            DOUBLE    = Array[100, 3542, 2]
   : Results of the linear line fit of each ramp.
   : [#pixels, #ramps, coeff]
   : [*, *, 0] = offset, [*, *, 1] = tilt.

ERROR            DOUBLE    = Array[100, 3542, 2]
   : Uncertainty of the linear fit.

EG_GL_CNT        INT       = Array[100, 3542]
   : Number of glitches detected in each ramp.

CAL_FLG_TOT      INT       = Array[3542]
   : Number of data points with calibration lamp is ON in each ramp.
   : If not zero, the ramp contains calibration lamp signal

SHT_FLG_TOT      INT       = Array[3542]
   : Number of data points with shutter open - number of data points
   : with shutter close.

DRV_MASK_TOT     INT       = Array[3542]
   : Number of data points with calibration lamp is ON or
   : shutter is closed per ramp. If not zero, the ramp
   : does not contain sky observation data.

Q_MEAN           DOUBLE    = Array[4, 3542]
   : Quarternion averaged over each ramp.

AA_MEAN          DOUBLE    = Array[3542]
   : Earth Avoidance Angle (EAA) averaged over each ramp.

AOT              STRING    = 'P12_FIS01'
AOTPARAM         STRING    = '0.5;8;70'
DATA_TYPE        STRING    = 'FIS_SW'
   : Information about the observation.

N_INT            INT       =        1
   :  Value given by N_RAMP_DIV option. 1: default (data point
   :  corresponds to each ramp).

RST              STRING    = '05N'
   : Internal status to identify the reset mode.

RST_INT          DOUBLE    =      0.47468354
   : The actual reset interval in seconds.

AOCU_ADS         INT       =        0
```

```
GLITCH_RMV_OFF  INT        =         0
RAMP_COR_OFF    INT        =         0
   : Options for ss_init_proc.pro. 1 : ON.
```

    ∗ cal.sav, ∗ dark.sav, ∗ flat.sav contains calibration information.

```
FISDR> restore, 'FIS_SW_20070705213613_1770_cal.sav'
FISDR> help
FLUX_CAL        DOUBLE    = Array[4, 100, 7]
   : Signal level of calibration lamp data.
   : [#data, #pixel, #cal.lamp_data].
   : An FIS01 observaton data file contains seven calibration
   : lamp data and an FIS02 data file has five.
   : [0, *, *] = Pixel index.
   : [1, *, *] = Average calibration lamp strength [V/s].
   : [2, *, *] = Uncertainty of the averaged value (rms/sqrt(N-1)).
   : [3, *, *] = Number of data samples N.


FISDR> restore, 'FIS_SW_20070705213613_1770_dark.sav'
FISDR> help
FLUX_DARK       DOUBLE    = Array[4, 100, 8]
   : Signal level of dark data (shutter close signal).
   : [#data, #pixel, #dark_data].
   : An FIS01 observaton data file contains eight dark
   : measurements and an FIS02 data file has six.
   : The meaning of the first dimension is the same as FLUX_CAL.


FISDR> restore, 'FIS_SW_20070705213613_1770_flat.sav'
FISDR> help
FLUX_FLAT       DOUBLE    = Array[4, 100]
   : Signal level of the flat-field data.
   : [#data, #pixel].
   : The meaning of the first dimension is the same as FLUX_CAL.
```

    /MK␣TXT␣FILE option additionally creates the following text format files. The contents of the files are almost the same as those in the .sav files. They are only left for compatibility and are not recommended to use by the observers.

```
FIS_[SW|LW]_20061225081641_1770_dark_[0,1,2,...].txt
FIS_[SW|LW]_20061225081641_1770_cal_[0,1,2,...].txt
FIS_[SW|LW]_20061225081641_1770_cal_dark.txt
FIS_[SW|LW]_20061225081641_1770_flat.txt
FIS_[SW|LW]_20061225081641_1770_flat_dark.txt
FIS_[SW|LW]_20061225081641_1770_fit_pr.txt
FIS_[SW|LW]_20061225081641_1770_fit_ar.txt
FIS_[SW|LW]_20061225081641_1770_ctof.txt
```

Co-add image processing: `ss␣make␣map.pro`

`ss␣make␣map` reads the output files of `ss␣init␣proc`, applies calibration, and creates the co-add image in various formats. The procedure `ss_init_proc` is called from `ss␣run␣ss` with all options. Therefore users are not required to use this routine directly.

ss_make_map procedure makes use of the following routines:

ss_resp_corr returns the absolute responsivity.

ss_q_to_radec calculates equatorial coordinates for each pixel from the quaternion in the `GADS` or `AOCU` data.

ss_trans_corr improves transient effects after calibration lamp operation.

ss_eg_lpf applies median/boxcar-smooth low-pass filtering to extract DC/slow components Earth shine.

ss_eg_slrmv extracts slow component and stray light from time-series data by an easy way with median/boxcar smooth filter.

ss_coad_image Constructs co-add images of the entire array.

ss_make_map produces the following output files:

```
FIS_[SW|LW]_*_ar.sav
   : Time series processed data, RA & DEC position, and parameters
   : ({\tt "ar"} denotes After-Reduction).

FIS_[SW|LW]_*_img.sav
   : Co-add image data, RA & DEC position, and parameters.

FIS_[SW|LW]_*_img_[w|n].fits
   : image map of wide/narrow band
FIS_[SW|LW]_*_err_[w|n].fits
   : error map (statistical uncertainty of each pixel)
   : of wide/narrow band image
FIS_[SW|LW]_*_num_[w|n].fits
   : density map (number of data points contributed to each pixel)
   : of wide/narrow band data

FIS_[SW|LW]_*_img.jpg
   : co-add image as jpeg image.

(with /CUBE_FITS option the following files are created instead of
*_img, *_err, *_num files).
FIS_[SW|LW]_*_cube_[w|n].fits
```

Description about the image files are given in the previous section. `FIS_[SW|LW]_*_ar.sav` are the IDL save file that contains the following information. The following example data are time sequential 879 data points of the SW (=100 pixels) detector.

```
IDL> restore, 'FIS_[SW|LW]_*_ar.sav'
IDL> help
RA              DOUBLE     = Array[100, 879]
DEC             DOUBLE     = Array[100, 879]
   : Position information of every pixels at every
   : sampling points.
```

```
DET             DOUBLE   = Array[100, 879]
   : Calibrated detector signal.

ERR             DOUBLE   = Array[100, 879]
   : Uncertainty of the detector signal.

EG_GL_CNT       INT      = Array[100, 879]
   : Number of glitches detected in each ramp.

BAD_FLG         INT      = Array[100]
   : 1 for band pixels (not used in the processing).

X               DOUBLE   = Array[879]
   : Data sampling index averaged over each ramp.

AOT             STRING   = 'P12_FIS01'
DATA_TYPE       STRING   = 'FIS_SW'
   : Information about the observation.

N_INT           INT      =        1
   :  Value given by N_RAMP_DIV option. 1: default (data point
   :  corresponds to each ramp).

RST             STRING   = '10N'
RST_INT         DOUBLE   =       0.94936709
   : The actual reset interval in seconds.

AOCU_ADS        INT      =        1
GLITCH_RMV_OFF  INT      =        0
RAMP_COR_OFF    INT      =        0
   : Options for ss_init_proc.pro. 1 : ON.
```

A.3   The FIS Data Visualizer (FISv)

The FIS Data Visualizer (FISv) is a Graphical User Interface (GUI) tool that has been created in order to provide a method of easy access to the FIS data (Time Series Data: TSD) and to easily display time series data such as the "detector signal", "Instrument status", "flags", etc...

FISv is distributed as part of the Slow-Scan toolkit and is written in IDL. To begin the FISv tool, you simply start a fisdr session as explained at the beginning of this chapter and type **fisv** or **FISV**.

Then you will see a window similar to that shown in Figure A.3.1.

A.3.1   Main Functions: Input/Output

There are four action buttons to open and save TSD files and to close the FISv application. When a TSD file is opened all the different options and functions become active as shown in Figure A.3.1.

The option "Open TSD file from LDS" is not applicable to the users as it is for accessing the Local Data Server at ISAS (Japan).
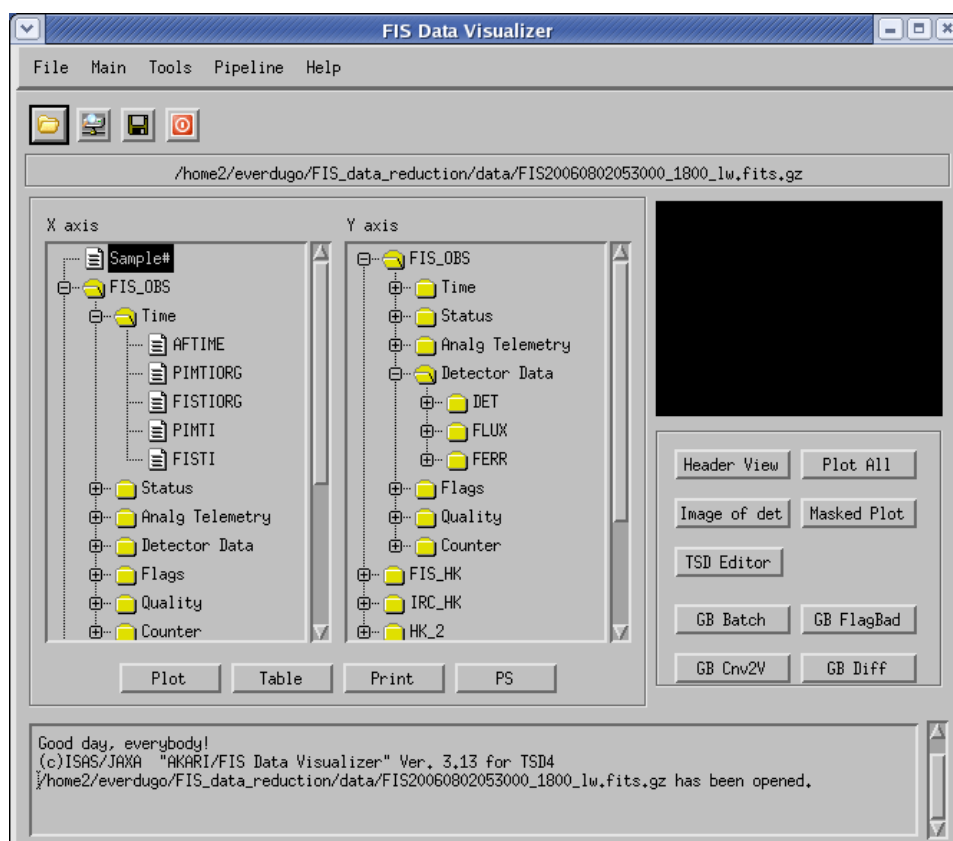
Figure A.3.1: TSD file opened with FISv

In the two windows, labeled "X axis" and "Y axis", appear all the extensions contained in the TSD file (that can be visualized using the Header View button) and the items under the extension FIS_OBS. Any of these items can be plotted against one another by selecting the appropriate entry in the corresponding "X" and "Y" axis windows. A Preview graph appears as is shown in Figure A.3.2.
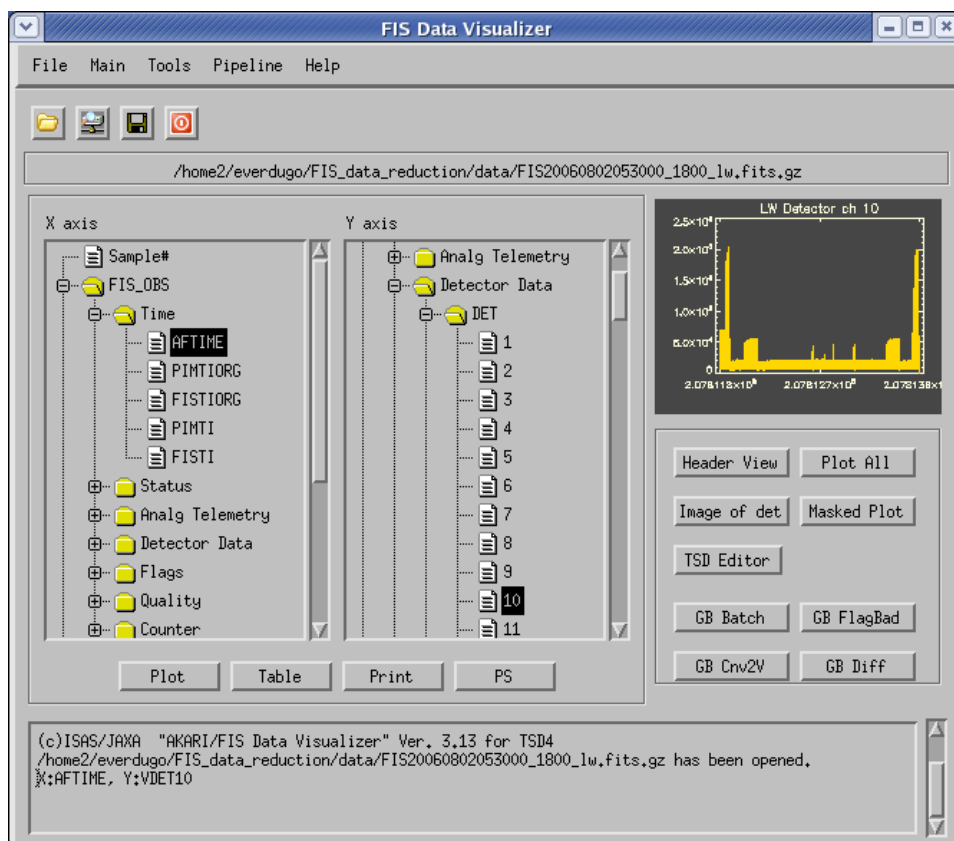
Figure A.3.2: Detector 10 signal plotted against AKARI satellite time

Output options include:

Plot. The currently displayed graph image can be plotted by clicking on the action button "Plot". A FISv plot window as the one shown in Figure A.3.3 will appear.
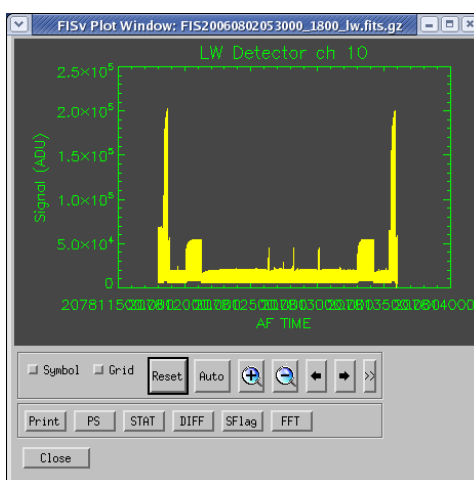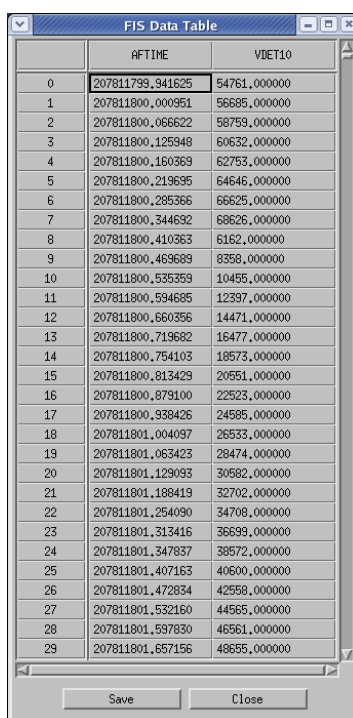
Figure A.3.3: Detector 10 signal plotted against AKARI satellite time

Table. A Dump of the data into a text format file is also possible with the action button "Table" (see Figure A.3.4).

Figure A.3.4: Dump of data into text format file

Print. Print out the currently displayed graph image. Button "Print" will give the option to print out the currently featured graph or to save it as a postscript file.
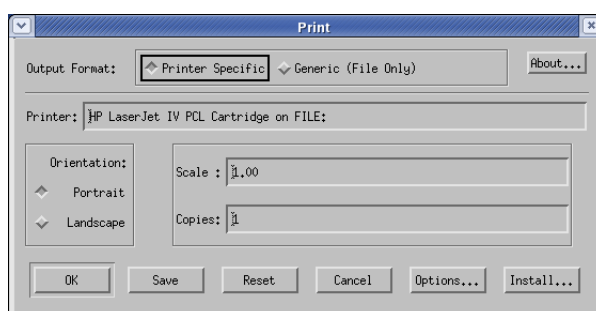

Figure A.3.5: Printer setup dialog

PS. A postscript file can also be generated from the "PS" button. A window with the configuration options will appear.
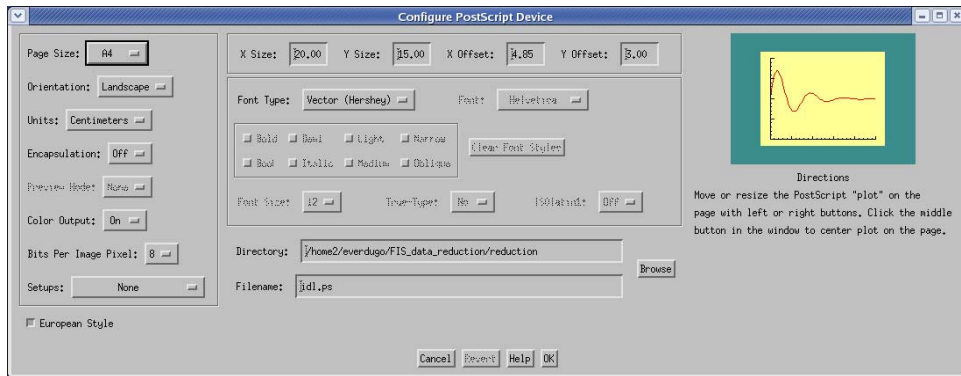
Figure A.3.6: Postscript output setup dialog

Processed data can also be saved into another TSD file (FITS binary).

A.3.2 Main Functions: Display

As shown in the previous section it is possible to display detector signals (for each pixel) and the status (Shutter open/closed, calibration lamp on/off, etc...). More than one value can be plotted at once by selecting multiple items using the [Ctrl] or [Shift] key on your computer keyboard. They will be plotted in the same graph as shown in Figure A.3.7 where the detector signal and Shutter Open status (ShtOp) are selected.
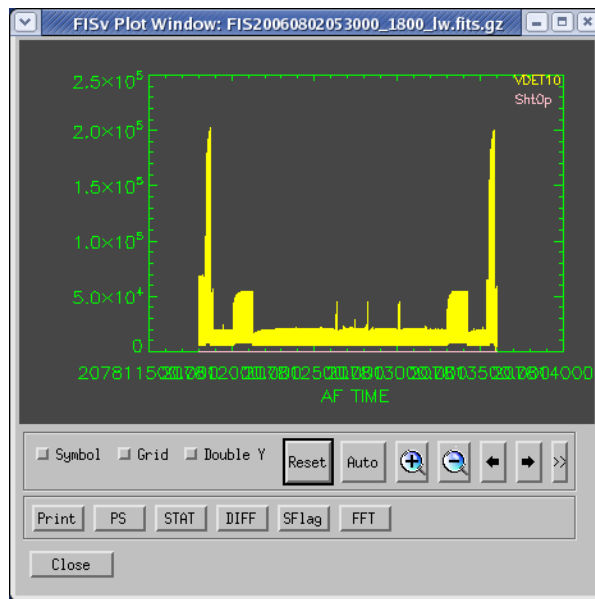

Figure A.3.7: Detector signal and Shutter Open plot

The button "SFlag" on the plot window allows both keywords to be displayed separately on a Double Y axis as shown in Figure A.3.8.
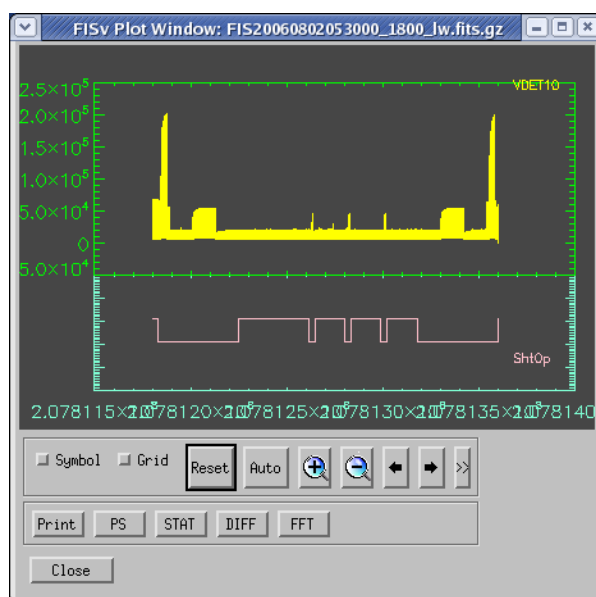
Figure A.3.8: Detector signal and Shutter Open plotted separately using the SFlag option

The plot window also allows one to perform simple statistics (STAT), differentiation (DIFF) and Fast Fourier Transforms of the signal in the time domain (FFT).

Other display functions allow the display of all the pixels (see Fig A.3.9) and the display of a 2D and 3D image of the detector array (Fig A.3.10).
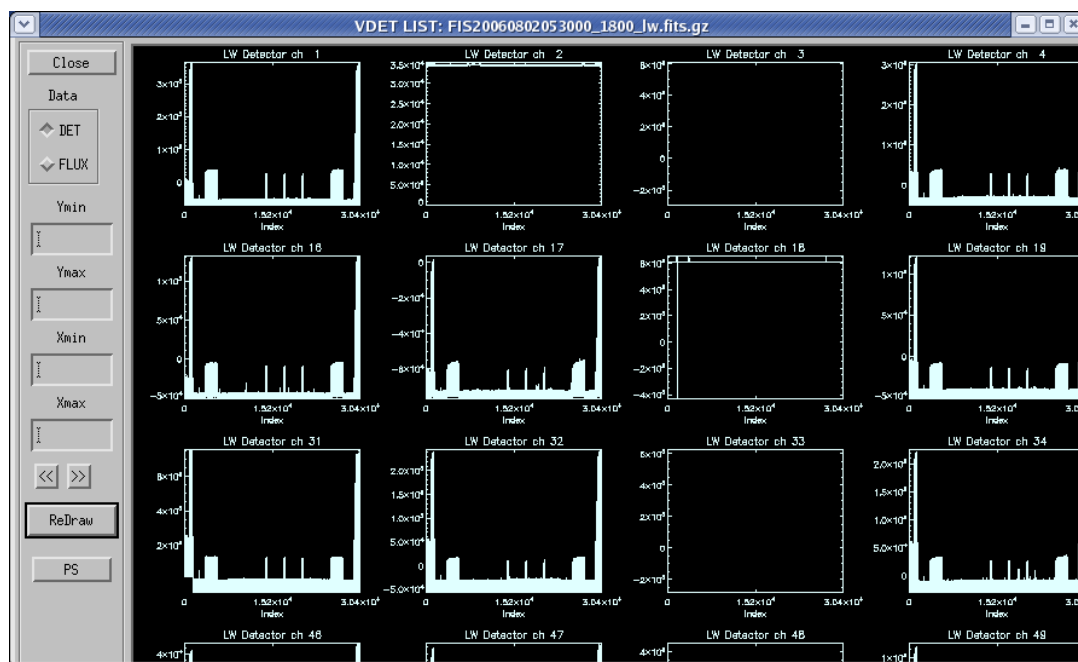

Figure A.3.9: Signal plot of all pixels

Figure A.3.10: 2D and 3D images of the detector array

A.3.3 Main functions: Processing

FISv also allows some simple calculations and processing besides the mentioned statistics, differentiation and FFT.

- A subset can be made from the TSD interactively. The current TSD will then be replaced by the subset.

- Plots can also be masked by some of the defined flags.

- Signal processing can be carried out by calling the GB pipeline modules (see Chapter 4). However, FISv is not intended to be at the moment a data reduction tool. It should be noted that using GB pipeline functions will override the original processing of the data. A history of the GB modules used is kept in the primary header of the TSD file.

A.4   Contribution tools

Contribution tools are extra tools which provide additional functions to the standard processing
package, or tools for data reduction/analysis beyond the scope of the standard tool.

A.4.1   Making mosaic images from multiple observations

Program Name

> `ss_mosaic_image.pro`

Developers

> M. Shirahata and S. Matsuura (ISAS)

Purpose

> This tool is prepared to make mosaic images map using multiple scan data. It is useful for
> observations of wide area covered by multiple pointings, and deep imaging by repeating
> the pointed observations.

Calling Sequence

```
ss_mosaic_image, targetdir, SIGMA=sigma, $
     T_START=t_start, T_END=t_end, $
     GRID_SW = grid_sw, GRID_LW = grid_lw, $
     LON_CENTER = lon_center, LAT_CENTER = lat_center, $
     LON_SIZE = lon_size, LAT_SIZE = lat_size, $
     ECLIPTIC = ecliptic, GALACTIC = galactic, $
     CUBE_FITS = cube_fits, $
     TAG_NAME = tag_name, $
     aot_mix=aot_mix, NO_DISPLAY=nodisp
```

Input

> `targetdir` : directory that contains `*_ar.sav` files produced by `ss_run_ss` you want to
> combine.

Output

> Image files in IDL save file and FITS format in the directory.

Options

> Most of the options for `ss_mosaic_image` are the same as `ss_run_ss` and already explained
> in the previous section. An only unique option for this module is `AOT_MIX`. Note that no
> lower limit is applied for `GRID_SW` and `GRID_LW` parameters.

> ```
> /AOT_MIX
>    : Use all available data in the directory. See Explanation below.
> ```

Explanation

> `ss_mosaic_image` searches for all processed scan data (`*_ar.sav` file) in the target directory
> and constructs images using all available data. It assumes that the directory contains a
> 'uniform' data set, i.e., same AOT and AOT parameters. If data files of different data

sampling modes are in the target directory the program takes the mode of the first found file (normal OS list order). `/AOT_MIX` option forces the program to use all available data, regardless of their sampling modes. The internal algorithm and the results are the same as those of the standard `ss_run_ss` tool. Note that this program attempts to make an image that covers all available data. If the directory contains scan data that is (spatially) far from the others, the program tries to allocate a huge amount of memory for the creation of the image plane which could cause many problems.